Aus dem Max-von-Pettenkofer Institut für Virologie

der Ludwig-Maximilians-Universität

Vorstand: Prof. Dr. med. U. Koszinowski

The subcellular trafficking of the prion protein: Characterisation of the function of the PrP^c N-terminus

Dissertation

zum Erwerb des Doktorgrades der Humanbiologie

an der Medizinischen Fakultät der

Ludwig-Maximilians-Universität zu München

vorgelegt von

Maximilian Nunziante
aus
Catania (Italien)

Jahr
2003

Mit Genehmigung der medizinischen Fakultät

der Universität München

Berichterstatter:	Prof. Dr. rer. nat. K. Conzelmann
Mitberichterstatter:	Priv. Doz. Dr. H. Steiner
	Prof. Dr. J. Herms
Mitbetreuung durch den promovierten Mitarbeiter:	Prof. Dr. med. H. M. Schätzl
Dekan:	Prof. Dr. med. Dr. h. c. K. Peter
Tag der mündlichen Prüfung:	26. 09. 2003

Table of contents

1 Introduction

1.1 Historical Background

Although at least some of the closely related neurodegenerative conditions known as transmissible spongiform encephalopathies (TSEs) or prion diseases have been recognised for many years, only in the last two decades decisive steps have been made in the characterisation of their underlying causes. These rapidly progressing fatal syndromes can affect both humans and animals and present scientists and public health with distinctive phenomena and challenges. This is because of the unique biology of the transmissible agent and because of the fear that the epidemic of the bovine prion disease BSE, with more the 180,000 cases in the U.K. and numerous confirmed cases in other European countries, could represent a threat to public health through dietary exposure. In 1996 a direct link between BSE and a novel form of the human Creutzfeldt-Jakob disease was argued for (Will *et al.*, 1996; Collinge *et al.*, 1996b;Will, 1998).

The nature of the agent in these disorders has been a matter of debate for many years. The naturally occurring scrapie disease affecting sheep and goat present in many countries world wide was first described as early as 1732. In 1936 inoculation between sheep (and goat) showed that scrapie could be transmitted after prolonged incubation. Some kind of virus was therefore assumed to be the causative agent and in 1954 Sigurdson referred to it as a "slow virus", due to incubation times as long as 20 years. Five years later Hadlow drew attention to the similarities between scrapie and kuru, a disease of New Guinea highlanders, at a neuropathological and clinical level. Intracerebral inoculation of chimpanzees with brain homogenates a few years later established the transmissibility of kuru (Gajdusek *et al.*, 1966). Similarities in the pathology of the central nervous system (CNS) also showed a link between these and another human disease, the Creutzfeldt-Jakob disease (CJD), a rare neurodegenerative condition, the etiology of which had been unknown for decades (it had first been described in 1920). In 1968 also the transmission of CJD to chimpanzees after intracerebral inoculation was reported (Gibbs, Jr. *et al.*, 1968).

In spite of the initial assumption for the causative agent of TSEs, no virus or immunological response was found. In 1966 Tikvah Alper and colleagues found that the scrapie agent was resistant to UV- inactivation and ionising radiation, treatments that would inactivate nucleic acids, whereas infectivity could be reduced by procedures that hydrolyse or modify proteins (urea or treatment with NaOH) (Alper *et al.*, 1966). These findings led to the conclusion of an agent devoid of nucleic acid and in 1967 Griffith suggested that the transmissible agent might

be a protein (Griffith, 1967). In 1982 the Prusiner group isolated a protease resistant glycoprotein which was the major constituent of the infective fraction in affected brain homogenate and sometimes formed amyloid deposits in form of filamentous structures called scrapie-associated-fibrils (SAFs) or prion rods (Lehmann and Harris, 1996; Hilmert and Diringer, 1984; Prusiner *et al.*, 1981;Prusiner, 1982). Prusiner therefore proposed the definition "prion" as a proteinaceous infectious particle that lacks nucleic acid. In enriched fractions of Syrian hamster (Sha) brains the isolated proteinase-K (PK)-resistent protein was of 27-30 kDa (PrP27-30) and was derived from a larger molecule of 33 to 35 kDa, designated PrP^{Sc} (denoting the infectious scrapie character of this protein). Determination of the NH2-terminal sequence of the PrP^{Sc} by Edman degradation finally made molecular cloning studies of the PrP gene (*prnp*) possible (Prusiner *et al.*, 1984). The findings that PrP mRNAs were identical in uninfected and scrapie infected tissues, and that antibodies raised in mice against infected hamster PrP also reacted with uninfected tissues led to isolation of a non- infectious cellular isoform of the prion protein denoted PrP^{c} (Oesch *et al.*, 1985; Meyer *et al.*, 1986). The two isoforms of the prion protein shared the same amino acid sequence, but differed significantly in their biochemical properties (Prusiner, 1991).

Characteristics	PrP^{c}	PrP^{Sc}
Infectivity	No	Yes
Secondary structure	Mainly α-helical	Mainly β-sheet
Half life time	2-6 hours	16-24 hours and longer
Proteinase-K (PK) digestion	Sensitive	Partially resistant
Ultracentrifugation in detergents	Soluble	Insoluble

Table 1: Features of the cellular and pathogen isoforms of the prion protein: a comparison

1.2 Animal prion diseases

Both human and animal prion diseases share common histopathological features. Examination of the CNS typically shows spongiform degeneration affecting different parts of the grey matter, neuronal loss and astrocytic proliferation which can be accompanied by amyloid plaques. The degree of spongiform vacuolation is quite variable and the extent of astrocytic proliferation correlates with the degree of neuronal loss.

Disease	Host	Cause
Scrapie	Sheep/ Goat	Vertical and horizontal infection in genetically susceptible sheep; oral transmission; sporadic
TME (transmissible mink encephalopathy)	Mink	Infection with contaminated meat from sheep and cattle
CWD (chronic wasting disease)	Deer, elk	Unclear, possibly similar to scrapie
BSE (bovine spongiform encephalopathy)	Cattle	Infection with prion-contaminated food; sporadic (?)
FSE (feline spongiform encephalopathy)	Cats	Infection with contaminated bovine tissue and food

Table 2: The animal prion diseases

Besides scrapie, more recently recognised animal diseases like transmissible mink encephalopathy (TME) (Marsh and Hadlow, 1992) and chronic wasting disease (CWD) in deer and elk (Shyng *et al.*, 1995b) were described in captive animals, mainly in the USA together with the bovine spongiform encephalopathy or BSE in the United Kingdom (Wells *et al.*, 1987). Chronic wasting disease seems to be a common condition in wild deer and elk in areas of Colorado, Wyoming and Montana (Spraker *et al.*, 1997). The routes of transmission remain unclear. Transmissible mink encephalopathy has occurred as infrequent epidemics along captive mink in UK and USA, long before BSE, and in Russia. The disease is probably caused by exposure to sheep and cattle prion via contaminated food.

BSE was first described in UK cattle in 1986 and evolved rapidly to an epidemic. The cows initially became apprehensive and uncoordinated, their mental status deteriorated and they became hard to handle. In some cases they progressed to frenzy, which led to the name “mad cow disease”. Contaminated meat and bone meal prepared from carcasses of sheep and cattle as a high protein nutritional supplement for dairy cows was recognised to be its probable cause. One possibility for the raise of BSE is that changes in the rendering processes introduced in the United Kingdom in the late 1970s (e.g. the use of hydrocarbon organic solvents had been stopped) allowed scrapie prion from sheep to survive and to be passed to cattle. An alternative hypothesis is that epidemic BSE resulted from recycling of rare sporadic BSE into cattle by oral inoculation with food. More than 180,000 clinical BSE cases have been confirmed in cattle in the UK although the total number of infected animals has been estimated at around one million (Anderson *et al.*, 1996). The ban of food derived from animal

carcasses in 1988 to sheep and cattle has now led to a drastic reduction of the epidemic. In the 90s, a number of BSE cases has been reported in other European countries like Switzerland, Ireland and Portugal. Recently diagnosed BSE cases in German cattle due to import of food from the UK has led to compulsory testing for all slaughterhouse cows older than 24 months in Germany, following the EU-regulations introduced in 2001. So far more than 100 animal were tested positive. Immunoassays for PrP^{Sc} in the brainstem of cattle might provide a reasonable approach to establishing the incidence of subclinical BSE. Newly recognised prion diseases can also affect domestic and wild cats (Lehmann and Harris, 1996) and a number of zoo animals (Jeffrey and Wells, 1988; Kirkwood *et al.*, 1990). These new diseases have developed at the same time or following the emergence of BSE, and several of these have been seen to be caused by the BSE prion strain (Bruce *et al.*, 1994; Collinge *et al.*, 1996b). Nevertheless, many domestic animals show resistance to infection with prion: no case of TSEs could be detected in dogs or birds, and pigs could not be orally infected, so far.

1.3 Human Prion Diseases

Depending on their etiology, human prion conditions can be divided into three categories: sporadic, acquired and inherited. Accidental exposure to human prions through medical or surgical procedures as for iatrogenic Creutzfeldt-Jakob disease (iCJD) or participation in cannibalistic ceremonies as in the case of kuru are the origin of acquired prion diseases in humans. The appearance in the UK in 1995 of a novel human prion disease, variant CJD (vCJD) probably derived by dietary exposure to cattle BSE has extended the list of acquired TSEs. Around 10-15 % of all human prion diseases are inherited and have been associated with autosomal dominant mutations in the prion protein gene. Over 20 distinct point mutations have been characterised (Collinge, 1997) and can be diagnosed by *prnp* analysis. This has allowed recognition of a range of atypical dementias and of the fatal familial insomnia (Collinge *et al.*, 1992; Gambetti *et al.*, 1995). No pathogenic PrP mutations are present in sporadic prion diseases.

Disease	Mechanism of infection
Kuru	Acquired through cannibalistic rituals
CJD:	
Familial	Inherited (mutation in the PrP gene)
Sporadic	Spontaneous conversion of PrP^{c} into PrP^{Sc} (?)
Iatrogenic	Acquired from contaminated instruments, dura mater grafts or growth hormone
Variant CJD	Acquired (infection by bovine prions)
GSS (Gerstmann-Sträussler-Scheinker disease)	Inherited (mutation in the PrP gene)
FFI (fatal familial insomnia)	Inherited (mutation in the PrP gene)

Table 3: The human prion diseases

Classical (sporadic) CJD is a rapidly progressive multifocal dementia occurring in all countries with an incidence of one per million inhabitants. Usually, the age of onset of the disease is 45 to 75 with death occurring 3-6 months after onset of the symptoms. Insomnia, fatigue, depression, loss of weight, headache and general pain sensations are characteristic symptoms, neurological features include ataxia, pyramidal signs and cortical blindness.

Kuru provides the largest experience of acquired human prion disease with the earliest cases dating back to the beginning of the 20^{th} century. This disease affected a defined population living in the Eastern Highlands of Papua New Guinea (the Fore linguistic group and their neighbours) reaching epidemic proportions. It affected predominantly women and children of both sexes and was the most common cause of death among women in affected villages. Kuru was transmitted during cannibalistic rituals when deceased members of the community were consumed by their close relatives. Women and children predominantly participated in these feasts and ate brain and internal organs, which might explain age and sex of incidence. The epidemic probably originated from a sporadic case of CJD which occurred in this population and was re-introduced when the individual was consumed. The precise estimate of the incubation period of the disease is complicated by the multiple exposure that individual kuru patients might have had. Infrequent cases of kuru recorded in children as young as 4.5 years indicate incubation times of this order or less. However, although dietary exposure was the

principal route of transmission, inoculation with brain or other tissue via cuts or sores was also likely (Prusiner *et al.*, 1982). On the other hand, occasional cases of kuru still occur in some individuals exposed during the last ceremonies held in their villages in the 1950s and are consistent with incubation periods longer than 40 years. After cession of cannibalism in the late 1950s the number of cases decreased significantly and none of the individuals born after the ban showed symptoms. The central clinical feature of the disease is progressive cerebellar ataxia and, in contrast to CJD, dementia is often absent. The mean clinical duration of illness is 12 months.

Although prion diseases can be transmitted experimentally to animals by inoculation, they cannot be transmitted to humans via family or sexual contact. Besides cannibalism, the only documented human case-to-case spread occurred by the use of inadequately sterilised intracerebral electrodes, dura mater and corneal grafting and from the use of human cadaver growth hormone or gonadotropin. Of note, cases arising from intracerebral or optic inoculation clinically manifest as classical CJD, with rapidly progressive dementia, whereas peripheral inoculation often results in kuru-reminding ataxia. Even incubation period after intracerebral inoculation is shorter (19-46 months for dura mater grafts) compared with peripheral cases (mean estimation 15 years).

The pathogenic mutations identified in the prion protein gene are all autosomal dominant and can be divided into two groups: point mutations resulting in amino acid substitution (or truncation) in the PrP molecule or insertions encoding additional copies of two or more of the five octapeptide repeats usually present in the normal PrP. These mutations are believed to destabilise the prion protein, which then undergoes spontaneous conformational change (Owen *et al.*, 1989; Ghetti *et al.*, 1996). Besides familial cases of CJD (10 % of all CJD cases), the Gerstmann-Sträussler-Scheinker disease (GSS) is another autosomal dominant disorder presenting with chronic cerebellar ataxia and dementia occurring later in a more prolonged clinical course than in CJD. Histologically, amyloid PrP-plaques represent a hallmark of the disease. The mean duration is approximately 5 years, with onset in the third or fourth decade. First associated with the P102L *prnp* mutation (Hsiao *et al.*, 1989), GSS is now linked to seven different PrP mutations and forms part of the phenotypic spectrum of inherited prion diseases.

The phenotypes in families with inherited prion diseases can show remarkable variability ranging from classical CJD to GSS as well as to other cases that do not conform to either of those syndromes. The classical histological features can be seen in variable combinations or lack completely. The latest discovered inherited form of prion disorder is the fatal familial

insomnia (FFI), characterised by mutation of codon 178 of *prnp* from Asp to Asn (Parchi *et al.*, 1998; Goldfarb *et al.*, 1992) associated with the PrP-allele methionine at codon 129. Affected individuals are usually over 50 years of age and usually die one year after onset of symptoms. A possible rare sporadic origin of this disease has been recently suggested (Kretzschmar, unpublished data).

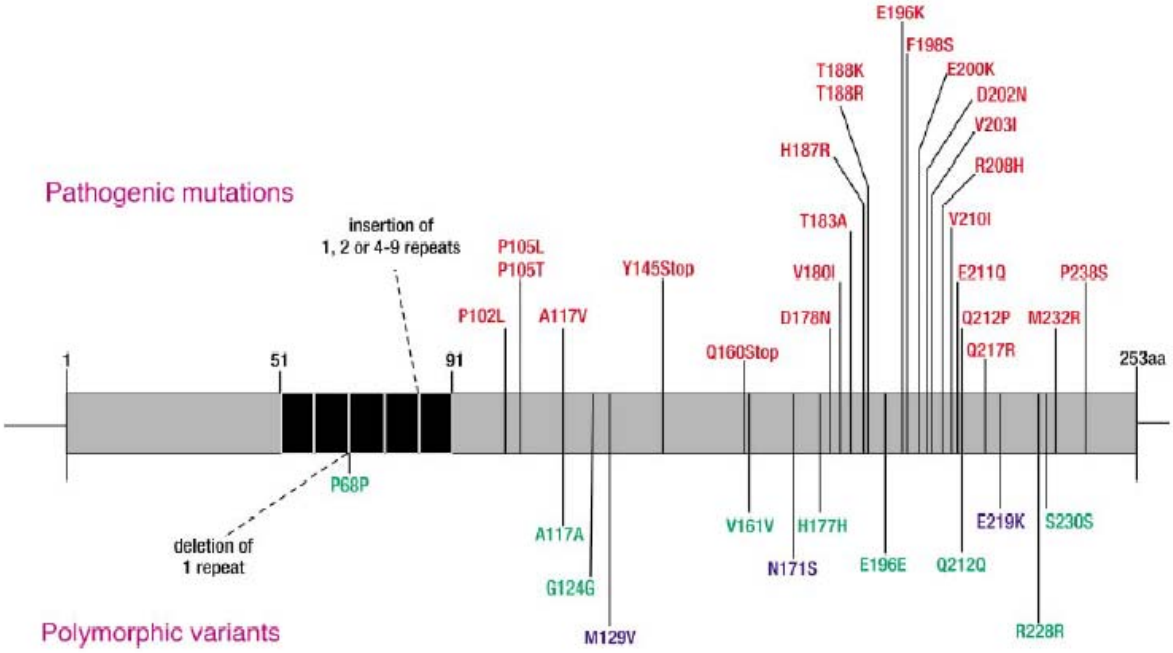

Figure 1. Mutations causing inherited prion diseases and polymorphisms in humans.

Above the line of the human sequence are mutations that cause prion disease. Below the lines are polymorphisms, some but not all of which are known to influence the susceptibility as well as the phenotype of disease. (From Collinge, 2001)

1.3.1 Variant CJD

Concern over the possibility of transmission of BSE to humans led to re-establishment in 1990 of a comprehensive system of national surveillance for CJD in the UK directed toward detection of any rise in the incidence of human prion disease. In fact, in 1994 (Will *et al.*, 1996; Collinge and Rossor, 1996) several cases of CJD in teenagers and young adults were observed and reported. Up to November 2002 a total of 117 probable cases have been referred in the UK with 6 cases in France, one in the Republic of Ireland and one in Italy. The disease, initially named new variant CJD, now simply variant CJD (vCJD), presented a clinical picture that contrasted with all forms of classical CJD. The most striking clinical difference between classic and variant CJD is the downward shift in the average age of affected individuals for vCJD with a range of 16 to 53 years. The rate of progression is marginally slower than that of cCJD with a mean duration of 14 months. In the clinical presentation, behavioural and

psychiatric disturbances predominate (Zeidler *et al.*, 1997), (Hill *et al.*, 1999) and the most dominant symptoms are depression and behavioural changes. Cerebellar syndromes and ataxia also develop, dementia usually appears later in the clinical course. The most remarkable neuropathological characteristic is the accumulation of PrP amyloid plaques in cerebral and cerebellar cortex, consisting of kuru-like spongiform vacuoles ("florid plaques") (Will *et al.*, 1996). Another unique characteristic is that PrP^{Sc} can be detected in tonsils and other lymphoreticular tissues in patients affected with vCJD, which is not the case in other forms of human prion diseases. All patients to date are homozygous for methionine at *prnp* codon 129 (Collinge *et al.*, 1996b).

A number of data today indicate a direct link between BSE and vCJD initially supported by the restricted geographical occurrence and chronology of vCJD. Molecular strain typing showed that the glycoform ratios of PK digested PrP^{Sc} in vCJD were identical with those seen in BSE passaged in a number of mammalian species (Collinge *et al.*, 1996a). In 1997 inbred mice that had been inoculated with homogenates of brains from three vCJD patients were reported to show the same BSE strain characteristic (incubation period and lesion profile) (Bruce *et al.*, 1997; Hill *et al.*, 1997). Macaque monkeys also developed neurologic disease several years after inoculation with bovine prions exhibiting plaques similar to those found in vCJD (Lasmezas *et al.*, 1996). In 1989 the British banned the use of specified types of bovine offal in food for human consumption. Until then homogenates of pooled bovine brains had been used as binders for foods such as hamburgers and sausages. Humans could therefore have ingested food with high titers of infected agent. If the cases of vCJD were contracted before this ban, the minimal incubation period would probably be around 10 years.

So far it remains difficult to usefully estimate the total magnitude of a possible vCJD epidemic by extrapolation from the current. Statistics and reports of the number of individuals who will develop vCJD in the next years range from hundreds to many thousands (Donnelly *et al.*, 2002; Ghani *et al.*, 2002).

1.4 Therapeutic and prophylactic approaches

Numerous approaches have been undertaken for experimental prophylaxis or therapy of prion diseases. Since the brain suffers severe damage during the course of TSEs, including widespread neuronal loss, even in the early clinical phase of the disease, it is difficult to think that this damage can be reversed by pharmacological treatment. A different strategy is the use of substances which might prolong the incubation time and decelerate the pace of the disease by inhibiting the accumulation of PrP^{Sc} or the conversion of PrP^{c} into its pathogenic isoform.

Among these, Congo Red, polyene antibiotics, anthracycline derivatives, sulphated polyanions, porphyrins, branched polyamines, Suramin and β-sheet breaker peptides have been seen to exert an effect in animal models or in cell culture systems. The effects exerted by some of these agents result primarily from their ability to interfere with trafficking of PrP^c either by stimulating its endocytosis (as in the case of Pentosan and Dextran Sulphate) or by re-routing the protein to acidic compartments (as for Suramin), so that the location of conversion is by-passed. Strategies for intervention in case of post-exposure prophylaxis also deal with the fact that, in some TSEs, follicular dendritic cells (FDC) and secondary lymphoid organs are essential for prion replication (Hilton *et al*., 1998; Hill *et al*., 1999, Brown *et al*., 1999; Beekes and Mc Bride, 2000, Mabbot *et al*., 2000, Bruce *et al*., 2001). The molecules involved in this replication and accumulation step can therefore represent attractive targets for post-exposure prophylaxis. Recent data on the role of the immune system in prion diseases (Klein *et al.*, 1997; Klein *et al.*, 2001; Mabbott and Bruce, 2001) and immunisation studies in mouse models for Alzheimer disease (Ingram, 2001) have suggested a possible vaccination strategy against prion infection. Anti-PrP monoclonal antibodies and recombinant Fab fragments have shown pronounced effect in suppressing prion replication in cultured prion-infected cells. A humoral immune response against PrP^c and PrP^{Sc} is difficult to induce due to the fact that PrP^c is a ubiquitous endogenous protein and an autotolerance within mammalian species represents a major obstacle in a vaccination approach. This is not the case when *prnp* is ablated or when PrP of a different species is used as an immunogen (Prusiner *et al.*, 1993; Williamson *et al.*, 1996). Of note, no innate or antigen-induced immune response is observed in natural prion infections (Prusiner, 1998; Weissmann *et al.*, 2001). In a recent work, transgene expression of the heavy chain of an anti PrP antibody in mice prevented scrapie pathogenesis after intraperitoneal inoculation with prions (Heppner *et al.*, 2001).

1.5 PrP gene structure

The PrP gene is mapped to the short arm of human chromosome 20 and to the homologous region of mouse chromosome 2 (Robakis *et al.*, 1986; Sparkes *et al.*, 1986) and is highly conserved in evolution (Schatzl *et al.*, 1995; Wopfner *et al.*, 1999). The entire open reading frame (ORF) of all known PrP genes resides within a single exon (Hsiao *et al.*, 1989; Gabriel *et al.*, 1992; Schatzl *et al.*, 1995). The mouse, sheep, cattle and rat PrP genes contain three exons with the entire ORF in exon 3 (Westaway *et al.*, 1991; Saeki *et al.*, 1996) which is analogous to exon 2 of the Syrian hamster (Sha) gene (Basler *et al.*, 1986). Exon 1 of the ShaPrP includes a portion of the 5′ untranslated leader sequence, while exon 2 includes the

ORF and the 3´ untranslated region. The promoters of PrPs are devoid of a TATA box and contain multiple copies of G+C rich repeats for binding of the transcription factors Sp-1 and AP-1 (McKnight and Tjian, 1986). Since the entire protein coding region is contained within a single exon, there is no possibility for the two protein isoforms to be the product of alternatively spliced mRNA (Basler *et al.*, 1986).

1.6 The function of the prion protein

PrP has been identified in mammals, birds (Harris *et al.*, 1993), marsupials (Windl *et al.*, 1995) and amphibians (Strumbo *et al.*, 2001). The highest PrP^c concentration is found in neurons (Kretzschmar *et al.*, 1986), the protein follows an axonal pathway (Borchelt *et al.*, 1994) and localises mainly at synaptic (Fournier *et al.*, 1995) or presynaptic ends (Herms *et al.*, 1999). Although the highest levels of expression are seen in the central nervous system, the protein is found in most tissues and is widely expressed in cells of the immune system (Dodelet and Cashman, 1998). Its precise function has so far remained obscure. Gene knock-out of *prnp* in mice did not lead to pronounced phenotype (Bueler *et al.*, 1992) although these mice were completely resistant to prion following inoculation and did not replicate prions (Bueler *et al.*, 1993). These knock-out animals were eventually shown to have abnormalities in the synaptic physiology (Collinge *et al.*, 1994) and in circadian rhythms and sleep (Tobler *et al.*, 1996). A second physiological phenotype for *prnp* knock-out mice was reported later, with a reduction of slow after-hyperpolarisations evoked by trains of action potentials (Colling *et al.*, 1996). This effect could be explained by abnormal homeostasis of intracellular Ca^+. One of the possible roles for PrP^c might be that of a receptor for an extracellular ligand. The transmembrane laminin receptor precursor (LRP) was shown to bind to PrP on the surface of mammalian cells (Rieger *et al.*, 1997; Gauczynski *et al*., 2001). Other identified intracellular interactors include HSP 60 (Edenhofer *et al.*, 1996) and Bcl-2 (Kurschner and Morgan, 1996). Several data argue for a role of the prion protein in copper metabolism related to the finding, that the prion protein can bind copper ions (Brown *et al.*, 1998; Pauly and Harris, 1998). It has been shown that the Cu^{2+} content in membrane preparation of $PrP^{0/0}$ mice was reduced to 50 % of that of wild type mice (Brown *et al.*, 1997b). These mice also show a higher sensitivity to copper toxicity in oxidative stress conditions (Brown *et al.*, 1996; Pauly and Harris, 1998). A superoxide-dismutase activity or a role as a carrier protein for uptake and delivery of metal ions from the extracellular space into the cell have been discussed, (Brown *et al.*, 1997a; Brown *et al.*, 1999). Synthetic peptides corresponding to the histidine rich octapeptide repeats (residues 50-90), and to peptides encompassing residues 60-91 or 23-98

have been seen to bind copper (II) ions (Pauly and Harris, 1998; Hornshaw *et al.*, 1995). Studies done with CD spectroscopy and NMR (Viles *et al.*, 1999) or mass spectrometry (Whittal *et al.*, 2000) confirmed this affinity proposing a pH dependence of binding and stoichiometry. Recently, a second site around histidines 96 and 111 of human PrP, a region of the molecule known to be crucial for prion propagation, has been described (Jackson *et al.*, 2001).

1.7 The structural properties of the prion protein

Numerous data support the concept that prions consist principally or entirely of an abnormal isoform of the cellular prion protein (PrP^c), named PrP^{Sc}. The pathogenic protein acts as a template promoting a conformational change of PrP^c (Borchelt *et al.*, 1990; Caughey and Raymond, 1991) in a postranslational contact.

Following translation of the PrP-mRNA the mouse PrP is composed of 254 amino acids, the first 22 of which function as signal peptide for translation of the polypeptide chain into the endoplasmic reticulum (Oesch *et al.*, 1985). After cleavage of another C-terminal peptide, the molecule acquires a glycosyl-phosphatidyl-inositol (GPI) anchor. The polypeptide chain undergoes further posttranslational modifications resulting in the possible addition of 2 N-linked carbohydrate chains at Asn181 and Asn197. A single disulphide bond between Cys179 and Cys214 stabilises the conformation of the protein. After cleavage of the N- and C-terminal signal peptides, the mature human protein comprises 209 amino acids.

A **B**

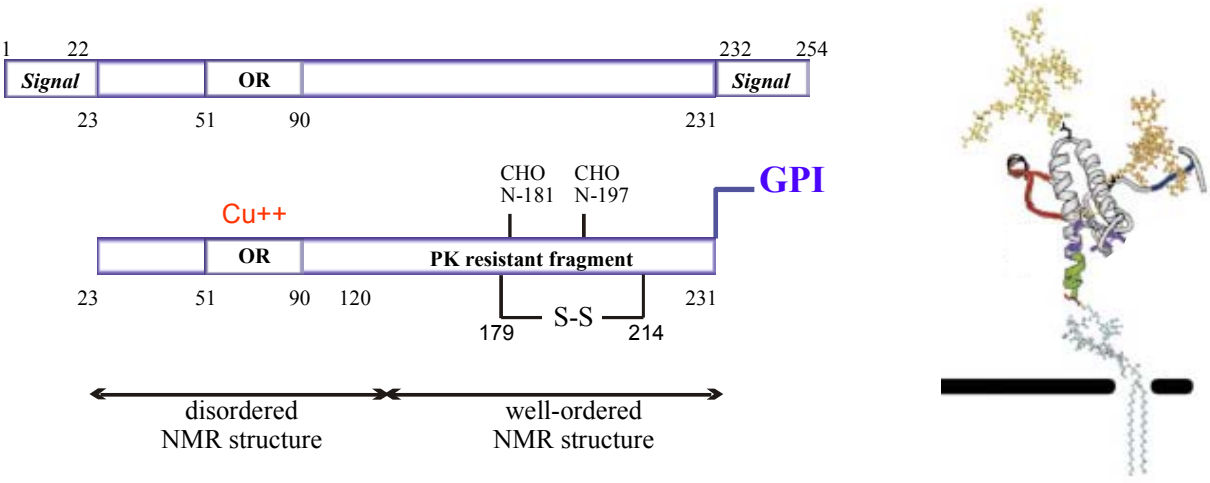

Figure 2. **Primary structure of human PrP^c before and after maturation**.

(**A)** The N- and C terminal signal peptides are cleaved from the translation product and a glycosyl phophatidyl inositol (GPI) anchor is attached to the C-terminal end of the protein. The molecule can be N-glycosylated twice (CHO), and disulfide bond (S-S) is built. The final product consists of 209 amino acids. (**B**) Structure of PrP^c as it is attached to the outer leaflet of the plasma membrane via its GPI anchor. Carbohydrate molecules are shown in yellow (from Peretz, 2001)

Properly folded PrP^c transits through the Golgi compartment and the secretory pathway and is attached to the outer leaflet of the cellular plasma membrane by the GPI-anchor (Borchelt *et al.*, 1990; Taraboulos *et al.*, 1990b;Caughey, 1991). From here internalisation seems to occur through caveolae-like domains (CLD) or in rafts, membranous domains or invaginations of the plasma membrane rich in cholesterol and glycosphingolipids (Taraboulos *et al.*, 1995). Cell surface localisation of PrP^c is thought to be essential for subsequent conversion into PrP^{Sc} (Borchelt *et al.*, 1990; Taraboulos *et al.*, 1990b;Caughey, 1991) since conversion into PrP^{Sc} has been reported to occur close to the plasma membrane along the endocytic pathway, probably in CLD or in rafts (Taraboulos *et al.*, 1995). Here also the first steps in PrP degradation occur (Vey *et al.*, 1996; Kaneko *et al.*, 1997a). After internalisation, PrP is transported to endosomes, from where it can either recycle to the cell surface (Vey *et al.*, 1996) or reach acidic compartments for final degradation. Late endosomes or lysosomes might be another compartment for prion propagation, as the low pH might facilitate un- and re-folding (Taraboulos *et al.*, 1992; Arnold *et al.*, 1995). After conversion, PrP^{Sc} accumulates in lysosomes and its degradation occurs at a very low rate.

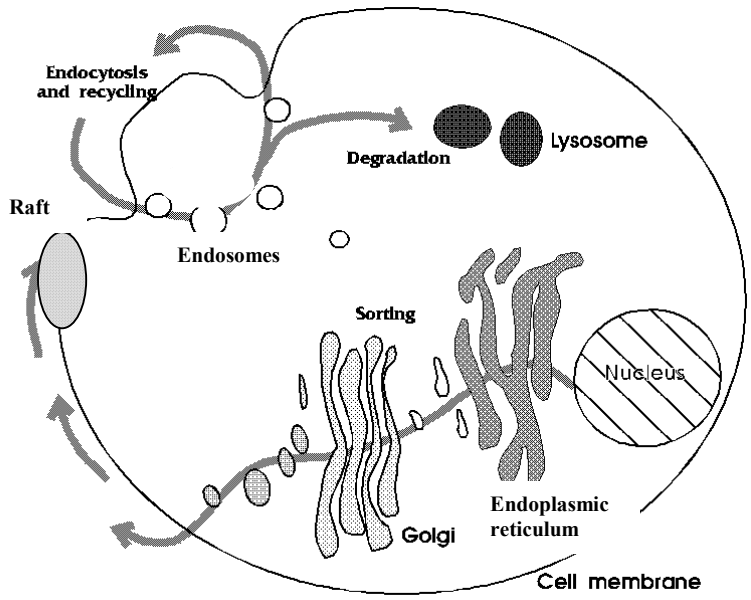

Figure 3. Cellular trafficking of PrP^c

After being transported along the secretory pathway and reaching the cell surface, where it is localised in cholesterol rich rafts. PrPc is internalised into endosomes and reaches lysosomes for degradation or is recycled back to the plasma membrane. (Modified from Lehmann, 1997)

1.7.1 The conformation of PrP^c and PrP^{Sc}

For many years, the idea that the amino acid sequence specifies one biologically active conformation of a protein had been accepted (Anfinsen, 1973). Nevertheless when purified PrP^{Sc} and PrP^c were isolated, the secondary structure of the two PrP isoforms sharing the same amino acid sequence were compared by optical spectroscopy and were found to be different (Pan *et al.*, 1993). The structure of the prion protein seemed to adopt two different conformations. Fourier-transform infrared spectroscopy (FTIR), mass spectrometry (Stahl *et al.*, 1993) and circular dichroism (CD) studies showed that PrPc contains about 42 % α-helix and 3 % β-sheets, whereas PrP^{Sc} is composed of about 30 % α-helix and 45 % β-sheet (Pan *et al.*, 1993; Gasset *et al.*, 1993; Pergami *et al.*, 1996). Since it has been impossible so far to produce crystals of PrP, the three dimensional structure of PrP^c has not been measured by crystallographic analysis. The structure of a fragment of purified and refolded mouse PrP encompassing aa 121-231 expressed in *E. coli* was nevertheless analysed by nuclear magnetic resonance (NMR) (Riek *et al.*, 1996) which confirmed a short two stranded antiparallel β-sheet and 3 of the four α-helices predicted earlier (aa 144-154, 175-193, 200-219) by computer modelling (Cohen *et al.*, 1994). The tertiary structure of the full length protein (aa 23-231) was subsequently characterised (Riek *et al.*, 1997), a defined structure of the N-terminal part of the protein (aa 23-120) could not be identified. Since then, NMR measurements on recombinant hamster (James *et al.*, 1997) human and bovine PrP (Hosszu *et al.*, 1999) show that they have essentially the same conformation. The N-terminal part of most known PrPs contains a region formed by the repetition of five consecutive, eight residue long peptides, rich in glycine, proline and histidine (octarepeats). In mouse, they comprise amino acid 50 to 90. Binding of this region in vivo to metal ions and other possible ligands might nevertheless lead to a defined globular conformation. New data indicate the possible presence of a poly-L-proline type II –helix structure in the in vivo conformation of the prion polypeptide chain (Gill *et al.*, 2000).

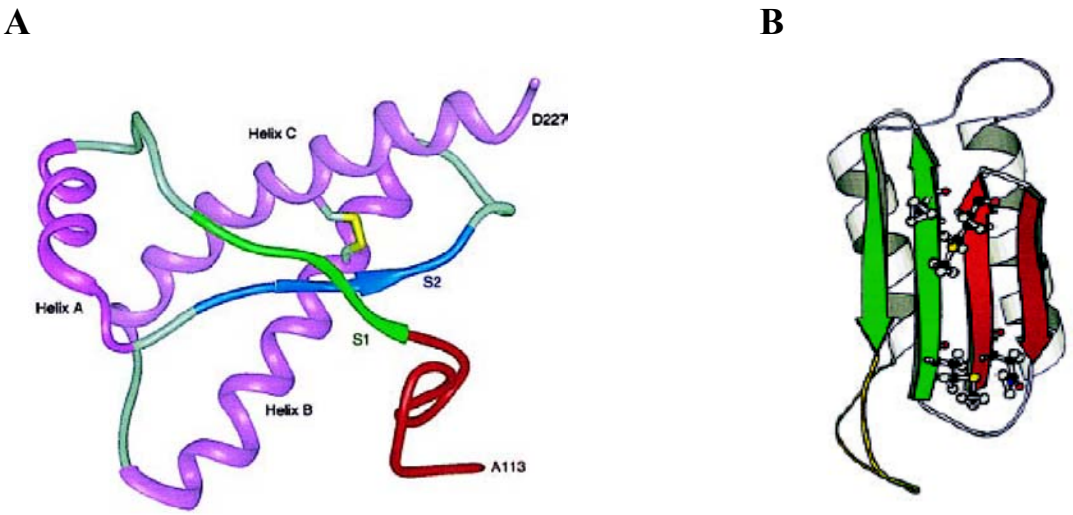

Figure 4. Proposed NMR structure of PrP^{c} and PrP^{Sc}

(**A**) Syrian hamster recombinant PrP^{c}(113–231) is viewed from the interface where PrP^{Sc} is thought to bind to PrP^{c}. Residues 90-112 are not shown. Three main α-helices A (residues 144–157), B (172–193), and C (200–227) can be seen. (**B**) Plausible model for the tertiary structure of $HuPrP^{Sc}$ with predominant β-strands structure (From Prusiner, 1998)

1.7.2 Mechanisms of prion conversion

The protein-only hypothesis for the propagation of prions proceeds from the assumption that the PrP^{c} of the host is converted into PrP^{Sc} by a direct interaction with exogenous scrapie protein. The major conformational change that causes PrP^{c} to become pathogenic is thought to involve refolding of the region between residues 90 and 112, which would lead to conversion of the two short β-sheet structures and the first α-helix into a large β-sheet formation. However, the remaining C-terminal structures including the other two α-helices and the disulphide bonds need to be preserved for PrP^{Sc} to be infectious (Prusiner, 1998; Hornemann *et al.*, 1997; Wille *et al.*, 2002). By these means, the predominantly β-sheet conformation of the pathogenic protein is transmitted to the native α-helical structure of the cellular isoform. Two current models provide possible explanations for this mechanism.

According to the heterodimer hypothesis proposed by Prusiner (Prusiner *et al.*, 1990; Cohen *et al.*, 1994), PrP^{c} is partially unfolded into a transitional state designated PrP* and then refolded under the influence of PrP^{Sc}, which results in the formation of a homodimer complex, possibly along with a hypothetical molecular chaperone. The newly generated PrP^{Sc} can again induce conversion of PrP^{c} in an autocatalytic process. The energy barrier for this conversion is probably very high (Cohen *et al.*, 1994) and spontaneous forms of the disease

only appear at an advanced age. Specific mutations promoting β-sheet conformation can therefore explain hereditary form of disease by lowering the energy barrier.

The nucleation dependent polymerisation model was first defined by the group around Gajdusek in 1990 (Brown *et al.*, 1990) and then developed by Landsbury together with Byron Caughey (Come *et al.*, 1993; Caughey *et al.*, 1995). According to this theory the host PrP^{c} can deposit on a polymerisation seed consisting of an infectious PrP^{Sc} oligomer. No unfolded transition state is needed and, upon deposition, PrP^{c} adopts the specific structure of the seed. leading to high molecular aggregates of PrP^{Sc}. These aggregates can then separate again and form new seeds. This model also explains the existence of different prion strains, since the PrP^{Sc} seed can determine the structure of the polymeric aggregates. The conformation does not have to be an intrinsic property of the PrP monomer but is induced by the scrapie oligomer. These two models, which are not mutually exclusive, are applicable to familial as well as infectious manifestations of prion diseases, since the presence of a pathogenic mutation presumably favors the spontaneous formation of either PrP^{Sc} nuclei or PrP*.

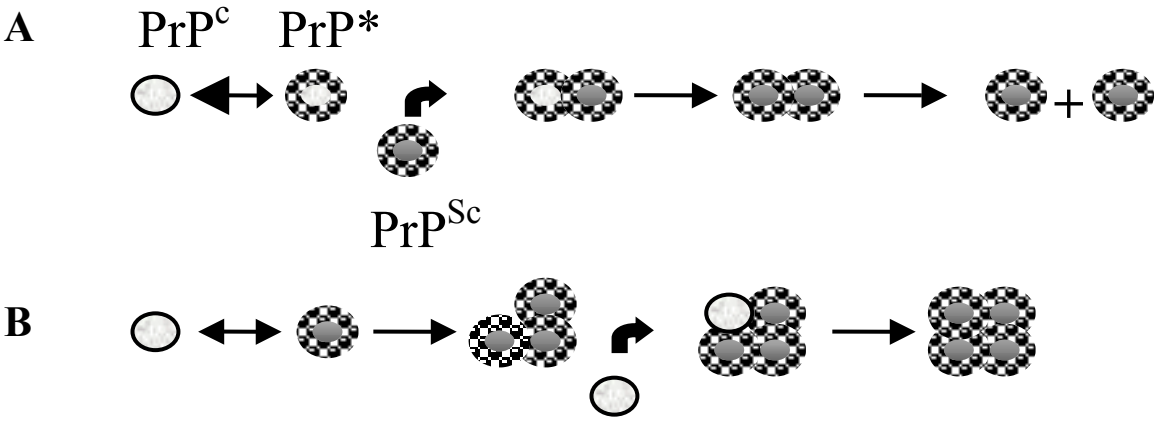

Figure 5. Two models for prion conversion and replication. (**A**) Heterodimer model; (**B**) the nucleation dependent polymerisation model.

1.8 Prion strains and the species barrier

Multiple isolates or strains of naturally occurring sheep scrapie have been isolated. Such strains differ in their biological properties: they produce distinct incubation periods and patterns of neuropathological targets (lesion profiles) in inbred mice and hamsters having the same PrP primary sequence. These features are not altered upon cross-species propagation. Furthermore, they can be re-isolated in mice after passage in intermediate species with different PrP primary structure (Bruce *et al.*, 1994). Two different mink prion strains

designated hyper (HY) and drowsy (DY) were serially propagated in hamster and showed different biochemical properties as well as specific migration patterns on polyacrylamide gels following limited proteolysis. Recently, several human PrP^{Sc} types have been identified which associate with different phenotypes of CJD (Parchi *et al.*, 1996) (Collinge *et al.*, 1996b). The different fragment size seen on Western Blots after PK-treatment suggests that there are several PrP^{Sc} conformations. Studies done with transgenic mice expressing human PrP^{c} showed that different CJD isolated maintained their fragment size and the ratio of the three glycolylation isoforms (diglycosylated, monoglycosylated and unglycosylated PrP) (Collinge *et al.*, 1996b). Transmission of human and bovine PrP^{Sc} to wild type mice resulted in murine PrP^{Sc} characterised by the strain phenotype of the inoculum. These data support a model in which the strain of the prion, which seems to be encyphered by the conformation of PrP^{Sc}, conspires with PrP^{c} sequence specified by the recipient to determine the tertiary structure of the nascent PrP^{Sc}. For human PrP^{Sc}, Collinge and collegues described three types among cases of sporadic and iatrogenic CJD and a distinctive fourth pattern for all vCJD cases. Recent work has shown that PrP^{Sc} conformation may be influenced by binding to metal ions in vitro and that different methodologies can lead to discrepancies in the classification of the strain types (Wadsworth *et al.*, 1999).

The transmission of prions between different species is almost always characterised by prolonged incubation time during the first passage in the new host when compared to transmission within the same species. This prolongation is referred to as “species barrier” (Pattison, 1965). De novo synthesised prions reflect the sequence of the host PrP. Upon subsequent passage in a homologous host, the incubation time shortens and resembles within-species transmission. Studies done with transgenic mice have shown that factors contributing to the species barrier are the difference in the PrP sequences between the donor and the recipient protein, the strain of prion and the species-specificity of the protein-X, a still undetermined host factor binding to PrP^{c} and promoting PrP^{Sc} formation (Telling *et al.*, 1995; Kaneko *et al.*, 1997b).

The concept of protein X has been introduced to explain the result of experiments with transgenic mice expressing both human and mouse PrP (Telling *et al.*, 1995). These mice proved to be resistant when inoculated with human prions, whereas mice expressing only human PrP could be infected and so were mice expressing mouse PrP and a chimeric mouse-human PrP. These results were interpreted in terms of a host (mouse) encoded factor (protein X) necessary for conversion, which binds to PrP^{c} of its own species with higher affinity than to that of a different species thus protecting form conversion by foreign PrP^{Sc}. This protein

has not been characterised, yet and still remains a merely genetic factor. Whether protein X functions as a molecular chaperone participating in the structural transitions during prion propagation is still unknown. Possible binding sites for the interaction with protein X have been identified at the COOH terminus of PrP^c (Kaneko *et al.*, 1997b).

1.9 The N-terminus of the prion protein

Numerous studies on the conformation of the mature recombinant prion protein revealed a properly folded globular structure only limited to the C-terminal domain of the protein, which also contains the glycosylation sites and the disulphide bond. In contrast, neither computer modelling techniques nor spectroscopic analysis provided evidence for a defined secondary structure of the N-terminal part of the PrP encompassing residues 23-120, which displays the properties of a random coiled peptide (Riek *et al.*, 1998; Donne *et al.*, 1997; Liemann and Glockshuber, 1998). However, since this segment has been seen to contain at least some of the binding sites for copper ions, a structured conformation might be acquired in vivo after the binding has occurred. Upon conversion of PrP^c into PrP^{Sc}, residues 23-89 can be digested with Proteinase K, whereas the rest of the molecule becomes PK resistant and retains the infectivity (Basler *et al.*, 1986; Meyer *et al.*, 1986). The N-terminus of PrP shows a general basic character especially in its N-proximal part with four lysines out of eight residues.

A comparative sequence analysis has evidenced a high conservation of the segment encompassing amino acids 23-50 in evolution, where differences between species mainly concern insertions and deletions (Wopfner *et al.*, 1999), suggesting a possible function of the N-terminus, besides the mentioned copper binding. The role of the N-terminal part and of the octapeptide repeats of the prion protein in the formation of PrP^{Sc} was examined in infected neuroblastoma cells. Elongation of PrP with extra octapeptides or deletion of amino acids 23-88 did not alter the synthesis of PrP^{Sc} (Rogers *et al.*, 1993). The relevance of the N-terminal part of PrP^c was also investigated in *in vivo* studies with mice expressing a transgene encoding various truncated PrP molecules (Flechsig *et al.*, 2000). In these studies, deletion of residues 23-93 allowed propagation of mouse scrapie in these mice, although with reduced levels of detectable PrP^{Sc} and altered pathology. These results are in line with *in vitro* cell-free conversion assays performed with hamster PrP^c, where the deletion of amino acids 32-94 reduced the amount of generated protease resistant PrP and showed an alteration in the ability of these deletion mutants to bind to PrP^{Sc} when compared to wild type PrP (wtPrP) (Lawson *et al.*, 2001). Other studies done with N-terminally truncated PrP have suggested that this region of the protein might stabilise the C-terminal domain of the molecule or modulate the

binding to auxiliary factors participating in the conversion into the pathogenic isoform (Zulianello *et al.*, 2000). On the other hand, extra copies of the octapeptide region are associated with familial CJD in humans (Owen *et al.*, 1992) and prion disease in transgenic mice (Chiesa *et al.*, 2000).

1.10 The *Xenopus laevis* prion protein

Recently, a sequence belonging to a portion of the *Xenopus laevis* prion protein was deposited in the EST Database (Washington University Xenopus EST project). Soon afterwards, the isolation and characterisation of the whole cDNA sequence of *X. laevis* PrP was reported (Strumbo *et al.*, 2001) together with the deduced amino acid sequence. This represents the first amphibian prion protein isolated and is, with its 216 residues, 15 to 20 % shorter than all other known PrPs. Comparison of sequences reveals about 28 % identity to mammalian and more than 44 % to avian and turtle prion protein. Preliminary analysis of the structural characteristics shows a 22 aa long signal peptide followed by a basic region (four lysines out of nine residues) similar to the N-proximal part of the mammalian PrP. The main differences, when compared to mammalian PrPs, is the absence of the octapeptide repeats whereas sequences immediately preceding and following this region show considerable conservation. At the C-terminus, the hallmarks of other PrPs are conserved: an intramolecular disulphide bond between two cysteines, two N-glycosylation sites, where the second one probably corresponds to an extra glycosylation site present in avian PrPs. The last 22-23 amino acids at the C-terminus might represent the signal peptide for the GPI-addition. A model for the three dimensional structure of the *Xenopus* PrP shows three α-helices at the C-terminal part, as seen in other species as well as an extra short helix downstream of the first one.

1.11 The subcellular trafficking of proteins

In the past years insight has been gained in the understanding of the trafficking of proteins to and from the plasma membrane. The transport machinery consists of small membranous vesicles. Newly synthesised proteins are cotranslationally transported into the endoplasmic reticulum (ER) where they are properly folded under direction of specific chaperones like BiP, Calnexin and Calreticulin, and carbohydrate side chains are added to glycoproteins (Matlack *et al.*, 1998). For GPI-proteins, the anchoring step resulting in the addition of the GPI moiety to the protein probably occurs in the lumen of the ER. Sorting from the endoplasmic reticulum (ER) is an important step in the biosynthetic pathway of secretory and membrane proteins. Misfolded or incompletely assembled proteins are subjected to ER

associated degradation (ERAD) by the cytoplasmic proteasome, whereas correctly folded proteins are incorporated into vesicles and directed to the Golgi stack. From here, sorting of proteins and lipids via several routes to different domains is achieved by the trans-Golgi network (TGN), which represents the principal sorting station for targeting of proteins to different localisations inside the cell. This organisation is particularly evident in polarised cells, where the plasma membrane is divided into functionally distinct domains: the apical and the basolateral domains in epithelial cells, the axonal and the dendritic membrane domains in neurons. For apical sorting, the sphingolipid- and cholesterol-rich rafts forming in the lumenal leaflet of the Golgi membranes work as microdomains for inclusion of proteins destined for the plasma membrane (Simons and Ikonen, 1997).

Sorting of proteins also characterises endocytosis. Many transmembrane receptors segregate into clathrin coated pits before internalisation and from here they are transported to sorting endosomes (SEs) and delivered to the recycling endocytic compartment (REC) (Mellman, 1996; Mukherjee *et al.*, 1997)or recycled to the plasma membrane (Hao and Maxfield, 2000). Certain proteins that recycle between the TGN and plasma membrane are delivered to the TGN via the endocytic pathway, involving the REC or the mannose-6-phosphate receptor pathway. Secretory and endocytic pathway are connected by sorting and separate packaging of lysosomal cargo in the Golgi and from the plasma membrane (Hunziker and Geuze, 1996; Mallet and Maxfield, 1999). The intracellular fate of GPI-proteins in the endocytic pathway is still a matter of debate but seems to be cell type dependent: in Chinese hamster ovary (CHO) cells, these proteins were found to be transported to the GPI-proteins enriched endosomal compartment (GEEC), probably a sub-compartment of early endosomes and then to pericentriolar recycling endosomes before returning to the plasma membrane (Mayor *et al.*, 1998). In baby hamster kidney cells (BHK) they were transported to early and then to late endosomes (Fivaz *et al.*, 2002). The common theme in these sorting processes is the recognition of targeting signals. Transmembrane proteins use sequence motifs in their cytoplasmic tails (for instance tyrosine or dileucine based motifs), which are recognised by specific sorter or adaptor proteins (Bonifacino and Dell'Angelica, 1999; Matter, 2000).

For proteins lacking cytoplasmic domains sorting to specific cellular destinations is not exclusively based on protein sequence: N- and O-linked glycosylations can act as sorting determinants (Scheiffele *et al.*, 1995). Lipid attachment (e.g. palmitoylation) can also serve as a targeting signal in cooperative protein-lipid affinities (Zhao *et al.*, 2000). In line with these results, several studies have shown that the GPI-anchor can act as a component in a targeting signal in polarised cells (Brown *et al.*, 1989; Lisanti *et al.*, 1989). Of note, for some proteins

the N-terminal stretch was reported to contain a plasma membrane localisation determinant (Lecat *et al.*, 2000).

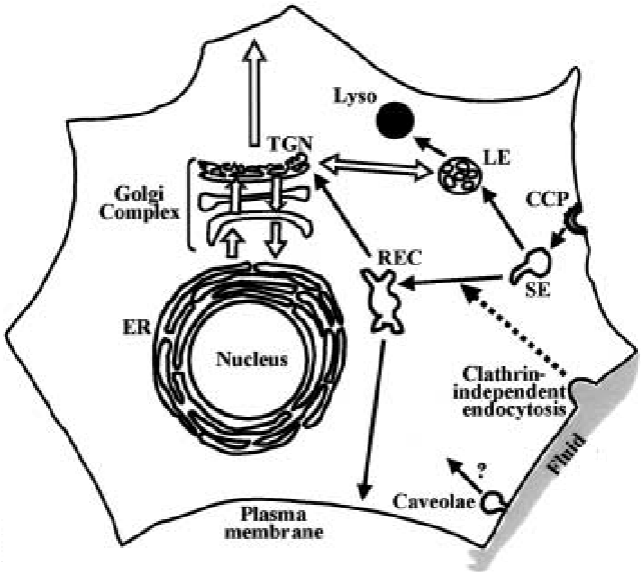

Figure 6: Sorting steps for the biosynthetic (thick open arrows) and endocytic (thin solid arrows) pathways.

LE: late endosomes; Lyso: lysosome; REC: recycling endocytic compartment; CCP: clathrin coated pits

1.11.1 Subcellular trafficking of the prion protein

Studies on the intracellular trafficking of the cellular prion protein have revealed that, following transport through the secretory pathway, the protein is present at the cell surface one hour after synthesis (Caughey *et al.*, 1989). Further work done with chicken PrP reported rapid endocytosis of PrP^c and cycling between the cell surface and endocytic compartments (Shyng *et al.*, 1993) before degradation in lysosomes with a half life of 3-6 hours (Caughey *et al.*, 1989; Borchelt *et al.*, 1990). Other studies on the endocytosis of PrP^c reported that its internalisation might be conditioned by metal ions binding to the octapeptide region (Sumudhu *et al.*, 2001).

Mutations and deletions characterising various forms of familial prion diseases often lead to misfolding and mistrafficking of PrP. Some of these mutants are partially retained in the ER and subjected to the quality control mechanisms of the cell and to degradation by the proteasome (Zanusso *et al.*, 1999; Stewart *et al.*, 2001). Studies done with PrP constructs lacking the GPI-anchor revealed slower transport through the secretory pathway when compared to wild type PrP^c ($wtPrP^c$) (Walmsley *et al.*, 2001), although conversion of these constructs into PrP^{Sc} was previously not found significantly compromised (Rogers *et al.*, 1993). Prevention of glycosylation affected the transport to the cell surface and changed the biochemical properties of PrP^c (Taraboulos *et al.*, 1990a; Lehmann and Harris, 1997). Addition of a transmembrane moiety to the C-terminus of PrP^c has been shown to affect

subcellular trafficking and to inhibit conversion into the scrapie isoform (Taraboulos *et al.*, 1995).

1.12 Aim of this work

This study aimes at devising a physiological function to the unstructured N-terminal part of PrP^c in subcellular trafficking. Expression of wild type mouse PrP, of specific N-terminally truncated mouse prion proteins and of one chimeric *Xenopus laevis*-mouse PrP construct in murine neuroblastoma cells allowed further characterisation of the intracellular trafficking and turn-over of the prion protein. Metabolic labelling techniques and surface-biotinylation assays were performed in order to follow the internalisation from the exofacial plasma membrane, the transport along the secretory pathway in a comparative analysis. These results provide deeper insight into the life-cycle of the cellular prion protein, raising the novel possibility of a targeting function of its N-proximal part by interacting with the secretory and the endocytic machinery. They also indicate the conservation of this targeting property in evolution.

Numerous attempts have been undertaken in animal and cell-culture models in order to interfere with conversion of PrP^c into infectious PrP^{Sc} (Aguzzi *et al.*, 2001). Several compounds analysed for their properties to interfere with this fundamental step in the propagation of prions seem to modulate the subcellular trafficking of PrP (Shyng *et al.*, 1995a; Gilch *et al.*, 2001). Characterisation of the cellular life-cycle of the prion protein and of the mechanisms underlying this process is therefore important in order to be able to optimise strategies leading to effective interference with prion propagation.

2 Material and methods

2.1 Antibodies

The following antibodies were used for detection of wtPrP^c and PrP mutants in immunoblot assay, immunoprecipitations or FACS analysis:

Primary antibodies

Name	Specificity	Origin	Company
3F4	3F4 epitope (residues 109-112 in human PrP)	Mouse monoclonal	Signet Pathology System, USA
A7	Prion protein	Rabbit polyclonal	Our laboratories

Secondary antibodies

Name	Specificity	Origin	Company
Peroxidase - labeled IgG	Anti-mouse	Sheep	Amersham Pharmacia, Freiburg
Peroxidase - labeled IgG	Anti-rabbit	Donkey	Amersham Pharmacia, Freiburg
Fluorescein - Isothyocianate (FITC)- linked IgG	Anti-mouse	Donkey	Dianova, Hamburg

2.2 DNA cloning

2.2.1 Polymerase chain reaction (PCR)

Oligonucleotides — Metabion (Germany)
MWG (Germany)

Deoxynucleotide	1 mM each dATP, dTTP, dGTP, dCTP (Amersham Pharmacia, Freiburg, Germany)
DNA polymerase	Taq Gold (Roche Diagnostic, Mannheim), Pfu Turbo (Stratagene, The Netherlands)
10x PCR reaction buffer	Roche Diagnostic, Mannheim; Stratagene, The Netherlands

Polymerase chain reaction procedure was used to amplify specific DNA sequences *in vitro*. A 50 µl reaction was set as follows:

DNA template	50-100 ng
5´ primer	2 µl (100 nM)
3´ primer	2 µl (100 nM)
dNTP-mix	50 µM
Polymerase	10 units
10 x polymerase reaction buffer	10 % volume
Aqua dest.	ad 50 µl

Reaction mix was set in 0.5 ml reaction tubes and was carried out in a PE 9600 Thermocycler (Perkin Elmer). The temperature for hybridisation of oligonucleotides with single strand parental DNA (Annealing) was generally set at 55° C. For more specific reactions the temperature was adjusted according to the following formula:

T_A (°C) = 60+ [(G+ C) x 41/ Nt] – (600/ Nt)

where T_A represents the annealing temperature, C+G the amount of guanine and cytosine in the primary sequence of the priming nucleotide and Nt the length (number of nucleotides) of the primers).

Amplification parameters:

95° C	5-10 min initial denaturation (once)
35 cycles with:	
95° C	1 min amplification
55° C (or required T)	1 min annealing temperature
72° C	1,5 min elongation
72° C	7 min final elongation (once)

Amplified DNA fragments were loaded on agarose gels for electrophoresis and purification.

PCR primers	**Sequence (5´-3´)**
PrP Bam HI 1 fwd	GCG GAT CCG TCG CCA CCA TGG CGA ACC TTG GCT A
PrP Eco RI 254 rev	ATC GAA TTC ATC ATC CCA CGA TCA GGA AGA
PrP Eco RI 91 fwd	GCG AAT TCG GAG GGG GTA CCC ATA ATC AG
PrP Eco RI 66 rev	GCG AAT TCT TGT CCC CAG CCA CCA CCG TG
PrP Pst I 22 rev	GCC TGC AGG CAG AGG CCA ACA TCA GTC C
PrP Pst I 90 fwd	CAC TGC AGC AAG GAG GGG GTA CCC ACA ATC
PrP Kpn I 48 fwd	AGC CCT GGA GGC AAC GGT ACC CAC CTC AGG GTG
PrP Kpn I 48 rev	CAC CCT GAG GTG GGT ACC GTT GCC TCC AGG GCT
PrP Pst I 51 fwd	CAC TGC AGG GTG GCA CCT GGG GGC AG
PrP Xba I 91 fwd	CGC TCT AGA GGA GGG GGT ACC CAT AAT CAG
Xen PrP Pst 23 fwd	CGC CTG CAG AAG AAG AGC GGT GGT GGG AAA
Xen PrP Xba I 69 rev	CGC TCT AGA CCT GTT ATA ACC GCT AGG ATT
Sequencing Primers	
PcDNA 3.1 +	CTA TAT AAG CAG AGC TCT C
PcDNA 3.1 -	TAG AAG GCA CAG TCG AGG
T7	TAA TAC GAC TCA CTA TAG GG
M13 fwd	GTA AAA CGA CGG CCA G
M13 rev	CAG GAA ACA GCT ATG AC
MHM2	GAA GCA TAT GGC AGG TGC T

2.2.2 Agarose gel electrophoresis

Agarose	Gibco/ BRL Life Lab., Paisley, Scotland
TAE- buffer	40 mM Tris-Acetate 1 mM EDTA, pH 8.0
5x loading buffer	50 % glycerol in TAE- buffer 0.05 % bromphenol blue
100 base pair DNA ladder	Gibco/ BRL Life Lab., Paisley, Scotland

Agarose gels (0.5 to 2 % depending on the length of the DNA fragment) were prepared by dissolving agarose in TAE-buffer by boiling the buffer in a microwave. After the solution had cooled to ca. 60° C, 1.5 µl ethidium bromide were added and the mixture was transferred into the appropriate gel chamber for solidification. The gel was then covered with TAE buffer and DNA samples to which the sample buffer had been added as well as 1,5 µl of the DNA ladder marker were loaded onto the gel. The gel was run under constant voltage (110V) in order to separate DNA fragments. After the electrophoresis, the ethidium-bromide-stained DNA was visualised under the UV-light and photographed with an “eagle eye” processor (Stratagene, The Netherlands).

2.2.3 Isolation and elution of DNA fragments from agarose gel

After electrophoresis separation, agarose gel fragments were excised from the gel with a scalpel and eluted to 20-50 µl in water using GFX^{TM} Purification Kit (Amersham Pharmacia, Freiburg, Germany) according to manufacturer ´ s procedures.

2.2.4 Enzymatic digestion of DNA

Restriction endonucleases	New England Biolabs, USA
10 x reaction buffer	New England Biolabs, USA

Restriction enzymes were used for DNA digestion applying the recommended buffers in a 20 or 40 µl final volume. 1-3 µg DNA were usually digested with at least 10 units of the required enzyme, either for 2 h or over night at 37° C.

2.2.5 DNA dephosphorylation

Treatment of digested DNA with alkaline phosphatase (calf intestinal phosphatase, CIP, NEB) which catalyses the removal of 5´ phosphate groups was carried out in order to prevent self-re-circularisation of the plasmide vector. The reaction was set by adding 0.1 units CIP/ pmol DNA and 1 X CIP buffer to the digested DNA. The reaction mixture was incubated at 37° C for 1 h.

2.2.6 Ligation

Vector and DNA fragments were ligated with a molecular ratio of 1:3 using either the T4-ligase (Gibco/ BRL Life Lab., Paisley, Scotland) or the DNA Quick Ligation Kit (Roche Diagnostic, Mannheim). For ligation with T4-ligase, the 10 x ligation buffer and 1 unit of the ligase were used in a total volume of 20 µl and the reaction mixture was incubated over night at 16 ° C. Ligation with the Quick Ligation Kit was carried out according to manufacturer´s procedures and the reaction was incubated at room temperature for 8-9 min.

2.2.7 DNA sequencing

10 x TBE buffer	0.9 M Tris
	0.9 M boric acid
	0.02 M EDTA

The reactions were set using the ABI PRISM^{TM} Taq DyeDeoxyTerminator Cycle Sequencing Kit (Perkin Elmer) according to manufacture´ s directions. 100 ng of isolated PCR fragments or 1µg of plasmid DNA were used for the reaction in a GeneAmP PCR 9600 thermal cycler (Perkin Elmer). The amplification was carried out as follows:

96° C 15´´
50° C 15´´
60° C 4´
25 cycles

The DNA was precipitated with 1/10 Vol. Na-Acetate (1.5 M, pH 5.2) and 2.5 Vol. EtOH (96 %) and was then centrifuged for 30 min at room temperature. The precipitate was washed with 70 % EtOH and centrifuged again for 10 min. The pellet was dried and dissolved in the appropriate buffer and run on an ABI 373 DNA-Sequencer (Perkin Elmer) and analysed with a specific software. Five % polyacrylamide sequencing gel was prepared as follows:

30 g urea
16 ml 30 % (w/ v) acrylamide/ bisacrylamide (37.5:1) (National Diagnostics, Atlanta, USA)
6 ml 10 TBE buffer
22 ml H_2O

2.2.8 Preparation of Heat Shock competent bacteria

SOC medium	2 % Trypton
	0.5 % Bacto yeast extract
	10 mM NaCl
	2.5 mM KCl
	10 mM $MgCl_2$
	10 mM $MgSO_4$
	20 mM glucose

200 ml LB medium were inoculated with one colony from an LB agar plate and transferred to a shaking incubator at 37° C until an OD_{600} of 0.6-0.7 was reached. The bacterial culture was placed on ice for 15 min. After centrifugation at 3000 g for 15 min at 4° C the pellet was first suspended in 50 ml ice cold 100 mM $MgCl_2$, placed on ice again for 30 min and then, after a new centrifugation step suspended in 50 ml cold 100 mM $CaCl_2$. and placed on ice for 30 min Bacteria were pelletted again and incubated overnight in 5 ml $CaCL_2$ at 4° C. 0.5 ml glycerol and 2.5 ml $CaCl_2$ were added and 100 µl aliquots were stored at –80° C.

2.2.9 Heat shock transformation

Heat shock competent *E. coli* (100 µl aliquot) were thawed on ice and up to 1 µg plasmid DNA or ligation mixture (max. 10 µl) were added and incubated on ice for 30 min. Bacterial cells were then warmed to 42° C for 90 sec and immediately chilled on ice for 2 min. 400 µl SOC medium was added and the bacteria were transferred to a shaking incubator set at 37° C to allow the bacteria to recover and to express the antibiotic resistance. After incubation for 30 min, the cultures were plated onto an LB agar plate with the appropriate selective antibiotic and incubated at 37° C overnight.

2.3 DNA extraction and purification

2.3.1 Small scale preparation of plasmid DNA from bacteria (Minipreparation)

Solution I	10 mM EDTA, 400 µg/ ml RNase I 100 mM Tris-HCl, pH 7.5
Solution II	1 M NaOH 5.3 % dodecyl sulfate sodium salt (SDS)
Solution III	Buffered solution containing acetate

For isolation of plasmid DNA from bacterial culture, the GFX Micro Plasmid Prep Kit (Amersham Pharmacia, Freiburg, Germany) was used according to manufacturer´ s directions. 1.5 ml of an overnight bacterial cell culture were pelletted in a microcentirfuge tube and suspended in an isotonic solution containing RNA (Solution I). Cells were then lysed by alkali treatment, chromosomal DNA and proteins were denatured with addition of solution II. The pH of the solution was neutralised with an acetate solution (Solution III) and cell debris, chromosomal DNA and proteins were precipitated. After centrifugation, the supernatant cell lysate was transferred to a GFX glass fiber matrix matrix column to bind plasmid DNA. The matrix bound DNA was washed with an ethanolic buffer to remove salts and other residual contamination. The DNA was eluted from the matrix in 100 µl sterile bidest. water. The total yield of DNA was between 1 and 5 µg.

2.3.2 Large scale preparation of plasmid DNA from bacteria (Maxipreparation)

Resuspension buffer (P1)	50 mM Tris/HCl, pH 8.0
	10 mM EDTA
	100 µg/ ml RNase A
Lysis buffer (P2)	2 mM NaOH, 1% SDS (w/v)
Neutralisation buffer	3.0 M potassium acetate, pH 5.5
Equilibration buffer (QBT)	750 mM NaCl
	50 mM MOPS
	15 % (v/ v) EtOH
	0.15 % (w/ v) Triton X-100
Wash buffer (QC)	1 M NaCl
	50 mM MOPS
	15 % (v/v) EtOH
	pH 7
Elution Buffer (QF)	50 mM Tris/ HCl, pH 8.5
	1.25 M NaCl
	15 % (v/ v) EtOH

For purification of up to 500 µg plasmid DNA from bacterial culture, 2 ml of an overnight clone culture were diluted into 100 ml selective LB medium and were grown overnight at 37° C. After pelletting the cells at 4000 g and 4° C for 15 min, the commercially available Quiagen Maxi Purification Kit was applied according to manufacture´s direction. The protocol is based on an alkaline lysis procedure, followed by binding of plasmid DNA to an anion exchange resin columns under low salt condition. The DNA was eluted, concentrated and desalted by isopropanol precipitation. The pellet was dissolved in sterile H_2O dest.

2.3.3 Spectrophotometric determination of amount of DNA

DNA was diluted 1:20 in H_2O and its concentration was measured in a spectrophotometer (Beckmann). DNA shows a maximum absorbation at 260 nm which allows calculation of DNA concentration. The reading was also taken at a wavelength of 280 nm since the ratio between these two values (OD_{260}/ OD_{280}) provides an estimation of purity of the nucleic acid.

For pure preparation of DNA this value should be 1.8.Values higher than 1.8 indicate contamination with proteins.

2.4 Culture of bacterial cells

2.4.1 Bacterial cells used in this work

For amplification of plasmids *E. coli* bacterial strains XL1, Top 10 or DH5α were used.

2.4.2 Growing of bacterial cells

LB medium/agar	
bacto trypton	10 g
bacto yeast extract	5 g
NaCl	10 g
bacto agar	15 g
ad 1 l with aq. dest.	
ampicillin	500 µg/ ml
(Sigma, Munich)	
kanamycin monosulfate	500 µg/ ml
(Sigma, Munich)	

For isolation of single colonies bacterial suspensions were plated on a Petri dish with solid LB-medium containing the appropriate antibiotic. Single bacterial colonies were grown in autoclaved LB-medium after addition of the adequate antibiotic to the medium for selection. Growing of bacteria was achieved by growing cultures overnight (at least 8 hours) at 37° C in a shaking incubator until an OD_{600} between 0.6 and 0.8 was reached. LB- solid and liquid medium share the same ingredients, the difference being the addition of 15 g/l Agar for the solid medium.

2.4.3 Determination of cell density

The number of cells in the growing culture was monitored by measurement of the optical density at a wavelength of 600 nm in 1.5 ml plastic cuvettes, culture medium was used as a control.

2.4.4 Storage of bacteria

For storage of bacteria, 1 ml aliquots from a liquid culture (OD_{600} ca.0.8) were added to 400 µl glycerol and preserved in 1.5 ml storage tubes equipped with screw caps and stored at –80° C.

2.5 Working with mammalian cells

2.5.1 Mammalian cell lines used in this work

N2a (ATCC CCL 131) murine neuroblastoma (Butler *et al.*, 1988)

2.5.2 Culture media

DMEM, Dulbecco´s modified Eagle medium (Gibco/ BRL Life Lab., Paisley, Scotland) supplemented with	2 mM L-glutamin 100 IU/ml penicillin 0.1 mg/ ml streptomycin 10 % (v/v) fetal calf serum (FCS) (inactivated at 56° C for 30 min)
Optimem (Gibco/ BRL Life Lab., Paisley, Scotland)	100 IU/ml penicillin 0.1 mg/ ml streptomycin 10 % (v/v) fetal calf serum (FCS) (PAA, Marburg) (inactivated at 56° C for 30 min)

Trypsin-EDTA
(Gibco/ BRL Life Lab., Paisley, Scotland) 0.25 % trypsin, 1 mM EDTA- 4Na
Phosphate buffered saline (PBS)
(Gibco/ BRL Life Lab., Paisley, Scotland)

2.5.3 Culture of mammalian cells

Cells were cultivated on appropriate culture dishes (NUNC) and kept in an incubator in a 5 % CO_2, 90 % humidity atmosphere at 37° C. Medium was changed every two days. When 80 % confluency was reached, cells were washed with PBS, briefly treated with 1 ml trypsin-EDTA in order to remove cells from the dish. Cells were then suspended in culture medium and transferred to a new culture dish in a 1:10-1:20 volume ratio, unless otherwise specified.

2.5.4 Storage of eukaryotic cells

Dimethyl sulfoxide (DMSO) Sigma, Munich

For storage of mammalian cells, 75-80 % confluent adherent cultures were subjected to mild treatment with trypsin and suspended in culture medium with addition of 20 % total FCS and 10 % DMSO. 1 ml aliquots of the suspension were transferred to 1.5 ml cryotubes (NUNC) and frozen to –80° C for 24 h. Tubes were then transferred to liquid nitrogen for long-term storage. Thawing was achieved by incubating frozen cells at 37° C for 10-15 min. Cells were resuspended in 10 ml culture medium with 10 % FCS and centrifuged for 10 min at 1000 g in order to remove toxic DMSO. The supernatant was removed and the pellet resuspended in 10 medium and plated on culture dish.

2.5.5 Transient transfection of mammalian cells

Transfection with Superfect (Qiagen, Hilden)
Activated dendrimeric polyamides function as carriers for introduction of plasmid DNA into the mammalian cell membrane. On day of transfection cells were 50 % confluent. The Superfect tranfection reagent was added to the cells according to manufacturer ´ s directions, medium was changed after 4 h and cells were lysed after 72 h for analysis.

Transfection with Effectene (Qiagen, Hilden)

Effectene is a non-liposomal transfection reagent coating DNA into micelle structures which are then transferred into eukaryotic cells. 40- 80% confluent cells. Generally, 2 µg DNA were used to transfect 50-60 % confluent cells following the recommended protocol. DNA is first condensed by interaction with an enhancer, Effectene reagent is then added to produce a complex with the DNA which is mixed with the medium and then added to the cells.

Transfection with Fugene 6 (Roche Diagnostic, Mannheim)

Fugene 6 transfection reagent is a blend of lipids and other components supplied in 80 % ethanol. Standard transfection was performed by dissolving 2 µg DNA in serum-free medium. Transfection reagent was then added and the mix was incubated at room temperature for 15 min before adding to the cells.

2.6 Internalisation assay with cell surface biotinylation

Sulfo-biotin-X-NHS (Pierce)	250 µ/ml
Lysis buffer	100 mM NaCl 10 mM Tris-HCl, pH 7.5 10 mM EDTA 0.5 % Triton X-100 0.5 % DOC

Endocytosis of wtPrP^c and PrP mutants located on the cell surface was assessed by surface biotinylation. N2a cells were plated on 6 cm Petri dishes and transiently transfected. After 72 h, cells were placed on ice, washed twice with cold PBS and incubated on ice for 15 min with 1 ml PBS containing 250 µg sulfo-biotin-X-NHS. Cells were then washed again 3 times with cold PBS to remove unbound biotin and were either harvested directly with 1 ml cold lysis buffer on ice for 10 min or cultured for appropriate chase times as indicated for each experiment in the presence of complete medium at 37 °C to allow internalisation. Cells were then washed with PBS and either lysed directly or treated with 1 ml Trypsin-EDTA on ice for 10 min before lysis and immunoprecipitated as described above, using mAb 3F4 for detection of transfected constructs. Immunoadsorbed proteins were finally subjected to 12.5% SDS-PAGE and transferred to PVDF membranes (Amersham Pharmacia, Freiburg, Germany) for

electrophoresis. After blotting and blocking of unspecific binding sites in skim milk buffer, the membrane was incubated with 1:5000 horseradish peroxidase-conjugated streptavidin in TBST for 1 h at room temperature and visualised with enhanced ECL plus chemoluminescence kit (Amersham Pharmacia, Freiburg, Germany).

2.7 Metabolic labelling and radio-immunoprecipitation

Cys/ Meth-free medium	RPMI without cysteine or methionine (Gibco/ BRL Life Lab., Paisley, Scotland) with 1% FCS
[^{35}S]- cysteine and methionine Promix	L-[^{35}S]- in vitro Cell labelling mix 1000 Ci/mmol (Amersham Pharmacia, Freiburg)
Chase medium	complete culture medium with 10 % FCS
Lysis buffer	100 mM NaCl 10 mM Tris-HCl, pH 7.5 10 mM EDTA 0.5 % Triton X-100 0.5 % DOC
RIPA buffer-SDS	0.5 % Triton X-100 0.5 % DOC 1% SDS in PBS
Protein A- sepharose	50 % suspension in RIPA buffer-SDS (Amersham Pharmacia, Freiburg)

Pefabloc protease inhibitor	1 % stock solution (Roche Diagnostic, Mannheim)

For immunoprecipitation transiently transfected N2a cells (6 cm Petri dishes) with 80-90 % confluency were used. Cells were washed twice with phosphate-buffered saline (PBS) and placed into an incubator at 37° C for 1 h in the presence of 1 ml RPMI medium without methionine/cysteine containing 1% FCS to promote metabolism of endogenous methionine and cysteine. Subsequent radioactive labelling of proteins was carried out by adding 400 µCi/ml [^{35}S]-Met/Cys to the medium for 5 min or, for half-life studies, for 1 h, respectively, at 37° C (pulse). After incubation, cells were washed twice in cold PBS and harvested with 1 ml lysis buffer on ice for 10 min or further incubated at 37 °C for different lengths of time in 5 ml complete culture medium to allow transport to the cell surface (chase). After appropriate chase times, cells were washed with PBS and either directly harvested or subjected to mild trypsin digestion. 1 ml Trypsin-EDTA was added to the dishes for 10 min on ice. Trypsinised cells were transferred to 15 ml poly-propylene tubes and the reaction was stopped by centrifugation of the cells twice at 900 x g in PBS containig 20% FCS and 100 µl Trypsin inhibitor. After lysis, cell lysates were transferred to 1.5 ml tubes and debris was removed by centrifugation for 40 sec at 18000 g. After addition of 1% N-lauryl sarcosine, postnuclear lysates were boiled at 95 °C for 10 min. Samples were placed on ice and 20 µl Pefabloc protease inhibitor were added; lysates were then incubated with antibody A7 or 3F4, as indicated, overnight at 4 °C (dilution 1:300). The protein-antibody complexes were precipitated by addition of 100 µl protein A-Sepharose beads for 90 min at 4 °C. The beads were then centrifuged at 18000 g for 1 min and washed in RIPA buffer supplemented with 1 % SDS at 4 °C. The washing procedure was repeated five times. All samples were treated with 0.1 units/µl PNGase F at 37 °C overnight to remove N-linked oligosaccharides and analysed by 12.5 % SDS-PAGE after elution with 4x sample buffer and boiling for 10 min at 95° C. SDS- ploy acrylamide gels containing proteins radiolabelled with ^{35}S-labelled amino acids were subsequently fixed in blotting buffer for 15 min before placing on Whatman paper and fitting on a gel for 2 h at 80° C. Dried gel was then placed in a light-tight X-ray holder and covered with a sheet of X-ray film (Kodak biomax MR). The film holder was stored at – 80 °C for the appropriate length of time and then developed with an automatic film processor.

2.7.1 Trypsin digestion

Trypsin-EDTA	(Gibco/ BRL Life Lab., Paisley, Scotland)
Trypsin inhibitor	stock solution 50 mg/ ml (Sigma, Munich)

In order to separate intracellular from surface located proteins, 1 ml Trypsin-EDTA was added on the cultured cells before lysis for 10 min on ice. Trypsinised cells were transferred to 15 ml poly-propylene tubes and the reaction was stopped by centrifugation of the cells twice at 900 x g in 5 ml PBS containing 20% FCS and 100 µl Trypsin inhibitor. Centrifuged cells were then resuspended in 1 ml lysis buffer for lysis on ice.

2.7.2 Treatment with Endoglycosidase-H (Endo-H)

β-Mercaptoethanol/SDS for Endo-H	0.1 M β-Mercaptoethanol 0.1 % (w/v) SDS
Endo-H buffer	0.1 M Na-citrate pH 5.5 0.5 % PMSF (protease inhibitor) 6 mU Endo-H (Roche Diagnostic, Mannheim)

For Endo-H digestion of glycoproteins, immunoprecipitated proteins were incubated with 50 µl 0.1 M 2-mercaptoethanol/ 0.1% SDS and heated at 95 °C for 10 min. Samples were then centrifuged at 18000 g for 2 min and supernatants were divided into two halves: one aliquot was supplemented with 25 µl Endo-H buffer containing 10 mU Endo-H, the other half was incubated with buffer without Endo-H. All samples were stored overnight at 37 °C, then subjected to SDS-PAGE after addition of 4x sample buffer.

2.7.3 Digestion with N-Glycosidase F (PNGase F)

Et-SH/ SDS	0.1 M Mercaptoethanol

	0.5 % SDS
PNGase F buffer (1 sample)	20 µl lysis buffer (post-nuclear) 2.5 µl Pefabloc (1 %) 2.5 units PNGase F (Roche Diagnostic, Mannheim)

PNGase F treatment was carried out by re-suspending immunoprecipitated proteins in 20 µl Et-SH/ SDS and heating at 95 °C for 10 min. Supernatants were incubated with 25 µl PNGase F buffer overnight at 37 °C prior to analysis on SDS-PAGE. For Western blot, 200 µl post-nuclear lysates were boiled in the presence of Et-SH/SDS, then 10 µl Pefabloc (1 %) and 5 units PNGase F were added end the reaction mixture was incubated overnight at 37° C. Samples were precipitated with methanol and prepared for SDS-PAGE as described below.

2.8 Preparation of postnuclear lysates

Lysis buffer	100 mM NaCl 10 mM Tris-HCl, pH 7.5 10 mM EDTA 0.5 % Triton X-100 0.5 % DOC
TNE	50mM Tris/HCl pH 7.5 150 mM NaCl 5 mM EDTA
4 x SDS sample buffer	7 % SDS 30 % glycerol 20 % β-mercaptoethanol 0.01 % bromphenol blue 90 mM tris/ HCl pH 6.8
Pefabloc SC (AEBSF)	1 % stock solution (Roche Diagnostic, Mannheim)

Adherent cells were washed once with PBS and were subsequently covered with 1 ml lysis buffer at room temperature for 10 min. Total lysates were transferred to 1.5 ml reaction tubes for separation of cell debris by centrifugation for 40 sec at 14.000 rpm. 20 µl of the 1 % Pefabloc stock solution were added to the supernatants before precipitation with 10 vol. methanol overnight at –20° C or -80° C for 2 h. Samples were then centrifuged at 3500 rpm for 30 min at 4° C and the resulting pellet was resuspended in 50-100 µl TNE and 4x SDS-sample buffer was added. Samples were heated o 95° C for 10 min and placed on ice.

2.8.1 Detergent solubility assay

N-lauroyl sarcosine	10 % stock solution (Sigma, Munich)

Post-nuclear cell lysates were supplemented with 0.5 mM Pefabloc protease inhibitor and N-lauryl sarcosine to 1 %, and centrifuged for 1 h at 100 000 g and 4 °C in a Beckman TL-100 centrifuge. Soluble fractions (supernatant) were precipitated with ethanol as described above. Insoluble fractions (pellet) were resuspended in 50 µl TNE. Ethanol precipitated samples were centrifuged for 30 min at 3500 g, the pellets redissolved in TNE buffer with addition of SDS-loading buffer. Samples were analysed on 12.5 % SDS-PAGE.

2.8.2 Proteinase K (PK) digestion

Proteinase K (PK)	1 mg /ml stock solution (Merck, Darmstadt)

Aliquots of post-nuclear lysates were incubated for 30 min at 37 °C with 20 µg/ml PK; the digestion was stopped by addition of protease inhibitor Pefabloc. Samples were precipitated with ethanol and analysed in immunoblot assay.

2.8.3 SDS-PAGE

4 x Resolving solution	1.5 M Tris 0.4 % SDS

	pH ad 8.8
4 x Stacking solution	0.5 M Tris 0.4 % SDS pH ad 6.8
Ammoniumpersulfate(APS)	10% (w/ v) stock solution
N,N,N,N-tetramethylethylendiamin (TEMED)	Pharmacia/ LKB, Upplasa, Sweden
Resolving gel (12.5 % acrylamide)	25.9 ml 30 % (w/ v) acrylamide/ bisacrylamide (37.5:1) Protogel (National Diagnostics, Atlanta, USA) 15.4 ml resolving solution 20.3 ml aqua dest. 90 µl TEMED 192 µl 10% (w/ v) ammoniumpersulfate (APS) in H_2O
Stacking gel (5 % acrylamide)	2.8 ml 30 % (w/ v) acrylamide/bisacrylamide (37.5:1) 4.2 ml stacking solution 9.9 ml aqua dest. 30 µl TEMED 168 µl 10% (w/ v) APS
10 x SDS electrophoresis buffer	250 mM tris 2.5 M glycine 1 % SDS

Electrophoresis separation of proteins was carried out on denaturing SDS gels containig 12.5 % acrylamide (Laemmli, 1970). After polymerisation was completed, the glass plates containing stacking and resolving gels were mounted in an electrophoresis chamber and

covered with electrophoresis buffer. Samples were loaded on the gel (15-25 µl). Constant voltage (27 or 45 depending on the size of the gel) was applied for mass separation until the proteins had reached the bottom of the resolving gel.

2.8.4 Western blot

Blotting buffer	20 % methanol 3 g Tris 14.5 g glycine
10 x TBST	0. 5 % tween 20 100 mM NaCl 10 mM Tris/ HCl pH 7.4
Skim milk buffer	5 % (2.5 g) skim milk powder (Merk, Darmstadt) in TBST buffer (ad 50 ml)
PVDF membrane	Amersham Pharmacia Freiburg, Germany
Semi-Dry transblot machine	Bio-Rad, Richmond, USA
Detection kit	ECL^{PLUS} Western Blot Detection kit Amersham Pharmacia, Freiburg, Germany
X-ray films	Kodak Biomax XS

After electrophoretic mass separation, proteins were electro-transferred from polyacrylamyde gels onto a Hybond-P:PVDF membrane using a semi-dry-methode. The membrane was activated with mehanol and then equilibrated with dest. water. Gel was palced in contact with the membrane. They were then sandwiched together between 6 layers of Whatman paper which had been soaked in Blotting Buffer. A Semi-Dry Transblot electrophoresis apparatus was used for the transfer, a current of 2 A was applied for 30 min or 45 min (depending on the

size of the gel). The membrane was then incubated in 5% skim milk buffer for 30 min at room temperature for saturation of unspecific binding sites and then in TBST with the specific primary antibody and shaken overnight at 4° C. The membrane was washed 5 times (5 min each) with TBST and the secondary antibody (peroxidase conjugated) was subsequently added to TBST at a dilution of 1:7500 for 30 min. The membrane was washed again 3 times with TBST, finally with dest. water. The antibody-
protein complex was visualised with an enhanced chemoluminescence ECL-plus kit by incubating the membrane for 2 min in the ECL-solution (solution 1:solutioin 2: 1:40), drying it with Whatman paper and exposing it to X-ray films.

2.9 Detection and evaluation of radioactive signals

The autoradiographic signals were quantified by Phosphor Imager analysis of the gel (Molecular Dynamics). The amount of total or intracellular (after surface trypsin digestion) PrP present at each time point after the chase was expressed as percentage of nascent PrP rescued from the cell lysate directly at the end of the labelling period.

2.10 Detection and evaluation of non-radioactive signals (densitometric analysis)

Films were digitised using an APB Image Scanner and images quantified using Image Master 1D software (both Amersham Pharmacia Biotech).

2.11 Treatment of cells with lysosomal inhibitor Leupeptin

Leupeptin	1 mg/ ml stock solution (Roche Diagnostic, Mannheim)

For inhibition of lysosomal degradation the serine and thiol protease inhibitor leupeptin was added to cultured cells for 24 h. The inhibitor was dissolved in aqua dest. and added to culture medium at a concentration of 100 µM. Cells were subsequently lysed and subjected to immunoprecipitation as described above. The polyclonal antibody A7 was used for probing of wtPrP and PrPΔ(23-90).

2.12 Fluorescence Activated Cell Sorting (FACS) analysis

2.12.1 Cell surface analysis

FACS buffer	2.5 % fetal calf serum (FCS) 0.05 % Na- Acide in PBS
Propidium Iodide	0,02 % FACS buffer
EDTA	1 mM in PBS

For measuring of the cell surface expression of transiently transfected PrP constructs, N2a cells were detached from culture dish with 4 ml 1 mM EDTA after reaching 70-80 % confluence . About $1x10^5$ cells were transferred to FACS-Polystyrene round bottom tubes and pelleted by centrifugation at 1200 rpm for 5 min. Cells were resuspended in 500 µl FACS buffer and placed in ice for 5 min. The tubes were then centrifuged again for 2 min and cells were incubated with the primary antibody (3F4, 1:100 in FACS buffer) and placed on ice for 45 min. Cells were washed with 1 ml FACS buffer and centrifuged for 2 min. The wash-step was repeated for 3 times. For detection of 3F4-bound proteins, cells were resuspended in 100 µl buffer containing the Fluorescein-Isothiocyanate (FITC)-conjugated secondary antibody (goat anti mouse) and placed on ice for 30-45 min. cells were washed again for 3 times. After the third wash 500µl propidium-jodide were added for staining of dead cells. Flow cytometry was then performed on a FACS (fluorescence activated cell sorter) Calibur (Becton and Dickinson) equipped with a 488 nm emitting argon laser. Forward and side scatters were collected as linear signals and all fluorescent emissions on a logarithmic scale. A gate based on FSC and SSC was set to separate living and dead cells and ten thousand events were acquired inside the gate using Cell Quest software (Becton and Dickinson).
Throughout the analysis, cells incubated only with the second antibody were used as a negative control and the resulting fluorescence signals subtracted from the values obtained using both antisera.

2.12.2 Intracellular analysis

Saponin buffer	0.1 % Saponin in FACS buffer
Ammonium-Chloride/Glycine	50 mM/ 20 mM
Formalin (37 % formaldehyde)	10 %
	(Merck, Darmstadt)

70-80 % confluent cells were detached from culture dish with 4 ml 1mM EDTA in PBS. 1-2 ml of the suspension (100.000 cells) were transferred to FACS-Polystyrene round bottom tubes and pelleted by centrifugation at 1200 rpm for 5 min. Cells were resuspended in 200 µl 10% formalin at room temperature for fixation. Tubes were then centrifuged for 2 min in 1.5 ml PBS and the reaction was quenched with 200 µl ammonium-chloride/ glycine for 10 min at room temperature. Cells were washed once with 500 µl saponin buffer, resuspended in primary antibody (100 µl, concentration 1:100 in saponin buffer) and incubated on ice for 45 min. Cells were washed with 1 ml saponin buffer and centrifuged for 2 min. The wash-step was repeated for 3 times, they were then resuspended in 100 µl buffer with the FITC-conjugated secondary antibody and placed on ice for 30-45 min. Cells were washed again for 3 times and flow cytometry was performed as described above.

3 Results

Detailed studies performed with the sulphated bis-hexasulphonated compound Suramin have revealed strong reduction of the detectable PrP^{Sc} level in prion infected cells and a significant delay of onset of the disease in peripherally inoculated mice, when the drug was applied at the time of infection (Gilch *et al.*, 2001). The compound is known to down- regulate the cell surface expression of certain proteins and to interfere with their oligomerisation state (Stein *et al.*, 1995). Suramin was seen to modulate the folding of PrP^{c} inducing aggregation of fully matured molecules. Aggregates of misfolded full length PrP^{c} were subjected to the quality control mechanisms of the cell and were transported directly from the trans-Golgi network (TGN) to late endocytic compartments for degradation therefore by-passing the site of PrP^{Sc} conversion. Further analysis evidenced an important role of the pre-octapeptide segment located in the N-terminal part of the protein (residues 23-50) in the modulation of these effects and in the activation of the quality control mechanisms for recognition of misfolded proteins (Gilch, Nunziante and Schätzl, personal communications). Other compounds have been seen to influence the trafficking of PrP^{c}. Pentosan sulphate and related compounds dramatically reduced the amount of PrP^{Sc} by stimulating endocytosis thereby causing a redistribution of PrP^{c} from the plasma membrane to late endosomes and lysosomes (Shyng *et al.*, 1995). Since the N-terminal sequence of mammalian PrP^{c} is rich in basic amino acids and each contain a consensus site for heparin binding (XXBXBX, where B is a basic amino acid and X another residue) (Cardin and Weintraub, 1989), the same sites have been hypothesised to mediate the binding to other sulphated compounds. The suggested function of PrP^{c} as a chelator of extracellular ions or as a carrier for uptake and delivery of copper ions to intracellular targets (Pauly and Harris, 1998) has been linked to the binding sites for copper ions identified in the N-terminal histidine-rich octarepeats. In studies done with neuronal cells, a rapid endocytosis of PrP^{c} upon exposure to physiologically relevant concentrations of Cu^{2+} or Zn^{2+} has been reported. Here, deletions of the octapeptide repeats or mutation of histidine residues in the central two repeats abolished endocytosis (Sumudhu *et al.*, 2001).

The natural trafficking of the cellular prion protein has been characterised to some extend. The molecule is localised on the cell surface within one hour after synthesis (Caughey *et al.*, 1989). The chicken PrP^{c}, which shares a sequence identity of 33 % with the homologous mammalian protein, had been previously reported to constitutively cycle between the cell surface and endocytic compartments via clathrin coated pits (Shyng *et al.*, 1993). The full length molecule was internalised with a $T_{½}$ of 20 minutes and then returned to the cell surface

at a similar rate. Later reports however, evidenced that PrP^c re-enters the cell via caveolae-like domains or cholesterol- and glycosphingolipid-rich rafts (Vey *et al.*, 1996; Taraboulos *et al.*, 1995), where PrP^c undergoes an initial proteolytic cleavage to produce an N-terminally truncated protein designated PrP-II (Haraguchi *et al.*, 1989; Pan *et al.*, 1992).

The following work was carried out with the purpose to further characterise the transport kinetics of the cellular isoform of the prion protein along the secretory and endocytic pathway and to devise a function of the N-terminal amino acid sequence in this subcellular trafficking.

3.1 Biochemical characterisation of PrP^c constructs showing progressive N-terminal deletions

For the determination of the relevance of the N-terminal part of the prion protein on its subcellular processing, several constructs, each of them characterised by a different deletion in its N-proximal amino acid sequence were designed and cloned by standard cloning methods (**Fig. 7**). The PCR technique was utilised to introduce restriction sites into distinct mouse PrP DNA sequences, which were amplified and cloned into the mammalian vector pcDNA3.1. Since neuroblastoma cell endogenously express wild type PrP^c ($wtPrP^c$), an epitope was introduced into the transfected constructs which is recognised by the murine monoclonal antibody 3F4. This epitope corresponds to the human and hamster sequence 109-112 (when referred to the human sequence) and is not contained in the mouse PrP. All constructs were named referring to the human PrP sequence.

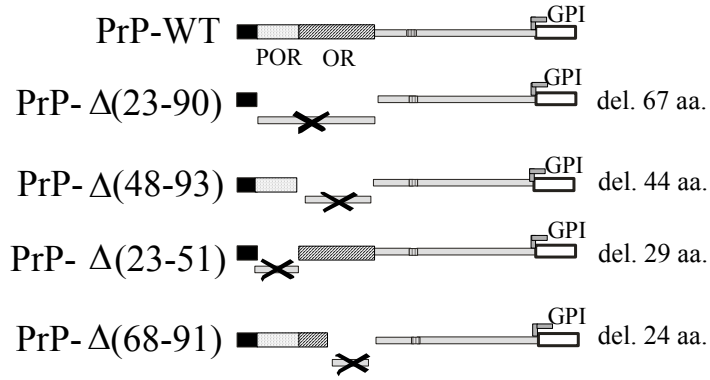

Figure 7. Schematic representation of examined PrP constructs

Wild type PrP and PrP deletion constructs used in this study were derived from murine PrP^c, and all contain the 3F4 epitope (amino acides 109-112, vertical bars), which allows detection by the monoclonal antibody 3F4. Numeration refers to the human PrP sequence. Black and open bars represent signal peptide and GPI-anchor, respectively, hatched bars the octapeptide repeats (51-90), dotted bars amino acids preceding the octapeptide region (23-50).

These constructs were then transiently transfected into the murine neuroblastoma cells N2a. All the experiments were carried out 72 hours after transfection, in order to allow significant expression of the constructs by the cells. Where necessary, the use of the antibody 3F4 allowed discrimination between endogenous and transfected prion proteins. All experiments with the deletion constructs described in this study were performed in parallel with transfected wtPrP^{c}, in order to rule out possible effects on the kinetics of the proteins due to overexpression or to metabolic stress upon the transfection. The deletion mutants were first characterised biochemically, and their properties compared to those of wtPrP^{c}, in order to assess whether truncation of residues within the N-terminal segments affected their folding and glycosylation patterns. N2a cells transfected with wtPrP^{c} or with the mutated proteins were lysed and then subjected to a solubility assay, which involves ultracentrifugation at 100,000 g for 1 hour in the presence of N-lauryl sarcosine for separation of the soluble from the detergent-insoluble fraction. Immediately after centrifugation, the supernatant was divided into two equal fractions and one of them subjected to digestion with Proteinase K (PK). These two assays are often applied for separation or differentiation of PrP^{c} (soluble in detergents and PK sensitive) from PrP^{Sc} (insoluble and partially PK-resistant). These features of PrP^{Sc} are related to its misfolded and aggregated conformation and can therefore give information about the folding of proteins, e.g. of the transfected constructs used in this study. The centrifuged pellets and the supernatants (+ and – PK) were then subjected to SDS-PAGE and analysed in a Western Blot, using the antibody 3F4. All were mainly detected in the soluble fraction and were found to be PK-sensitive, as was expected for wtPrP^{c} (**Fig. 8A**). It was therefore concluded that truncations within their N-terminal amino acid sequence did not significantly affect the solubility and PK-resistance of these proteins and therefore their conformation. On a polyacrylamide gel, wtPrP^{c} migrated with its characteristic glycosylation pattern: un-, mono-, and diglycosylated bands were detected at 25, 28 and 33 kDa, respectively (**Fig. 8A**, lane 2). To verify that the other constructs were also properly glycosylated, aliquots of the lysates were subjected to an N-glycosidase F (PNGase F) digestion (**Fig. 8B**). This glycosidase cleaves NH_2-glycans from their protein attachment sites, a glycosylated protein therefore migrates, upon treatment, in its unglycosylated form on an SDS-PAGE gel. For all deletion constructs, only one single band, corresponding to the unglycosylated form, was detected upon digestion with PNGase F. These results confirmed the N-glycosylation of the analysed proteins.

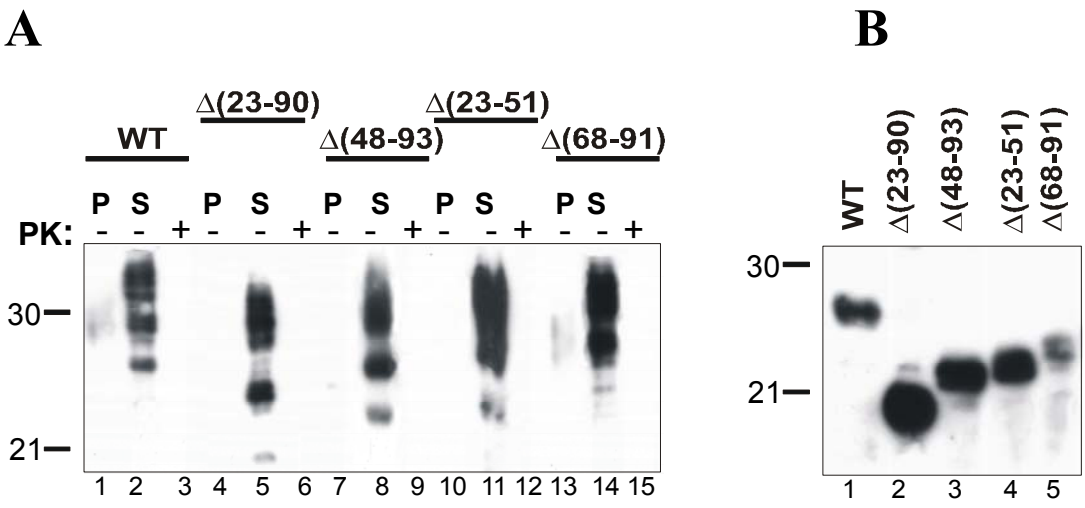

Figure 8. Biochemical properties of wtPrP^c and PrP deletion mutants

(A) For comparison of the biochemical behaviour of the different mutants used in this study with that of wtPrP^c, postnuclear lysates of N2a cells transiently transfected with wtPrP^c or with the described PrP deletion constructs were divided into two aliquots. One was subjected to a solubility assay, the other one was treated with 20 µg/ml proteinase K (PK). The detergent- insoluble pellets (lanes 1, 4, 7, 10, 13), the supernatants (lanes 2, 5, 8, 11, 14) and the PK-treated fractions (lanes 3, 6, 9, 12, 15) were all analysed by immunoblotting using the monoclonal antibody 3F4. All constructs were soluble in detergents and sensitive to PK treatment.
(B) Fractions (200 µl) of postnuclear lysates described in (A) were treated overnight with PNGase F for deglycosylation of the proteins and then subjected to immunoblotting with the antibody 3F4. All proteins migrated as single, unglycosylated bands. Molecular size markers are shown in kDa on the left.

3.2 Effect of progressive N-terminal deletion on the internalisation of murine PrP^c

The first step in the characterisation of the subcellular trafficking of the prion protein was the analysis of its endocytosis. For this purpose, internalisation of wtPrP^c was first compared to that of three constructs presenting deletions of different length in their N-terminal part: PrPΔ(23-51) lacked the 29 amino acids between the signal peptide and the octapeptide repeats, in PrPΔ(48-93) a segment of 44 residues encompassing the octapeptides was deleted, and in PrPΔ(23-90) the complete N-terminus (67 residues after the signal peptide, therefore comprising octapeptide repeats and the region preceding them) were missing. N2a cells transiently expressing these proteins were incubated on ice with PBS containing sulfo-NHS-biotin (pulse). This small molecule is membrane-impermeable and only binds to free amino groups of proteins localised at the outer leaflet of the plasma membrane. The low temperature inhibited further transport of proteins to and from the cell surface, so that only a defined population was labelled. The cells were then either lysed immediately after the labelling or were placed into an incubator at 37 °C for the described time periods to allow internalisation

of the labelled proteins (chase). Subsequent treatment of the cells with trypsin on ice which digests surface-located proteins, allowed discrimination of proteins that had been internalised during the chase from those still localised at the plasma membrane. All cells were then lysed and the wtPrP^c and the mutants were immunoprecipitated with the antibody 3F4. After SDS-PAGE, biotin-conjugated PrPs were detected by incubation with streptavidin, which binds with high affinity to biotin. Since all constructs could be detected upon labelling with biotin immediately before the chase, it was deduced that they were all localised on the cell surface. (**Fig. 9A**, lanes 1, 8, 14 and 18). Additionally, specific PrP signals disappeared upon mild treatment with trypsin. This assay therefore confirmed that the deletions in the N-terminus did not prevent the transport to the cell surface along the secretory pathway. After biotinylation, the different glycosylation bands were more difficult to devise. To confirm whether this was due to interference with the biotin molecules or to detection of unspecific signals, immunoprecipitation with N2a cells transfected with the unrelated plasmid pEGFP was performed using the antibody 3F4. In this case no signal could be detected, confirming that the bands monitored upon immunoprecipitation of the transfected PrPs were specific and represented the constructs. Analysis of the signals detected after trypsin treatment of wtPrP^c and of PrPΔ(23-51), the mutant missing the 29 amino acids preceding the octapeptide repeat sequence, after 45 min of chase, revealed that only the wild type protein had been efficiently internalised (**Fig. 9A**, lanes 4 and 11). On the other hand, after 60 min both constructs had entered the cells, although in different amounts. The intensity of the visualised bands was quantified with an appropriate computer programme and the signals detected after trypsin treatment compared to those untreated at the same time point. This quantification of the blots revealed that ~72 % of wtPrP^c had been endocytosed, whereas the amount of PrPΔ(23-51) only measured ~32 % (**Fig. 9B**). In contrast, neither PrPΔ(48-93), which lacked the octapeptide repeats, nor PrPΔ(23-90) in which the longest segment had been eliminated, could be detected inside the cell after 60 min (**Fig. 9A**, lanes 17 and 21).

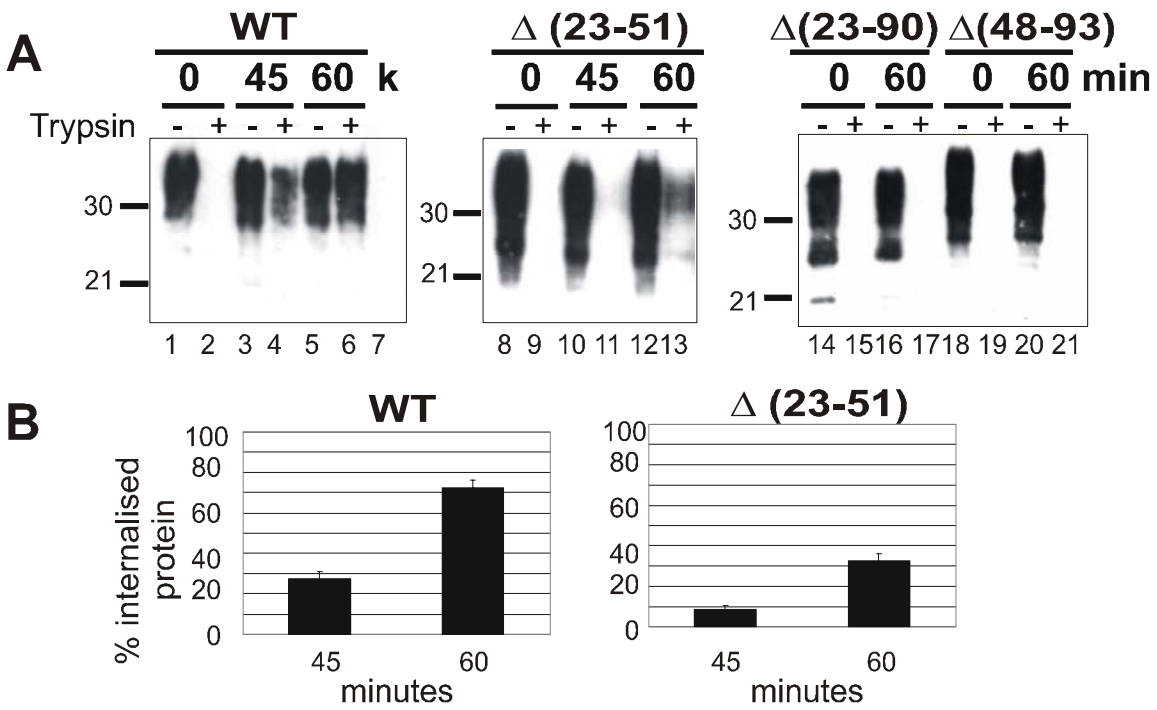

Figure 9. Comparison of internalisation kinetics of wtPrP^c and deletion mutants after 45 and 60 min of chase

(**A**) N2a cells were transfected transiently with wtPrP^c or PrP deletion mutants using Fugene transfection reagent. 72 h after transfection cells were surface-biotinylated on ice for 15 min and then incubated for 0, 45 or 60 min at 37 °C. They where lysed immediately (-) or treated with trypsin (+) for 10 min on ice before harvesting and were then immunoprecipitated with the antibody 3F4, in order to detect only the transfected proteins. Lane 7 depicts lysate from N2a cells transfected with the unrelated plasmid pEGFP and precipitated with the monoclonal antibody 3F4, as a control. The samples were subjected to SDS-PAGE and the signals were detected by 1 h incubation with peroxidase conjugated streptavidin. Molecular size markers are depicted on the left (kDa). The autoradiogram reveals a delayed internalisation for all analysed deletion constructs.
(**B**) The signals from (A) were quantified and the amount of internalised protein after 45 and 60 min was calculated as a percentage of protein without treatment with trypsin (100 %) at the same time point (each bar represents mean values from two independent experiments). The blot was digitised using an APB-Image Scanner and specific bands quantified with Master-1d analysis software.

In order to evaluate kinetics of internalisation for PrPΔ(48-93) and PrPΔ(23-90) in more detail, an analogous biotinylation assay with prolonged chase times was performed with these two constructs (**Fig. 10**). This experiment confirmed extremely impaired endocytosis for both proteins: after 3 and 6 h of chase almost no specific signals were detected within the cell (**Fig. 10A**, lanes 4, 6, 12 and 14). Quantitative evaluation of the blot revealed that the amount of PrP(48-93) molecules located intracellularly after 10 h was 65 % of the total amount of protein rescued at the same time point without treatment with trypsin (**Fig. 10A**, lane 15 and 16 and **Fig. 10B).** On the contrary, the levels of intracellular PrPΔ(23-90) remained extremely low throughout the chase (lanes 4, 6 and 8) and only reached ~7 % of the total amount of PrP after 10 h. Taken together, these two assays evidenced altered kinetics of endocytosis for all

PrP constructs analysed, longer deletions in the protein sequence caused stronger impairment. These results therefore argue for a correlation between the length of the N-terminal truncation and the efficacy of PrP internalisation.

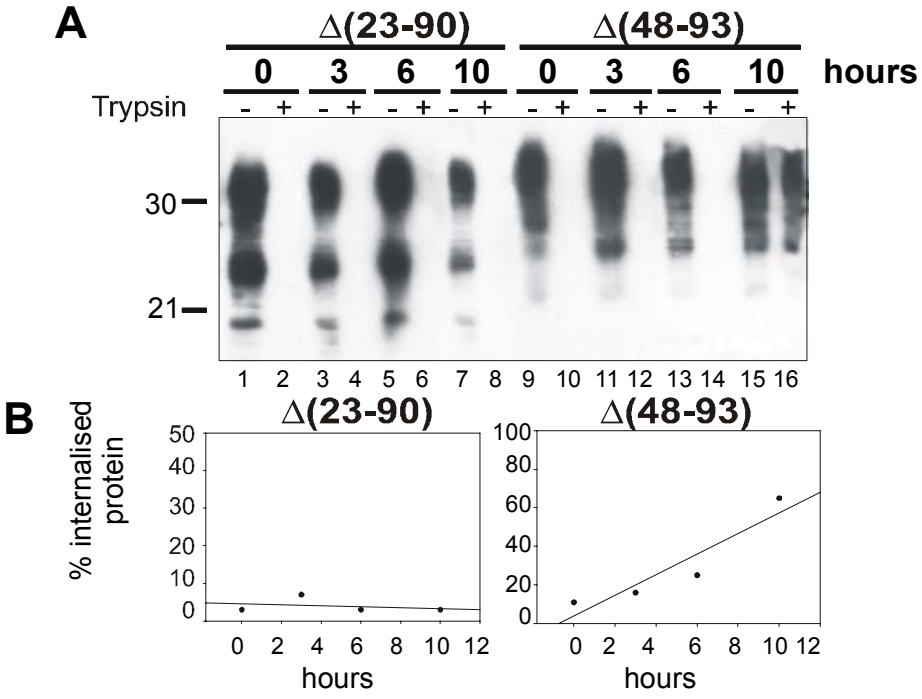

Figure 10. Internalisation kinetics of PrPΔ(23-90) and PrPΔ(48-93)

(**A**) Transiently transfected N2a cells expressing PrP deletion mutants were surface biotinylated on ice and then incubated at 37 °C for 0, 3, 6 and 10 h, respectively. Cells were harvested directly or treated with trypsin for 10 min on ice and then lysed. PrPs were immunoprecipitated with the monoclonal antibody 3F4. The blot shows samples treated (+) and untreated (-) with trypsin. The bold numbers on top indicate chase times (in hours) after the pulse. Molecular weight markers are indicated in kDa on the left. The construct with the longest deletion showed a more impaired endocytosis and was mainly localised on the cell surface even after 10 h of chase.
(**B**) Mean values from two independent experiments represent the amount of internalised protein expressed as a percentage of the total labelled protein without trypsin digestion (at the same time point) and plotted as a function of different time points.

3.3 Equal detection of wtPrP^c and PrPΔ(23-90) in the culture medium

The partial or complete removal of the N-terminal part of the prion protein prolonged the presence of the protein on the plasma membrane. Particularly for PrPΔ(23-90), the amount of protein which could be detected intracellularly, even after a long chase, was extremely low. A small quantity of PrP^c has been reported to be released from cultured cells and to be shed into the medium (Borchelt *et al.*, 1990; Caughey *et al.*, 1989; Parizek *et al.*, 2001), and a soluble N-terminally truncated PrP was seen to be released from human platelets (Perini *et al.*, 1996). To test whether inefficient endocytosis of the PrP deletion constructs results in a more

pronounced shedding into the culture medium as means to avoid accumulation, a pulse chase experiment was carried out. N2a cells transiently expressing wtPrP^c or PrPΔ(23-90) were metabolically labelled with [^{35}S]-methionine/cysteine for 1 h and then chased for 1 or 6 h at 37 °C. The transfected proteins were subsequently recovered from the cells after lysis or from the culture medium, upon immunoprecipitation with the antibody 3F4. All samples were subjected to PNGase F treatment for deglycosylation of the proteins in order to facilitate comparison of the signals and were run on an SDS gel. Upon deglycosylation, single bands were detected in the lysates at 25 kDa for wtPrP^c and at 19 kDa for the truncated PrP (**Fig. 11**). The levels monitored for both proteins in the medium after 6 h were comparable (**Fig. 11**, lanes 4 and 8), the slightly reduced amount of PrPΔ(23-90) in the lysates and in the medium probably due to the lower efficiency of transfection (when comparing lysates of the two constructs). Increased shedding of PrPΔ(23-90) could therefore be excluded.

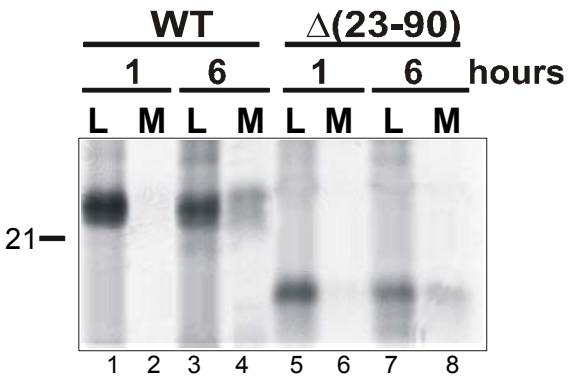

Figure 11. Detection of wtPrP^c and PrPΔ(23-90) in the culture medium

N2a cells transiently expressing wtPrP^c or PrPΔ(23-90) were metabolically labeled for 1 and then incubated for 1 or 6 h at 37 °C before lysis. The cells (L) and the corresponding culture medium (M) were then immunoprecipitated with the antibody 3F4. All samples were deglycosylated overnight with PNGase F and run on an SDS-PAGE gel. No increased release of PrPΔ(23-90) was detected in the culture medium.

3.4 Lysosomal accumulation of PrPΔ(23-90) upon treatment of the cells with leupeptin

Since no increase in the level of medium-recovered PrPΔ(23-90) had been registered, and only low amounts of this protein could be detected within the cell upon biotinylation, more information about the degradation route of this protein was collected with another pulse-chase experiment. Wild type PrP is normally internalised from the plasma membrane and transported along the endocytic pathway to late endosomes and lysosomes where the final degradation occurs. In the present assay, N2a cells were thus treated with the endosomal and lysosomal protease inhibitor leupeptin, which covalently binds to serine and thiol proteases, inhibiting their activity and the degradation of proteins in the lysosome. After immunoprecipitation of the transfectd proteins with the antibody 3F4 and PNGase F deglycosylation, specific bands for wtPrP^c and PrPΔ(23-90) were monitored (**Fig. 12**). For

both proteins the signals became stronger when the cells had been treated with leupeptin, implying that they follow the lysosomal pathway for degradation (**Fig 12**, lanes 2 and 4). In spite of the slower rate of endocytosis monitored in the earlier experiments, accumulation of PrPΔ(23-90) in the lysosomes upon inhibition of proteasomal activity, showed that the cells were still able to internalise this construct and to direct it to acidic compartments for final degradation. Whether the pathway used for endocytosis is the same as for wtPrP^c or whether an alternative one is adopted, still needs to be elucidated.

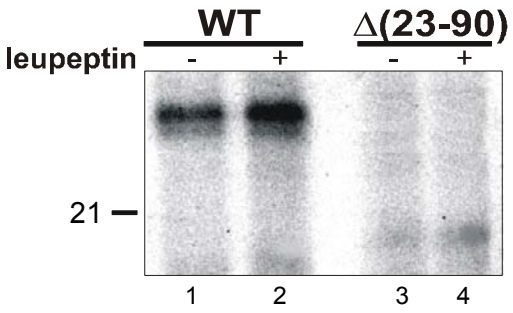

Figure 12. Effect of lysosomal inhibition on PrPΔ(23-90) degradation

N2a cells were transiently transfected with wtPrP^c or PrPΔ(23-90) and subsequently treated overnight with 100 µM lysosomal inhibitor leupeptin. They were then metabolically labeled for 1 h and chased at 37 °C for 6 h in the presence of leupeptin. The cells were lysed, and the PrPs were immunoprecipitated with the antibody 3F4. All samples were deglycosylated with PNGase F and then subjected to SDS-PAGE PrPΔ(23-90) accumulates in lysosomes upon treatment of the cells with leupeptin.

3.5 Effect of N-terminal deletion on the half-life of PrP^c

The experiments described above evidenced prolonged permanence of PrP deletion mutants on the cell surface and localisation in the same compartments of degradation evidenced for the wild type. The following assay was therefore aimed at a more detailed characterisation of the kinetic of degradation and stability of the truncated PrPs. In a pulse-chase experiment the half-lives of wtPrP, PrPΔ(23-90) and PrPΔ(48-93) were compared. N2a cells expressing these constructs were metabolically labelled with [^{35}S]-methionine/cysteine for 1 h and either directly harvested or chased for the indicated intervals of time in [^{35}S]-free culture medium before lysis. PrP present in the lysates was immunopurified with the polyclonal anti-PrP antibody A7, deglycosylated with PNGase F, and the decrease in the intensity of the signals in time was analysed by SDS-PAGE (**Fig. 13A**). The gel was evaluated by densitometric analysis and the specific signals quantified as fractions of the signal observed immediately after the pulse period (**Fig. 13B**). This analysis revealed a half life for newly synthesised wtPrP^c of 2.6 h. This turnover was comparable, although slightly slower than the one measured in other studies done with untransfected cells (Borchelt *et al.*, 1990). In contrast, the turnover of the deleted PrP molecules proved to be significantly prolonged. Quantification for

PrPΔ(48-93) and PrPΔ(23-90) indicated a half-life of ~4.2 and ~4.8 h, respectively. Both values were almost twice as long as those registered for wtPrP^c. As the antiserum used in this assay was the polyclonal antibody A7, which recognises both endogenous and transfected PrP, also the full length PrP^c was precipitated from the lysates of cells expressing the truncated proteins and could be monitored on the blot as a single band of 25 kDa. This phenomenon underlines the difference in the turnovers of the constructs. These data corroborate the model that prolonged localisation of PrP costructs on the plasma membrane due to N-terminal deletion also affects the degradation of these proteins.

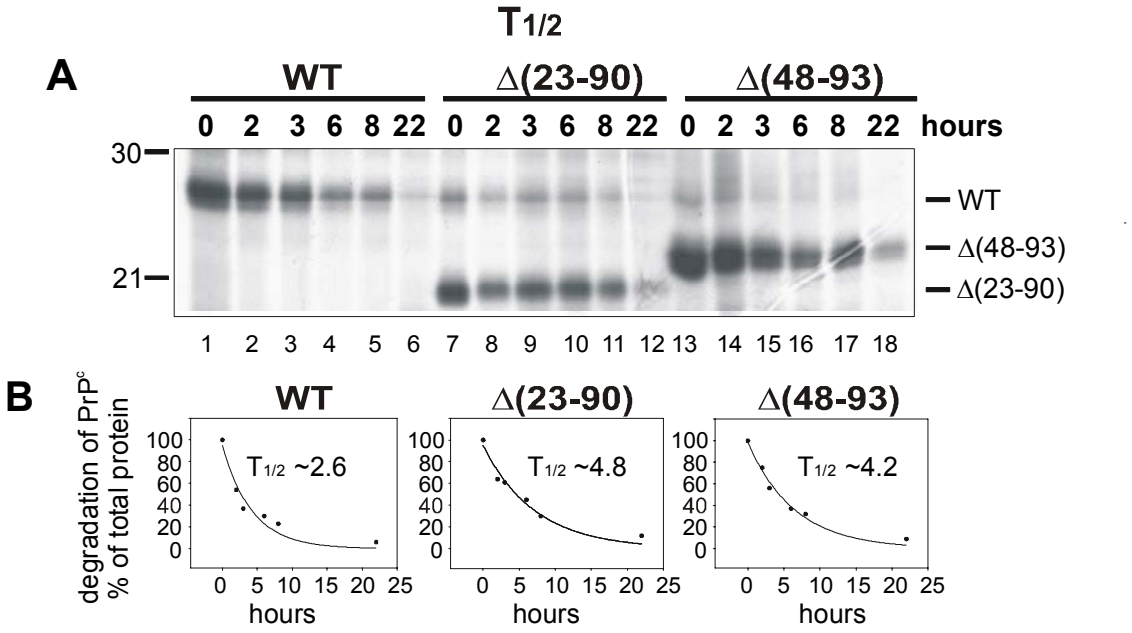

Figure 13. Deletion of the N-terminus prolongs turnover of PrP^c

(**A**) Confluent N2a cells transiently expressing wtPrP^c, PrPΔ(23-90) or PrPΔ(48-93) were metabolically labelled with [^{35}S]-Met/Cys for 1 h at 37 °C and were either lysed immediately after the pulse or incubated in culture medium without [^{35}S] at 37 °C for 2, 3, 6, 8 and 22 h before harvesting. Proteins were precipitated with the ployclonal antibody A7 and deglycosylated with PNGase F to facilitate molecular size comparison and quantification. Samples were subjected to SDS-PAGE and autoradiography. Molecular size markers are designated in kDa on the left. Bars on the right indicate unglycosylated PrP-specific bands belonging to each construct. The autoradiogram evidences that the PrP deletion constructs are degraded with a slower kinetic, compared to that of wtPrP.
(**B**) Evaluation of autoradiograms from three independent experiments performed as described in (**A**), to determine the half-life of the different PrPs. The amounts of protein are expressed as percentage of total protein rescued directly after the labelling period and are plotted as a function of the chase time points. The data points were fitted to an exponential curve using non-linear regression analysis.

3.6 Modulation of the transport through the secretory pathway by the N-terminal segment of the prion protein

Since the data collected so far had shown that the N-terminal part of PrP^c modulates endocytosis and stability of the protein, the transport of the prion protein and of the different deletion constructs through the secretory pathway was examined, to identify a possible function of the N-proximal segment also in this arm of the PrP life-cycle. Pulse-chase experiments coupled with trypsin digestion were used to evaluate the time required by $wtPrP^c$ and PrP deletion constructs to reach the plasma membrane. After transfection, a metabolic pulse of 5 min allowed the labelling of a more homogenous protein population shortly after translation and translocation into the ER. Cells were then harvested immediately or chased for the indicated time periods to allow transport to the cell surface. Molecules that had reached the plasma membrane were separated from those still undergoing synthesis or transport to the cell surface by mild trypsin treatment on ice for 10 min and were then immunoprecipitated with an anti-PrP antibody. All samples were deglycosylated with PNGase F for simplifying quantitative comparison of the constructs. Immediately after the pulse, $wtPrP^c$ and the PrP constructs were still protected from extracellular trypsin digestion (**Fig. 14**, lanes 2, 8 and 14), consistent with their localisation in the endoplasmic reticulum and/or Golgi apparatus. A relevant decrease in the $wtPrP^c$ signal was monitored after 60 min of chase (**Fig. 14A**, lane 4), and confirmed that most of the $wtPrP^c$ molecules reach the cell surface within 1 h after synthesis. This value was consistent with those reported earlier by other groups (Caughey *et al.*, 1989; Borchelt *et al.*, 1992). For the other two constructs analysed here, even after 60 min of chase, considerable amounts were still detectable intracellularly (**Fig. 14A**, lane 10 and 16). Of note, PrPΔ(48-93) was still clearly detectable after 75 min of chase. Phosphor-Imaging analysis evidenced that, whereas after 45 min 50 % of total $wtPrP^c$ could still be detected after trypsin treatment, this level rapidly decreased to ~25 % after 60 min. Quantification of the signals for PrPΔ(23-90) and PrPΔ(48-93) revealed that 50% of the labelled proteins were not susceptible to trypsin treatment after 65 and 75 min, respectively. These repeated and reproducible findings corroborated the notion that deletions within the N-terminal sequence negatively affect the transport of PrP^c also along the secretory pathway. The sorting of PrPΔ(48-93) to the cell surface seemed to be more delayed than that of PrPΔ(23-90), possibly due to a particular conformation of the construct.

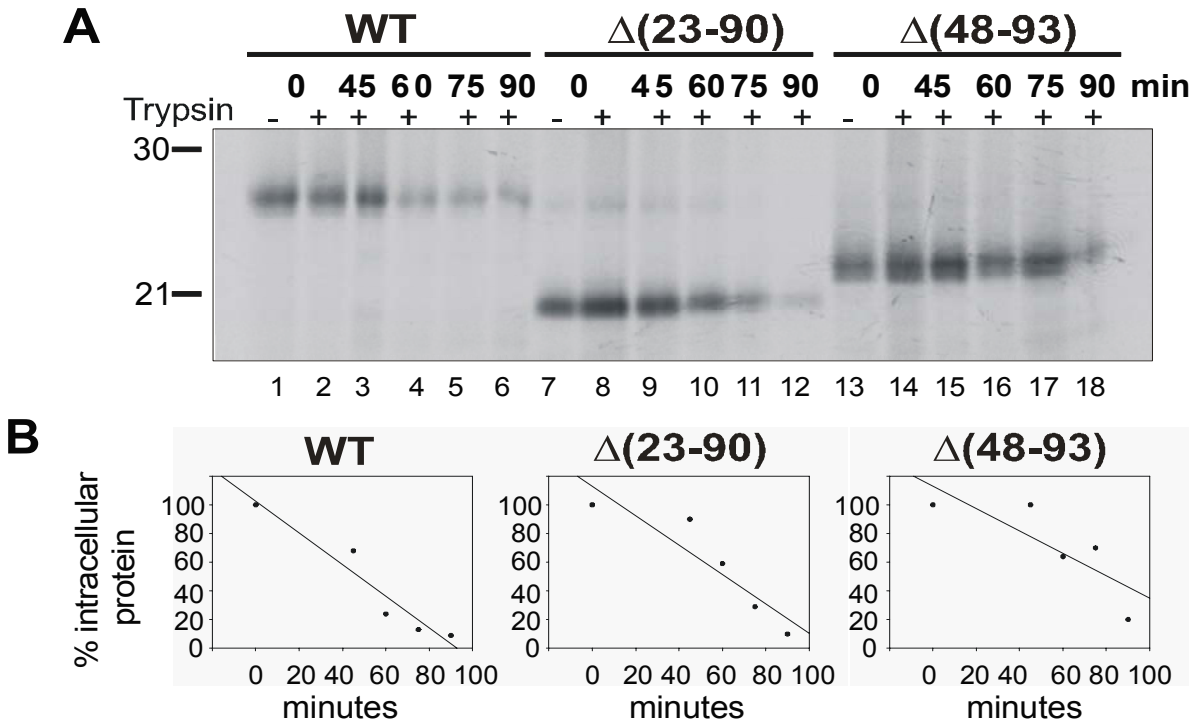

Figure 14. Kinetics of transport of wtPrP^c, PrPΔ(23-90) and PrPΔ(48-93) to the cell surface

(**A**) wtPrP^c and N-terminally truncated constructs were transiently transfected into N2a cells. They were then metabolically labelled with [^{35}S]-Met/Cys for 5 min on ice and chased at 37 °C in [^{35}S]-free culture medium for 0, 45, 60, 75, 90 min, respectively. For each construct, one plate was harvested immediately after the pulse or treated with trypsin for 10 min on ice and lysed. All other plates were subjected to digestion with trypsin after the chase. Proteins were immunoprecipitated with antibody A7, deglycosylated with PNGase F and subjected to SDS-PAGE. The autoradiogram shows PrP signals before (-) and after (+) treatment with trypsin. Molecular size markers in kDa are shown on the left. Deletion of the N-terminus results in a delayed transport along the secretory pathway.
(**B**) Phosphor-Imager evaluation of autoradiograms representing amount of proteins detected after digestion with trypsin. Each point represents a mean value of three independent experiments. Quantities are calculated as a percentage of protein precipitated immediately after the pulse without trypsin-treatment.

For further analysis of the domains involved in the trafficking of PrP^c, the transport of PrPΔ(23-51) and that of another construct in which three of the five octapeptide repeats had been removed (residues 68-91), were compared. Also in this analysis, a pulse-chase assay combined with trypsin treatment of transfected cells, using the same time points for easier comparison was used (**Fig. 15A and B**). In these two constructs, segments of similar length were deleted in distinct sections of the N-terminus. If different kinetics of transport were measured, these should therefore reveal the presence of a more limited domain with a dominant sorting role in the secretory pathway. The time for detection of 50 % of intracellular PrP was 65 and 70 min for PrPΔ(68-91) and PrPΔ(23-51), respectively, which was longer than that measured for wtPrP^c (45 min). The bands detected in this assay migrated as doublets under these conditions, rather due to incomplete deglycosylation than to the presence of

degraded forms of the proteins, since they were already present immediately after the pulse. From these results two conclusions can be drawn: truncation of even a reduced segment within the N-terminus negatively interferes with the efficiency of transport of PrP^c to the plasma membrane. More important, no specific domain within the stretch of the PrP analysed in this study displays a dominant role, since deletions encompassing or preceding the octapeptide repeat region similarly affect this pathway.

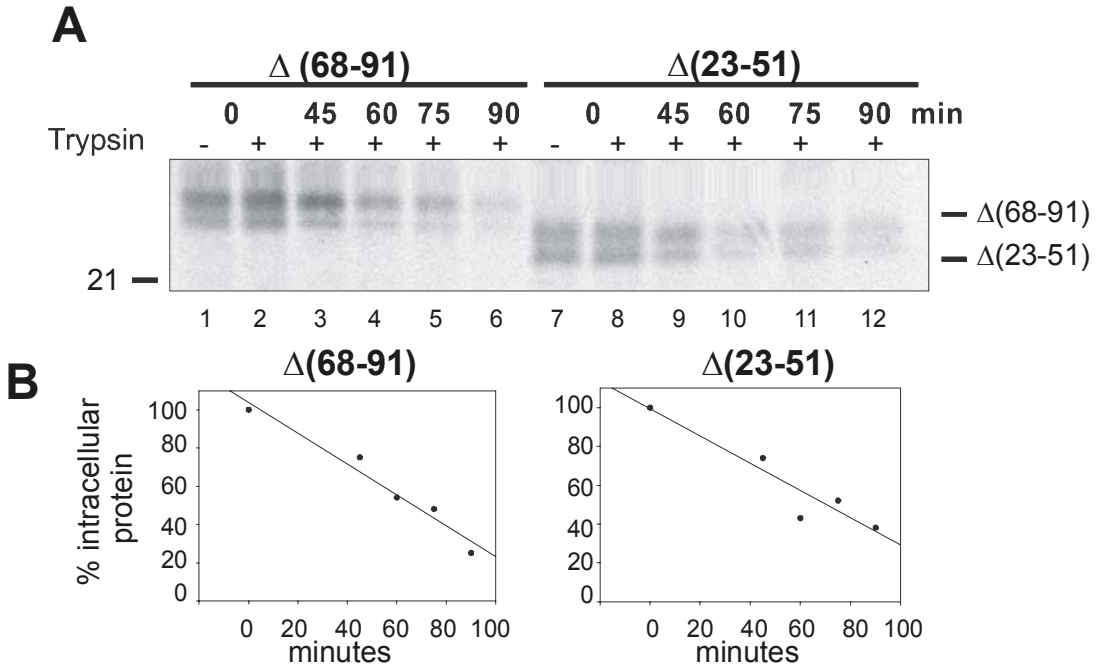

Figure 15. Kinetics of PrPΔ(68-91) and PrPΔ(23-51) transport through the secetory pathway monitored by pulse-chase experiments

(**A**) PrP deletion constructs were transfected into N2a cells and metabolically labelled with [^{35}S]-Met/Cys for 5 min. For both constructs one plate was lysed immediately after the pulse or treated with trypsin, the others were incubated for 45, 60, 75 and 90 min at 37 °C and then treated with trypsin for 10 min on ice before harvesting. Proteins were immunoprecipitated with the antibody A7, deglycosylated with PNGase F and subjected to SDS-PAGE. Bars on the right indicate PrP specific signals. Both constructs migrated as doublets, under these conditions. On the left molecular size markers are shown in kDa. Small deletions in different parts of the N-terminus can impair transport of PrP molecules to the cell surface.
(**B**) The diagrams show the amount of protein detected at each time point after treatment with trypsin. Signals from two autoradiograms were quantified by Phosphor-Imager analysis and depicted as percentage of protein precipitated immediately after the pulse without trypsin treatment.

3.7 N-terminal deletions and PrP glycosylation

The experiments described above have evidenced a general delay in the transport of PrP^c to the cell surface when segments within the N-terminal part were deleted. A more accurate characterisation of this impaired pathway was therefore necessary. In a first attempt to identify a specific compartment or membranous vesicles involved in the secretory pathway, in

which N-terminal truncation of PrP^c might result in a delayed transport to the cell surface, immunoprecipitated samples were subjected to Endoglycosidase-H (Endo-H) treatment. This enzyme hydrolyses high-mannose oligosaccharides linked to the proteins while these are in the ER or ER cis-Golgi intermediate compartment (ERGIC) preceding the medial Golgi stack. (Tarentino and Plummer, Jr., 1994). Once glycoproteins have reached the mid-Golgi compartment, removal of mannose residues by mannosidase I and II and addition of a single sugar residue by N-acetyl-glucosamine transferase generates a structure called "inner core" of the complex oligosaccharide, which is resistant to degradation with Endo-H (**Fig 16**). Treatment of proteins with Endo-H therefore enables characterisation of their glycosylation state and localisation.

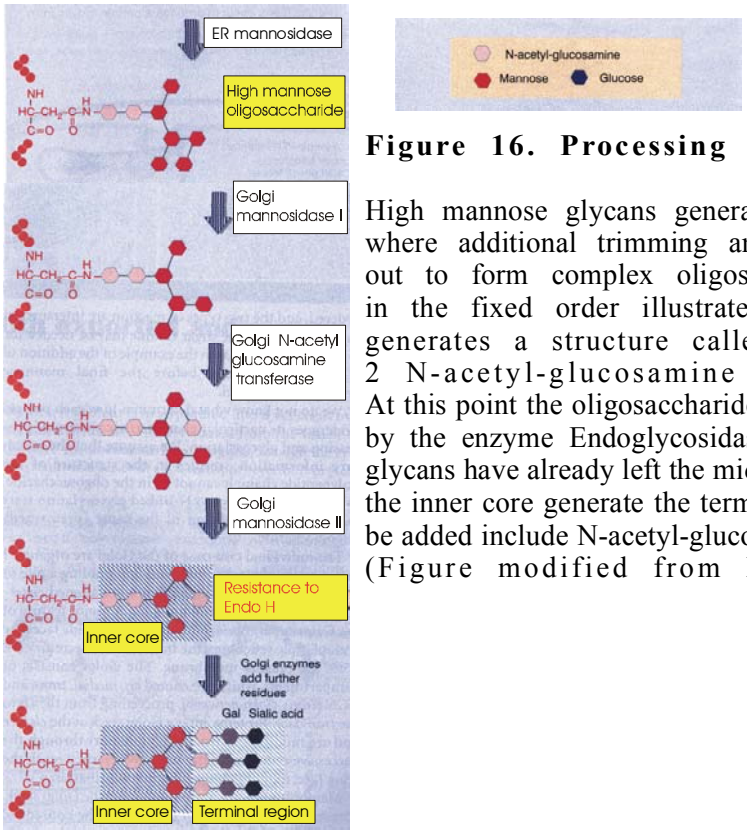

Figure 16. Processing of glycans in the Golgi.

High mannose glycans generated in the ER reach the Golgi where additional trimming and further additions are carried out to form complex oligosaccharides. Modifications occur in the fixed order illustrated in the figure. This process generates a structure called inner core, consisting of 2 N-acetyl-glucosamine and 3 mannose residues. At this point the oligosaccharide becomes resistant to degradation by the enzyme Endoglycosidase-H (Endo-H). Endo-H resistant glycans have already left the mid-Golgi compartment. Additions to the inner core generate the terminal region. The residues that can be added include N-acetyl-glucosamine, galactose, and sialic acid. (Figure modified from B.Lewin,Genes VII, 2000)

In pulse-chase experiments, the time points at which $wtPrP^c$, PrPΔ(23-90) and PrPΔ(48-93) acquired Endo-H resistance was measured (**Fig. 17**). Acquisition of Endo-H resistance at different time points for PrP^c and PrP deletion constructs would localise the compartment of delay before the mid-Golgi stack. If all constructs became resistant at the same time, then the trans-Golgi or a vesicular compartment between trans-Golgi and plasma membrane would represent the compartment where this impairment takes place. After metabolic labelling of prion proteins for 5 min, these were either immediately harvested or chased for different time intervals before lysis. All samples were immunoprecipitated with the antibody 3F4 and

subjected to Endo-H treatment. The experiment was performed twice with different chase times. Treatment of wtPrP^c with Endo-H immediately after labelling resulted in a shift of the 33 and 28 kDa bands to a band of ~25 kDa (**Fig. 17A**, lane 2). Initial signs of resistance for wtPrP^c were detected after 30 min of chase, when the mono-glycosylated form appeared (lane 6) and became more prominent after 40 min (lane 8). Observing the other two constructs, we could detect the conversion to unglycosylated molecules of 19 and 22 kDa for PrPΔ(23-90) and PrPΔ(48-93), respectively, when treated with Endo-H immediately after the pulse (**Fig. 17A** lane 12 and **Fig. 17B** lane 2). Partial resistance was detected after 40 min for both deletion mutants (**Fig. 17A** lane16 and **Fig. 17B** lane 8).

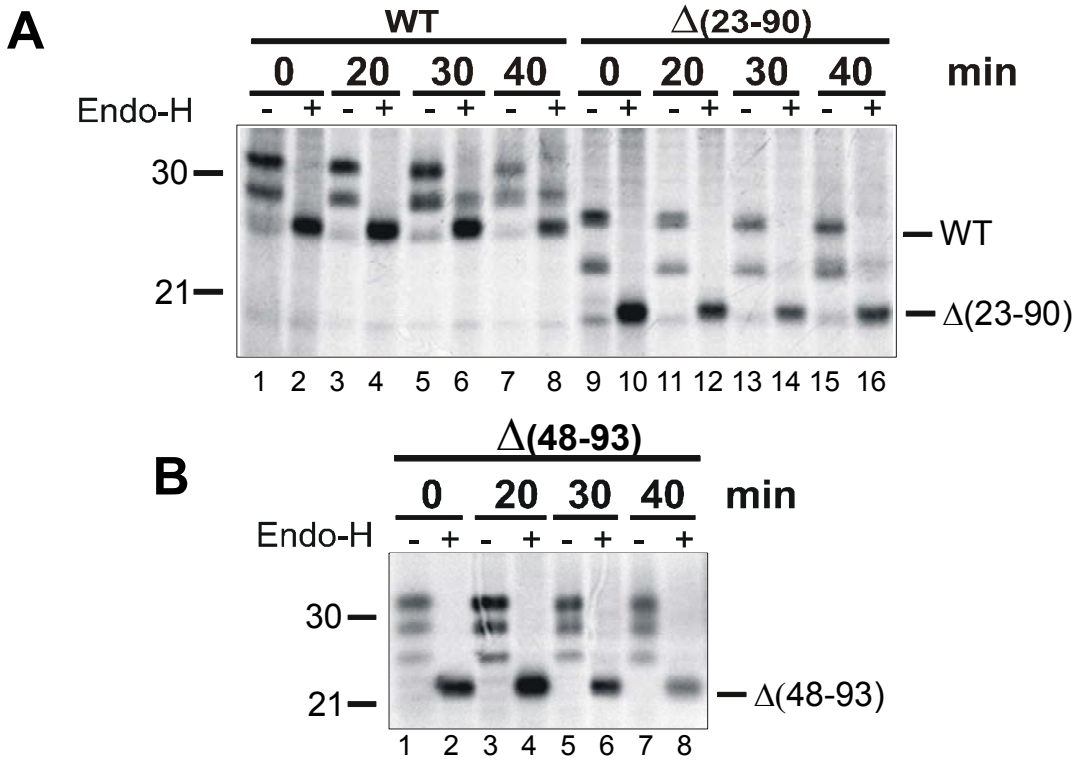

Figure 17. Endo-H digestion of wtPrP^c, PrPΔ(23-90) and PrPΔ(48-93)

Confluent N2a cells transfected with wtPrP^c, PrPΔ(23-90) or PrPΔ(48-93) were metabolically labelled with [^{35}S]-Met/Cys for 5 min on ice and then either immediately harvested or incubated in culture medium without [^{35}S] at 37 °C for different chase periods before lysis. Proteins were then immunoprecipitated with antibody 3F4 and treated with (+) or without (-) Endo-H overnight at 37 °C before analysing by SDS-PAGE. Bars on the right indicate unglycosylated PrP specific bands. Molecular size markers are shown (in kDa) on the left. None of the three proteins analysed became completely Endo-H resistant after 40 min of chase.

Since complete Endo-H resistance had not been monitored for any of the analysed constructs, the assay was repeated applying longer chase periods after the pulse (**Fig. 18**). Under these conditions, the mono- and di-glycosylated bands of wtPrP^c could be detected, after treatment

with Endo-H, between 40 and 50 min (**Fig. 18A**, lanes 4 and 6). Both the other deletion constructs became fully Endo-H resistant after 50 min (**Fig. 18A**, lane 16 and **18B**, lane 6). As deletions within the N-terminal part of PrP^c do not profoundly affect kinetics of glycosylation and transport of PrP^c to the Golgi, delay in reaching the plasma membrane seems to take place in a compartment downstream of the mid-Golgi.

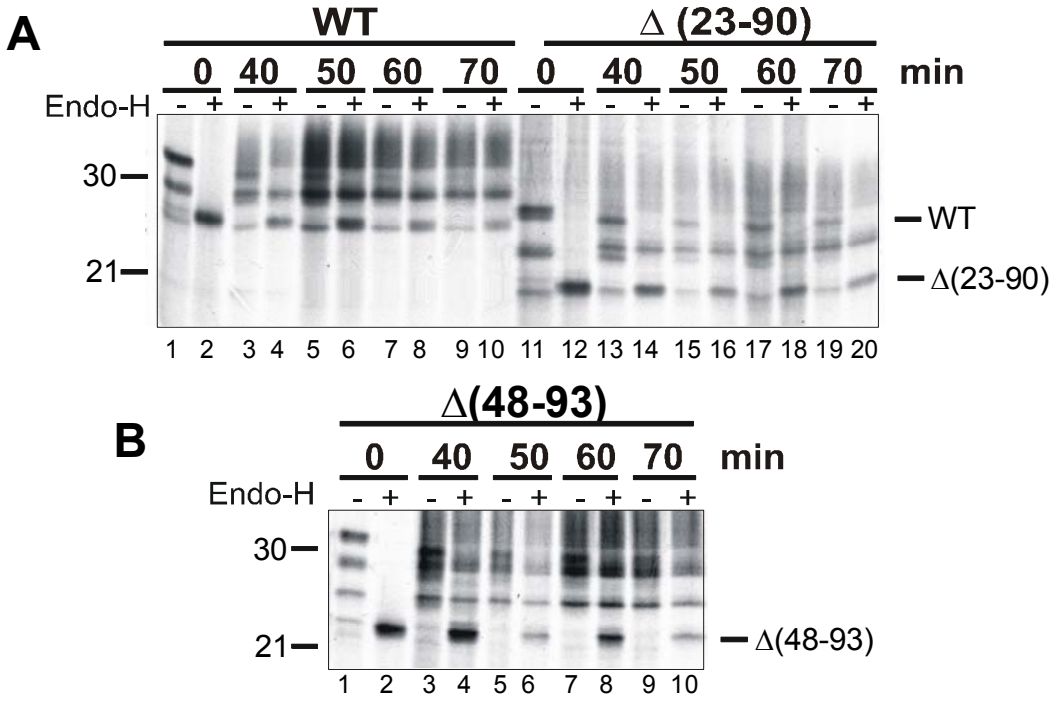

Figure 18. Endo-H digestion of wtPrP^c and PrP deletion constructs after 40-70 min chase periods

Confluent N2a cells transiently expressing wtPrP^c, PrPΔ(23-90) or PrPΔ(48-93) were metabolically labelled and chased as described in the previous figure. Proteins were then immunoprecipitated with antibody 3F4 and treated with (+) or without (-) Endo-H previous to analysis by SDS-PAGE. Bars on the right indicate unglycosylated PrP specific bands. Molecular size markers are shown (in kDa) on the left. All PrPs analysed became completely Endo-H resistant between 40 and 50 min of chase.

3.8 Biochemical characterisation of a chimeric prion protein

In light of the results described above, further analysis of the influence of the N-terminal part on subcellular trafficking was undertaken by substituting the mouse N-terminus with that of a far remote species in one of the analysed constructs. An IMAGE clone containing the cDNA comprising 387 bp of the coding sequence of the *Xenopus laevis* PrP was used for cloning of a chimeric protein. The 47 residues following the signal peptide represent the N-terminal end of the mature Xenopus PrP^c (amino acids 23-69), and were therefore inserted into the truncated mouse PrPΔ(23-90) with PCR cloning techniques. This segment, although showing

homology to the mouse PrP-N-terminus, especially in the basic N-proximal stretch, is 20 amino acid shorter than that of the mouse, mainly due to the lack of repeat structure (**Fig.19**).

A

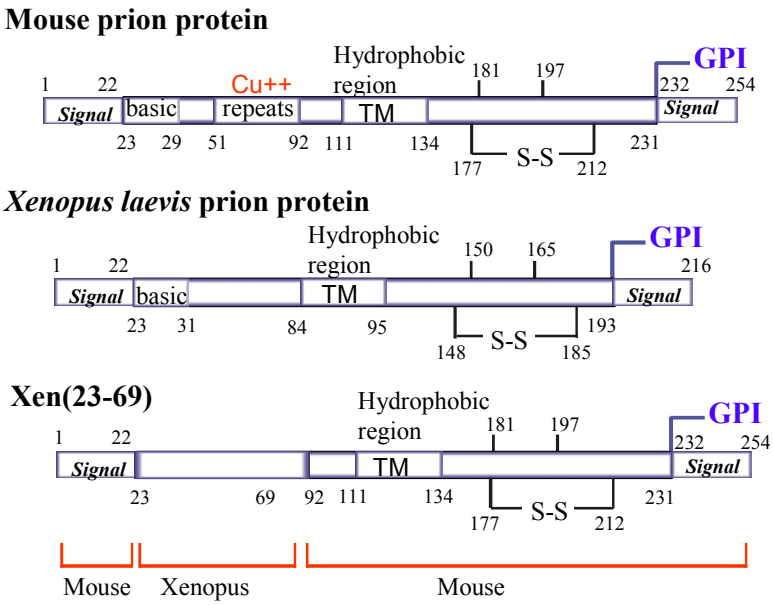

B

```
MPQSLWTCLVLISLVCTLT-VS-SKKSGGGKSKTGGWNTG-SNRNPNYPG--GYPGN-----52   Xenopus
MAN--LSYWLLALFVAMWTDVGLCKK-R-PKP--GGWNTGGS-RYPGQGSPGGNRYPPQGG-55   mouse

----------TGGSWGQQPYNPSG----Y-N-KQ  70   Xenopus
TWGQPHGGGWGQPHGGSWGQPHGGSWGQPHGGGWGQ----------GGGT--HN--Q  98   mouse
```

Figure 19. Schematic representation of mouse and *Xenopus laevis* wtPrP^c and of the chimeric construct Xen(23-69)

(**A**)The proteins are depicted with their structural features and post-translational modifications. The polypeptide chains are divided into distinct segments according to the different biochemical properties. The numeration of amino acids refers to the human PrP sequence. The figure shows that for construction of Xen(23-69), residues 23-69 of the *Xenopus* PrP have been introduced into the mouse PrPΔ(23-90), following residue 22.
(**B**) Comparison of the *X. laevis* prion protein N-terminal amino acid seqence with the mouse. Grey boxes denote identical residues.

The resulting protein Xen(23-69) was transiently expressed in N2a cells and was characterised biochemically in a solubility assay in the presence of N-lauryl sarcosine and upon PK-digestion, using the antibody 3F4. The construct appeared to be soluble and PK-sensitive and thereby had the characteristics of a properly folded, non aggregated prion protein (**Fig. 20**, lanes 2 and 3). After deglycosylation with PNGase F, the construct migrated

as a single band of about 23 kDa, consistent with its shorter amino acid sequence (**Fig. 20**, lane 4). Its biochemical properties did not differ relevantly from those of the murine PrP^c.

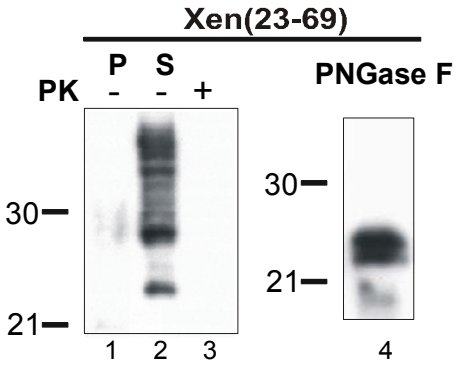

Figure 20. Biochemical characterisation of Xen(23-69)

The postnuclear lysates of N2a cells expressing the chimeric construct Xen(23-69) were analysed in a solubility assay or were subjected to treatment with 20 µg/ml PK for 30 min at 37 °C. One aliquot was used for PNGase F digestion. The resulting fractions were examined in a Western Blot developed with the antibody 3F4. Lane 1 and 2: detergent insoluble (P: pellet) or soluble (S: supernatant) fractions upon ultracentrifugation; lane 3: lysate fraction treated with PK; lane 4: aliquot treated with PNGase F for deglycosylation. No specific signals were detected in the pellet upon ultracentrifugation, nor after PK digestion.

The intracellular expression and the cell surface localisation of this protein were therefore analysed in a FACS analysis with a flow cytometry after immunofluorescence staining (**Fig. 21**). Also in this case, the monoclonal antibody 3F4 was applied, in order to avoid a cross-reaction with the endogenous PrP^c. Both the chimeric and the wild type protein showed similar pattern of expression, indicating that the introduction of the *Xenopus* N-terminal segment into the mouse protein neither altered the expression levels nor prevented cell surface localisation of the chimeric protein.

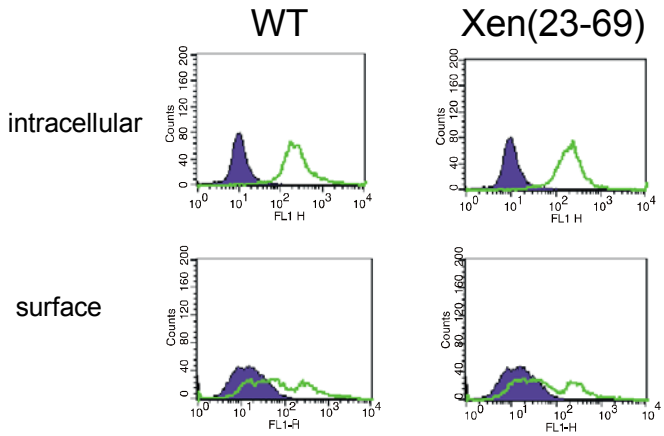

Figure 21. Similar levels of cellular expression for $wtPrP^c$ and Xen(23-69)

The expression levels in N2a cells transiently transfected with $wtPrP^c$ or Xen(23-69) were measured by cytofluorometry 72 h post transfection. The upper panels show fluorescence histograms for the intracellular expression of the two proteins in permeabilised cells for one representative experiment.

X-axes represent the fluorescence intensity plotted against the number of cells (y-axes). In each experiment the expression in transfected cells (open diagram) was measured against that of untransfected ones (filled diagram). For each cell population 10,000 events were measured. The lower panel shows the cell surface expression in non-permeabilised cells. Living and dead cells were separated by staining with propidium iodide and gating. The histogram only shows the cells contained in this gate. In both assays the monoclonal antibody 3F4 was used for detection of the constructs.

3.9 Restoration of the wild type phenotype by the *Xenopus laevis* N-terminus

Once the biochemical properties and the correct surface expression of Xen(23-69) had been assessed, this protein was used to examine how the intracellular trafficking of the truncated mouse PrP^c was affected by the N-terminal segment belonging to a phylogenetically remote species. The kinetic of endocytosis of this construct was analysed in a biotinylation assay followed by mild treatment of transfected N2a cells with trypsin, as described above. Immediately after the pulse, biotin labelled Xen(23-69) localised on the cell surface could be rescued upon immunoprecipitation with the antibody 3F4 (**Fig. 22A**, lane 1). Additionally, no signal was detected upon treatment of the cells with trypsin, confirming the presence of the protein at the outer leaflet of the plasma membrane (**Fig. 22A**, lane 2). Chase times of up to 45 min at 37° C showed no signals upon trypsin treatment, only after 60 min specific bands could be detected (**Fig. 22A**, lane 6). This experiment showed that endocytosis of this chimeric protein occurred at a slower rate when compared to $wtPrP^c$ which was detected in the intracellular space after 45 min. Nevertheless, the introduction of an N-terminal sequence, although belonging to a remote species accelerated the internalisation of PrPΔ(23-90). Quantification of the blot revealed an intracellular level of protein of almost 60 % 1 h after the pulse.

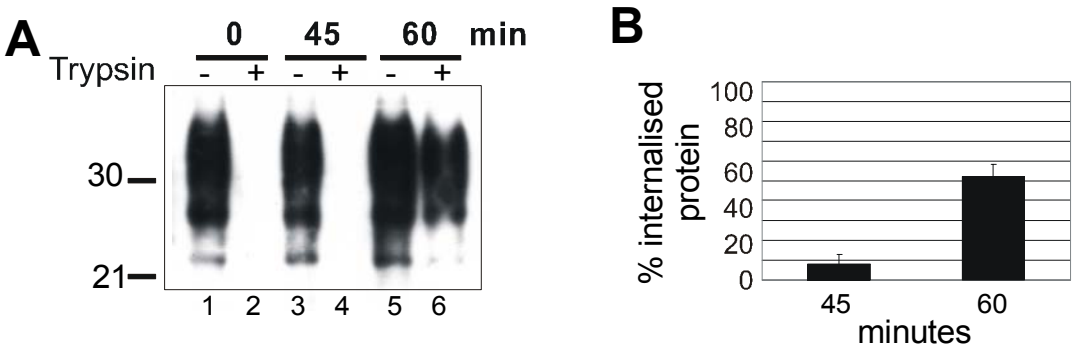

Figure 22. Internalisation kinetics of Xen(23-69)

(A) Transiently transfected N2a cells expressing chimeric PrP Xen(23-69) were incubated for 0, 45 or 60 min at 37 °C, after surface biotinylation on ice for 15 min. Cells were lysed immediately (-) after the labelling, or were subjected to trypsin digestion (+) for 10 min on ice previous to lysis, and were then precipitated with antibody 3F4. Samples were subjected to SDS-PAGE and signals were detected

by streptavidin. Molecular size markers are depicted on the left (kDa). Xen(23-69) is efficiently internalised.
(**B**) The bars represent the amount of PrPXen(23-69) internalised in the biotinylation assay depicted in (A), expressed as a percentage of total labelled protein without trypsin digestion (at the same chase time) and plotted as a function of different time points.

A similarly interesting result was obtained in a pulse-chase analysis performed in order to follow the transport of Xen(23-69) through the secretory pathway. After a short metabolic pulse of 5 min, the protein was chased for up to 75 min as done previously with other constructs, deglycosylated with PNGase-F and then precipitated with the antibody A7 (**Fig. 23**). Removal of surface localised proteins with trypsin revealed intracellular localisation of the chimeric construct until 45 min following the pulse; after 60 min of chase the signal became very faint (**Fig. 23A**, lanes 4 and 5). This kinetic of secretory transport for Xen(23-69) mirrored those recorded for wtPrP^{c}. Phosphor-Imager quantification revealed that 50% of Xen(23-69) moiety reached the cell surface after ~43 min (**Fig 23B**), a value very similar to that of wild type mouse prion protein. These data suggest that the N-terminus of *Xenopus laevis,* like the corresponding murine sequence, exerts the same intrinsic sorting functions and is able to restore the wild type trafficking kinetics.

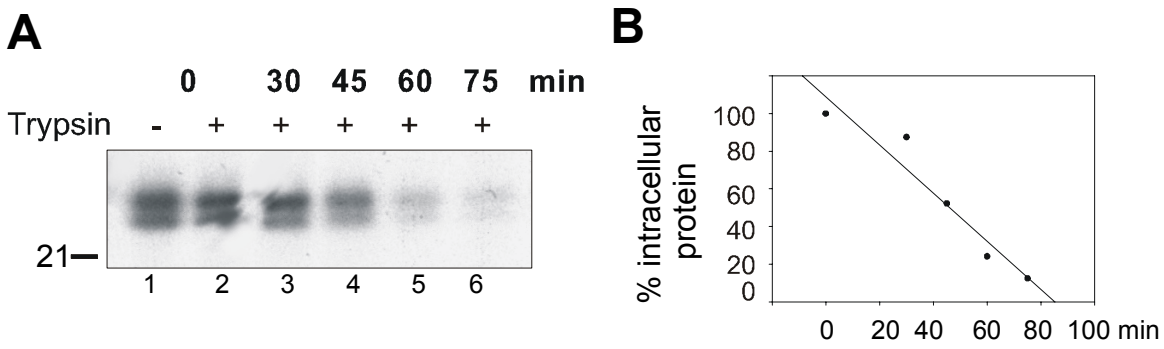

Figure 23. Transport of Xen(23-69) through the secretory pathway to the cell surface

(A) Xen(23-69) was transiently transfected into N2a cells, metabolically labelled with [^{35}S]-Met/Cys for 5 min on ice and then chased in [^{35}S]-free culture medium for 0, 45, 60, 75 min, respectively. One plate was harvested immediately after the pulse or treated with trypsin and then lysed. All other plates were subjected to treatment with trypsin on ice for 10 min before lysis. Proteins were immunoprecipitated with antibody 3F4, deglycosylated with PNGase F and subjected to SDS-PAGE. The blot shows PrP signals before (-) and after (+) treatment with trypsin. A molecular size marker in kDa is shown on the left. The transport of Xen(23-69) to the cell surface is not impaired.
(**B**) Phosphor-Imager evaluation of the autoradiogram. The curve represents the amount of Xen(23-69) detected at each time point, after digestion with trypsin. Each point represents a mean value of two independent experiments. Quantities are calculated as a percentage of protein precipitated immediately after the pulse without trypsin-treatment.

4 Discussion

When the term prion was proposed by Prusiner in 1982, as the proteinaceous infectious particle responsible for numerous infectious neurodegenerative diseases in animals and humans, researchers were confronted for the first time with a pathogen which does not rely on nucleic acid for its own propagation. Huge steps toward the characterisation of the chemical properties and mode of transmission of the protease resistant PrP^{Sc}, of which prions mainly if not solely consist, have been made since then. It is nevertheless clear that full understanding of the mechanisms underlying these diseases also requires the knowledge of the function and the metabolism of the host encoded cellular PrP^{c}, the protein undergoing profound conformational alteration and conversion into its pathogenic isoform. Despite the great body of knowledge obtained so far about structure and processing of the prion protein, several questions remain unanswered. Exceeding work has been done lately in order to characterise the still undefined function of this protein. The N-terminal part of the protein and its involvement in a cellular function have been a matter of intense study. In both, the mainly α-helical PrP^{c} and the PrP^{Sc}, with its high β-sheet content, the N-terminus of the protein is devoid of a globular structure and remains protease sensitive after scrapie conversion (Riek *et al.*, 1997; Donne *et al.*, 1997; Liemann and Glockshuber, 1998; Prusiner, 1998). Still, during evolution, this segment of the prion protein has remained highly conserved, suggesting a defined pressure or a reason for this conservation. Following the work of other groups, the study presented here assesses a possible targeting function of the segment comprising residues 23-90 of the mouse PrP^{c} in the life cycle of this protein.

4.1 N-terminal deletion does not affect the biochemical properties of the prion protein

The constructs analysed in this study were based on the mouse PrP sequence and lacked segments of different length in their N-terminal end. The first experiments aimed at the characterisation of their biochemical properties. These were compared to those of the wild type prion protein in order to exclude that conformational changes or overexpression might influence the outcome of the subsequent analysis. The assays chosen for this purpose have often been used to differentiate between the pathogenic and the cellular isoform of the prion protein according to their different solubility in detergent and their sensitivity to treatment with PK. They have also been applied for characterisation of several PrP mutants expressed in cell culture or rescued from *in vivo* studies (Taraboulos *et al.*, 1990a; Lehmann and Harris, 1997). The insolubility and partial PK-resistance of PrP^{Sc} reflects its aggregated, conformationally altered state. When the deletion constructs were expressed in N2a cells and

were subjected to the mentioned assays, their behaviour did not differ from that of the wtPrP^c. They all showed similar glycosylation patterns (un-, mono- and di-glycosylated form of the protein), although, according to their mobility on a polyacrylamide gel, some of the deletion mutants seemed to display glycans of higher molecular weight. Upon digestion with PNGase F, these proteins all migrated as a single unglycosylated band. The fact that in the following experiments membrane impermeable biotin could bind to them and that they could be cleaved from the cell surface by treatment with trypsin, confirmed that, at a steady state, these proteins were localised at the plasma membrane and showed similar levels of expression. Inside the cell, regulation of protein expression is ensured by quality control mechanisms operating at a the ER level and downstream along the secretory pathway. These mechanisms apply to misfolded and as well as to incompletely assembled proteins. The main strategies include retention in the ER, ER-associated degradation (ERAD) and retrieval to the ER from other organells. If proper maturation and folding with the assistance of ER-chaperones and folding enzymes fail, proteins are retranslocated to the cytosol and degraded by the proteasome. Truncations in the N-terminal polypeptide sequence of the PrP constructs did not seem to prevent correct folding in a way that would activate the quality control of the cell, as it was the case for other described PrP mutants (Rogers *et al.*, 1990 ; DeArmond *et al.*, 1997; Zanusso *et al.*, 1999). Even a Golgi/TGN-based system for re-routing and lysosomal degradation of aberrantly folded proteins, described in yeast (Ellgaard *et al.*, 1999) and recently proposed in an anti-prion study (Gilch *et al.*, 2001), does not seem to apply to N-terminally truncated prion proteins analysed in the present study.

4.2 Progressive deletions within the N-terminus of PrP^c result in reduced endocytosis

Previous work done by other groups has characterised the endocytosis of the chicken PrP^c (Shyng *et al.*, 1993; Shyng *et al.*, 1995b). Surface iodination and immunofluorescence microscopy have shown that this protein is rapidly internalised, with 40-50 % recovered inside the cell after 30 min of chase. This PrP^c cycles between the cell surface and endocytic compartments where it is subjected to a proteolytic cleavage to yield a COOH-terminal fragment. These results are consistent with earlier investigations in cell culture extracts and partially purified fractions from the brain of Syrian hamsters which identified an N-terminally truncated molecule labelled PrP^c-II representing a first degradation product of PrP^c (Haraguchi *et al.*, 1989; Pan *et al.*, 1992).

The analysis of the internalisation kinetics of mouse PrP^c in the present work revealed that the endocytic pathway was impaired for all PrP deletion constructs when compared to wtPrP^c

and that the degree of impairment correlated with the length of the deletion. About $^{3}/_{4}$ of the total surface labelled wtPrP^{c} entered the cell after 60 min of chase, whereas deletion of the pre-octapeptide segment negatively affected this pathway. The effect of the N-terminal truncation on the endocytosis of PrP was particularly evident when the internalisation of PrPΔ(23-90) and PrPΔ(48-93) was analysed: only after 10 h of chase 65 % of the total amount of surface labelled PrPΔ(48-93) could be detected intracellularly. At the same time point, PrPΔ(23-90) was still mainly localised on the cell surface. Interestingly, the glycosylation patterns monitored for the biotinylated contructs differed slightly from those monitored in the Western blot. One explanation for this evidence could be that the relative amount of glycosylation appears to be dependent on the cellular localisation of PrP^{c} (Vorberg and Priola, 2002) and the labelled population localised at the plasma membrane could therefore present different glycan ratios and profiles than the total PrP^{c} population monitored in a Western blot analysis. Of note, unglycosylated PrP, which was rarely detected upon biotin labelling in the present study, was reported to be transported with slower kinetics to the plasma membrane (Taraboulos *et al.*, 1992; Borchelt *et al.*, 1990). The biotinylation studies reported here support the work done on chicken PrP^{c}, although mouse PrP^{c} seems to have slower internalisation kinetics. These differences might be explained by relatively poor homology between mammalian and avian PrP (~30 %) and by the longer N-terminus of chicken PrP which contains 8 hexapeptide repeats (Harris *et al.*, 1991). The C-terminal fragment (20 kDa) described for chicken PrP upon proteolytic cleavage of the wild type protein in the endocytic compartments could not be detected in the biotinylation assays, either due to the slow rate at which this fragment is produced (~ 1 %/ h) or due to the slower kinetics monitored for mouse PrP. The endocytosis of murine PrP has also been analysed in other studies (Sumudhu *et al.*, 2001). The binding of copper to the histidine residues contained within the octapeptide repeats of PrP^{c} has been seen to affect the cell surface localisation of the protein by stimulating endocytosis (Pauly and Harris, 1998; Marella *et al.*, 2002). In these studies, deletions or mutations within the octapeptides abolished endocytosis. The assays presented here indicate that the octapeptide repeats are not the only element in the PrP sequence with an internalisation-promoting function, since considerable differences between the internalisation kinetics of PrPΔ(23-90) and PrPΔ(48-93) could be detected. The analysis of the endocytosis of PrPΔ(23-51) supported this hypothesis. This construct presenting deletion of the residues preceding the octapeptide repeats also showed impairment in its endocytosis, although not as strong as for PrPΔ(23-90). This would not be expected if only the octarepeat segment had a role in promoting internalisation.

The systems involved in importing proteins into the cell lead to several pathways in which proteins follow different routes. Transmembrane receptors that localise at the plasma membrane slide laterally into invaginations called coated pits surrounded by the 180 kDa protein clathrin for endocytosis (49-51 rev). These vesicles are released into the cytoplasm to form endocytic vesicles which transport their content toward the interior of the cell and fuse with the membrane of target compartments such as early endosome. The common mechanism in this process requires a relatively short sequence motif in the cytoplamic tail of the transmembrane proteins which is recognised by the multimeric adaptor protein complex AP-2, (Bonifacino and Dell'Angelica, 1999; Matter, 2000), leading to protein-protein interaction followed by internalisation. These domains are often characterised by the presence of a tyrosine residue to form a signal of the type YXXϕ (where X represents Tyrosin, XX other amino acids and ϕ a residue with a bulky hydrophobic side chain), or NPXY (Asn-Pro-X and Tyr) located close to the C-terminus. In proteins that are internalised in response to ligand binding, the internalisation signal may be generated by a change in the conformation as a result of the binding. The lack of cytoplasmic domains in GPI-anchored proteins requires different mechanisms for their internalisation than those described above. PrP^c, like most GPI-anchored proteins (Parton *et al.*, 1994; Skretting *et al.*, 1999; Nichols *et al.*, 2001), seems to be endocytosed via a clathrin-independent pathway, by associating with the glycosphingolipid- and cholesterol-rich raft membranes (Taraboulos *et al.*, 1995; Vey *et al.*, 1996). Functionally different GPI-proteins have been shown to cluster within sphingolipid rafts at different densities and on different domains on the plasma membrane of the same cell (Madore *et al.*, 1999). While, for example, the small adhesion molecule Thy-1 occupies a highly insoluble, fully ordered domain, rafts where PrP^c is clustered appear to form a marginal boundary of semi-ordered lipids flanking the glycerolipid domain in which transmembrane proteins are embedded. Several transmembrane receptors have been shown to have GPI proteins as ligand binding subunits or to bind to GPI-anchored proteins and to translocate between different plasma membrane domains (e.g. the receptor for ciliary neurotrophic factor) (Davis and Yancopoulos, 1993). As described for the urokinase-type plasminogen activator (uPA) receptor (Nykjaer *et al.*, 1992), clustering of PrP^c in an intermediate semi-ordered lipid domain could promote binding to an endocytosing transmembrane factor. The data shown in the present work support a similar model in which the N-terminal half of PrP^c binds, either directly or indirectly, to the extracellular part of a transmembrane protein containing internalisation motifs. The N-terminal segment of PrP^c (or multiple regions within it) can represent the element responsible for this binding. The impairment in endocytosis seen for the

deletion constructs could therefore be explained by a reduced ability of these PrPs to bind to a putative receptor due to deletions within the binding epitope. It can not be ruled out that other elements in the polypeptide chain of PrP^c might also play a role in this process.
Recently, cell-binding and internalisation assays done by other groups have shown that the 37-kDa laminin receptor precursor (LRP) and its mature form, the 67-kDa laminin receptor (LR), localise with PrP^c on the cell surface and promote endocytosis of PrP (Gauczynski *et al.*, 2001). It was therefore concluded that these molecules act as main cell surface receptors for PrP. As one of the two identified LRP-binding domains in the PrP sequence was mapped between amino acid 53 and 93 (Hundt *et al*., 2001), the 37-kDa/67-kDa laminin receptor might be involved in the impaired trafficking of PrP^c described here.

4.3 The N-terminal truncated form of the prion protein is not exceedingly released into the culture medium and accumulates in lysosomes upon protease inhibition

The prolonged presence of PrPΔ(23-90) at the outer leaflet of the plasma membrane identified in long chase period experiments led to first steps toward the characterisation of the fate of this protein. Several GPI proteins are shed from the cell membrane and exist as soluble proteins (Mizukami *et al.*, 1995; Smith *et al.*, 1997). Detectable levels (10-30 %) of PrP^c have been found in the medium of cultured neuroblastoma cells following chases of 4 and 16 hours (Caughey *et al.*, 1989). Recent work done with primary splenocytes monitored high amount of soluble PrP^c shed into the medium (Parizek *et al.*, 2001), probably due to the presence of phopspholipases contained in the culture medium, similarly to other GPI proteins (Lehto and Sharom, 1998). The levels of $wtPrP^c$ and PrPΔ(23-90) rescued in the medium of the transfected cells in the described assay were comparable, there was no indication of an increased amount of N-terminal deleted protein shed by the neuroblastoma cells. The molecular weights of the proteins recovered in the serum and deglycosylated did not differ form those detected on the cell surface or intracellularly in other experiments, which leads to the assumption that phospholipases which might cleave the GPI-anchor from PrP^c do not play a major role in this shedding process. As the level of actively released or catabolised PrPΔ(23-90) is not enhanced, it was concluded that this protein is eventually internalised by the cell, possibly via different mechanisms than those described for the wild type protein. Inhibition of lysosomal and endosomal proteases with Leupeptin showed that the deletion of the N-terminal part of PrP did not prevent lysosomal localisation of this protein. Replacement of the GPI addition signal of PrP^c with the transmembrane and cytoplamic regions of mouse CD4 (Taraboulos *et al.*, 1995) or with other C-terminal transmembrane domains (Kaneko *et al.*,

1997a) targeted the protein to clathrin coated pits instead of cholesterol-rich membrane domains for internalisation. A re-routing of PrP^c by the deletion of its N-terminal domain might be possible. Regardless of the pathway leading to endocytosis, this protein eventually reaches these acidic compartments for degradation. Additional degradation pathways for a subpopulation of this protein can not be ruled out and have to be assessed by use of specific inhibitors in the future.

4.4 Deletion of the N-terminal part significantly affects PrP^c turnover

The reduced efficiency in endocytosis of PrP molecules with extended deletions in their N-terminal sequence of their peptide chain allowed the assumption that these deletions might influence the turnover of these proteins. This hypothesis was confirmed in pulse-chase experiments which revealed a much longer half-life for the constructs with more pronounced truncations when compared to the $wtPrP^c$. The half-life monitored for $wtPrP^c$ in this assay was 2.6 h. This value was similar to that recently reported for PrP^c degradation in primary cell cultures derived from lymphoid and nervous tissues (Parizek *et al.*, 2001) and in neuroblastoma cells (Gilch *et al.*, 2001), although it is slightly shorter than that reported in studies done by other groups on endogenous PrP^c with scrapie infected and uninfected neuroblastoma cells (Caughey *et al.*, 1989; Borchelt *et al.*, 1990). On the other hand, the values registered for the two deletion constructs analysed in this study, the half-life was almost twice as long as for the wild type. These values correlate with the rate of endocytosis described earlier but they could also stand for a different pathway of internalisation. So far, it is not known whether raft specific proteases participate in PrP^c degradation. Several GPI-anchored peptidases have been described (Deddish *et al.*, 1990; Hooper *et al.*, 1990). Additional putative PrP^c cleaving enzymes could also be present at the cell surface. A shift in the plasma membrane localisation of the construct analysed here could lead to decreased affinity or accessibility to the polypeptide chain and therefore result in prolonged turnover of the deletion proteins observed in this study. The analysis of murine homologues of mutations in the PrP gene associated with human prion diseases showed that these mutations can affect their biochemical properties and intracellular trafficking (Lehmann and Harris, 1996), but prolonged half-lives were not described. Of note, the constructs described in the present work did not display any evident alteration of their biochemical properties but nevertheless showed a distinctive subcellular trafficking. Interestingly, several compounds which strongly inhibited PrP^{Sc} formation by enhancing the rate of PrP^c endocytosis, did not affect the turnover of PrP^c,

although they shifted the distribution of this protein from the cell surface to an intracellular location (Shyng *et al.*, 1995a).

4.5 The N-terminus of PrP^c and the secretory pathway

The sorting of proteins to the cells surface along the secretory pathway is not a simple default process, since specific signals, closely related to those used for internalisation, are required for the inclusion of cargo into secretory vesicles and for its transport to the plasma membrane. The evidence obtained in the above mentioned assays for a modulating role of the N-terminal part of the prion protein in the endocytic pathway which also interferes with its degradation, led to the question of whether these effects are symptomatic of a more general function of this amino acid segment as a sorting determinant. The assay performed in the present work in order to characterise the transport of $wtPrP^c$ and the deletion constructs evidenced that the majority of the wild type molecules reached the cell surface within 1 h after the pulse. These values are in line with those reported by other groups (Caughey *et al.*, 1989; Borchelt *et al.*, 1990). Conversely, the transport of all the constructs lacking more or less extended portions of the N-terminal part occurred with lower efficiency. Although the impairment monitored here was not as pronounced as for the endocytic pathway, the kinetics of the two constructs presenting the longest deletions were characterised by a delay of almost 50 % compared to the wild type protein. These results also evidenced that even relatively small deletions can considerably impair the trafficking of the PrP^c through the secretory pathway, as seen for PrPΔ(23-51) and PrPΔ(68-91). Of note, the different impact with which the N-terminal deletions affect the two pathways in the life cycle of the PrP^c analysed, argue for the specificity of these results.

The first attempt toward the characterisation of this impaired pathway in more detail was the Endo-H digestion of PrPs on the way to the plasma membrane. The aim was to localise a specific cellular compartment or vesicle in which the transport of the truncated proteins was hindered, which can be seen by the sensitivity of proteins to this enzyme depending on their localisation. This analysis revealed that, although first signs of complex oligosaccharides in the form of an Endo-H resistant monoglycosylated protein were detected at slightly different times (30 min for $wtPrP^c$ and 40 min for PrPΔ(23-90) and PrPΔ(48-93)), complete resistance of the fully glycosylated proteins was achieved for all constructs after ~50 min. These experiments also evidenced that immediately after 5 min of metabolic labelling $wtPrP^c$ as well as the deletion mutants were glycosylated. Since Endo-H hydrolysis of N-linked high mannose oligosaccharides attached to glycoproteins only occurs in the ER and cis/mid-Golgi,

the kinetics monitored here argue for the trans-Golgi or a post-trans-Golgi compartment as a probable site where the impairment in the transport to the cell occurs. A delay in the transport at an ER- or ER-Golgi intermediate compartment would result in retention in or retrieval to the ER from downstream organelles and in proteasomal degradation. Since all proteins are expressed on the cell surface, this is therefore less likely.

This finding is in line with several studies about the biogenesis of epithelial cell surface polarity. In polarised cells, where the plasma membrane comprises functionally distinct domains differing in protein and lipid composition (Simons and van Meer, 1988; Rodriguez-Boulan and Powell, 1992; Craig and Banker, 1994) , the development and maintenance of this polarised distribution is achieved by the sorting of protein and lipid cargo via different trafficking routes from the TGN (Winckler and Mellman, 1999; Mostov *et al.*, 2000). It is in the lumen of the TGN that glycosphingolipids and cholesterol associate into clusters linked together by hydrogen bonds involving the sugar head groups in the exoplasmic leaflet and acyl chains to form lipid rafts. Cholesterol molecules function as spacers in the cytoplasmic leaflet between associating sphingolipids. These microdomains represent the carriers for delivery of proteins to the cell surface via the apical route. Vesicular integral membrane proteins (VIPs) associate to these sorting platform as stabilisers or as linkers to other proteins in the rafts (Fiedler *et al.*, 1994). In this pathway, carriers move along microtubules to the apical surface (Lafont *et al.*, 1999). After having crossed the subcortical network of actin cytoskeleton (Ojakian and Schwimmer, 1988; Fath and Burgess, 1993), the apical carriers dock and fuse with the cell surface by a mechanism involving the ubiquitous SNARE (soluble N-ethyl maleimide-sensitive receptor). As mentioned above, several specific protein determinants are required for incorporation of proteins into rafts and correct basolateral or apical transport. These are based on protein-protein (Mellman, 1996) or protein-lipid affinities via sequences in their polypeptide chains (Eaton and Simons, 1995; Simons and Ikonen, 1997). Lipid attachment (e.g. palmitoylation) and N-glycans for secretory and membrane proteins can also serve as a targeting signal in cooperative protein-lipid affinities (Scheiffele *et al.*, 1995; Zhao *et al.*, 2000). The GPI anchor has been recognised as an important targeting domain for inclusion of proteins into rafts and correct delivery to the cell surface in different polarised epithelial cell types (Lisanti *et al.*, 1989; Brown *et al.*, 1989), beside acting as a sorting motif for exit from the ER (Muniz and Riezman, 2000). It was also seen to act in the sorting of PrP^{c}: the substitution of the lipid anchor with a transmembrane domain redirected the prion protein to clathrin coated pits and prevented conversion into PrP^{Sc} (Taraboulos *et al*., 1995, Kaneko *et al*., 1997a). More recent studies have evidenced a slower transport of

PrP^c trough the secretory pathway when the GPI- addition signal is missing and argue for glycosylation and membrane anchorage as co-operative processes (Walmsley *et al.*, 2001). The studies reported here suggest that also the N-terminal part of PrP^c is involved in subcellular trafficking and therefore represents one of the targeting signals for effective transport of PrP^c both through the secretory pathway and for endocytosis. The deletion constructs analysed in this study do not seem to activate the ER- or post-ER-based cellular quality control mechanisms and therefore reach the plasma membrane. Nevertheless, the deletions might still influence the conformation of the protein which can explain the differences in the glycosylation patterns seen between the deletion mutants. This phenomenon would confirm the hypothesis raised by other groups, that the N-terminal region of PrP^c might stabilise the conformation of the C-terminal domain of the molecule (Zulianello *et al.*, 2000). Indeed this could also explain the slightly slower kinetics of the monoglycosylated form of the deletion mutants for acquisition of Endo-H resistance. Given the function of glycans in stabilisation and correct folding of proteins, the double glycosylation might compensate for a change in the conformation of the N-terminal deletion mutants, which would otherwise make the protein less capable of travelling through the secretory pathway (as seen for the monoglycosylated form). Although the deletion mutants are not subjected to ERAD, the impaired trafficking described here shows reduced capacity of the cell to properly deal with these proteins. The model proposed earlier for the delay in the endocytosis of truncated PrPs, i.e. the binding of PrP^c via its N-terminus to a transmembrane receptor promoting internalisation of the PrP can also apply to the secretory pathway: The same amino acidic stretch could therefore, as a single motif or as part of a larger epitope, together with other elements of the molecule, serve as a determinant for inclusion into rafts, proper apical sorting and for internalisation from the cell surface. Truncations within this segment decrease the affinity for the specific transmembrane receptor and lead therefore to impaired trafficking. Since all mutants eventually reach the plasma membrane and can be detected in the endocytic pathway, it can be assumed that, as seen with other studies on the trafficking of PrP^c, other segments of the protein are also involved in the subcellular trafficking or the cells are able to switch on alternative pathways for proteins that escape the ER-based quality control. As a matter of fact, the plasma membrane domain in which the deletion mutants localise has not been characterised, yet. Of note, the phospholipid binding protein annexin XIIIb which binds to rafts budding off the TGN and acts at the TGN level and at the cell surface, is apically localised and is involved in the formation of apical transport vesicles (Lafont *et al.*, 1998). The apical targeting of this protein is determined by a 41 amino acid stretch in its N-terminal

tail, as its isoform annexin XIIIa lacks this sequence and is localised basolaterally (Lecat *et al.*, 2000). Several proteins interacting with PrP^c have been identified using different biophysical assays (Kurschner and Morgan, 1996; Edenhofer *et al.*, 1996; Rieger *et al.*, 1997; Chebassier *et al.*, 2001), yet the question of whether any of these interactors or a complete different molecule is involved in the correct trafficking of PrP^c remains open.

4.6 Targeting function of the PrP N-terminus is conserved in evolution

The involvement of the N-terminus of the mouse PrP in subcellular trafficking led to the question of whether the corresponding sequence in the PrP^c of more remote species might exert the same functions. The recent analysis of *Xenopus laevis* prion protein (Strumbo *et al.*, 2001) allowed the construction of a chimeric *Xenopus*/mouse prion protein and to characterise its trafficking. The chimeric and the wild type mouse PrP^c shared similar biochemical features. Surprisingly, the addition of the *Xenopus* N-terminal segment to the truncated mouse PrP almost restored the wild type trafficking phenotype, and the internalisation and the secretory kinetics monitored for this construct significantly differed from those reported for PrPΔ(23-90) and PrPΔ(48-93).

These data were quite unexpected. In spite of the relatively low identity between the mouse and the *Xenopus* PrP^c (28 % for the entire amino acid sequence), the first 34 residues following the N-terminal signal peptide in *Xenopus* mainly retain the character and composition of the regions immediately following or preceding the octapeptides in mammals, especially in the basic charged N-proximal segment. Still, the Xenopus PrP^c lacks the octarepeat region and is completely devoid of histidines (Strumbo *et al.*, 2001). The numerous lines of evidence collected *in vivo* and *in vitro* show that transition metals, especially copper, bind to PrP^c (Brown *et al.*, 1997a). This has suggested several functions for the protein all related to the metabolism of these metals. The cooperative binding of copper to the four histidines contained within the octapeptide repeats is assumed to be the mechanism underlying these functions. The absence of both octapeptides and histidine residues in *Xenopus* suggests that copper binding might not be the primary function of PrP^c. Recently, a previously unreported high affinity binding site for divalent transition metals around histidines 96 and 111 of the human PrP^c (Jackson *et al.*, 2001), and additional interaction of copper with the structured domain of mouse PrP^c was reported (Cereghetti *et al.*, 2001). These results seem to confirm the importance of copper in the function of PrP^c, and that neuronal damage in prion diseases might be a consequence of perturbation in copper transport upon conversion of PrP^c into PrP^{Sc}. Nevertheless, the observation that the histidine content of PrP

increases with the evolutionary level (1.5 % and 4 % of the amino acid residues in avian and mammalian PrP, respectively), the functional hypothesis concerned with copper binding might have developed later in evolution, with the development of the octapeptide repeats as a domain of the protein specialised in this role. The reported stimulation of PrP^c endocytosis upon exposure of neuronal cells to physiologically relevant concentrations of copper or zinc contained in the culture medium (Pauly and Harris, 1998; Sumudhu *et al.*, 2001) was not assessed in the present study, as no addition of metals was given into the culture medium. Nevertheless, relevant levels of copper could already be present in the culture medium. In the case of the chimeric *Xenopus*/mouse PrP^c which was internalised despite the absence of histidine residues, the additional binding sites in the C-terminal part of the molecule might possibly be sufficient for correct endocytosis. Despite the differences in the polypeptide chain, the N-terminal segment of the *Xenopus* PrP^c was able to properly direct subcellular trafficking when fused to PrP^c of another species. These data argue for a conserved, intrinsic sorting function of this segment.

Although deletion of residues 23-88 of the prion protein did not alter the synthesis of PrP^{Sc} in cell culture models (Rogers *et al.*, 1993) and mice expressing such a protein were still susceptible to prion propagation (Fischer *et al.*, 1996), several works argue for a physiological relevance of this segment of the prion protein. Flechsig and collegues showed that mice expressing a PrP devoid of residues 23-93 still sustain scrapie infection but with longer incubation times. Prion titres and protease resistant PrP are about 30 fold lower than in wild type mice, with no histopathology typical for scrapie (Flechsig *et al.*, 2000). These data were supported by the *in vitro* studies performed by Lawson and collegues in which PrP^c lacking a segment comprising residues 34-94 reduced the conversion efficiency in a cell-free conversion assay (Lawson *et al.*, 2001). In light of the results reported here, these findings could also be explained by altered intracellular trafficking of the mutated prion protein due to the alterations in the N-terminal part. In a different study, the basic N-proximal segment of PrP^c modifies the binding to the hypothetical protein X by altering the structure of the binding epitope therefore influencing the structure of the molecule (Zulianello *et al.*, 2000). Clinical studies have shown that addition of two to nine octapeptides to the normal five segregate with a familial form of Creutzfeldt Jakob disease (Owen *et al.*, 1989 ; Owen *et al.*, 1990; Owen *et al.*, 1992) and non-transmissible prion disease in transgenic mice (Chiesa *et al.*, 2000). Analysis of the biochemical properties of such PrP mutants in cell culture revealed aggregation and insolubility in non-ionic detergents, and resistance to protease digestion. These insertions caused a change in the conformation of the molecule which led to an

abnormal association with the plasma membrane when expressed in cultured cells (Shyng *et al.*, 1995a). In general, the question remains, whether alterations in the trafficking of PrP and of other neurodegenerative proteins are important in the pathogenesis of sporadic forms of neurodegenerative disorders.

The work described in this study adds to all this evidence and helps delineating a conserved biological role of the elusive N-terminus of the prion protein. Additionally, the finding that the trafficking of the chimeric *Xenopus*/mouse protein was not altered despite the absence of octarepeats, argues in favour of a model in which copper binding to the octapeptide repeats and subcellular trafficking represent separate aspects in the life-cycle of the prion protein.

5 Summary I (English version)

Transmissible spongiform encephalopathies (TSEs) are degenerative diseases of the central nervous system in humans and animals, and include Creutzfeldt-Jakob disease (CJD) in humans, scrapie in sheep and bovine spongiform encephalopathy in cattle. These spongiform encephalopathies can manifest as sporadic, familial and acquired disorders and are caused by the conformational alteration of the non-pathogenic cellular prion protein (PrP^{c}) into a infectious isoform denoted PrP^{Sc}. The latter therefore represents a pathogenic agent (prion) which does not contain nucleic acids. During biogenesis, PrP^{c} undergoes posttranslational modifications with the addition of two N-linked carbohydrate chains and a glycosyl-phosphatidyl-inositol-(GPI)-anchor. Properly folded PrP^{c} transits through the Golgi compartment and the secretory pathway and is attached to the outer leaflet of the plasma membrane by the GPI-anchor. The cellular function of the prion protein is still unknown, although binding of copper to the octapeptide repeat sequence located at its N-terminus suggests a role of PrP^{c} related to this phenomenon.

In the present work, the physiological function of the N-terminal part of PrP^{c} in subcellular trafficking was analysed. Metabolic labelling and surface-biotinylation assays were performed in order to compare the intracellular trafficking and turnover of PrP^{c} mutants showing specific deletions within their N-terminal sequence with those of wild type PrP^{c} ($wtPrP^{c}$). Upon transient expression of these constructs in murine neuroblastoma cells, these deletions, although not influencing the biochemical properties or the cell surface expression of these proteins, lead to a delay in their endocytosis. The prolongation of the internalisation kinetics was shown to be dependent on the length of the deletion: truncation of the complete N-terminus leads to the almost complete inhibition of internalisation. The analysis of the kinetics of degradation showed a similar correlation with the N-terminal part of PrP^{c}, since the half-life of the PrP-mutants was significantly prolonged when compared to that of the wild type protein. Additionally performed detailed analysis of the secretory pathway with immunoprecipitation assays showed that N-terminally truncated PrP molecules reach the plasma membrane at a later time point, when compared with $wtPrP^{c}$. A closer analysis of the processing of the sugar molecules linked to these proteins performing an Endo-H digestion revealed that this delay in the transport to the cell surface takes place in a cellular compartment following the mid-Golgi.

The following studies were done with a chimeric protein consisting of the short N-terminal segment of *Xenopus laevis*, which does not contain the copper-binding octarepeat region, fused to the N-terminally truncated mouse PrP^{c}. These studies showed that endocytosis of this

protein and its transport through the secretory pathway were comparable to those of the mouse wtPrP^c. It was therefore concluded that the N-terminus belonging to a phylogenetically remote species can rescue the wild type trafficking phenotype.

These results indicate that the N-proximal domain of the prion protein functions as a targeting element and is essential for both transport to the plasma membrane and modulation of endocytosis. The data support a model in which the N-terminal part of PrP^c represents an epitope for binding to a transmembrane receptor containing internalisation-promoting motifs or for inclusion of PrP^c into the secretory raft-compartments. The present work also indicates for the first time that copper affinity of the octarepeats and subcellular trafficking represent separate aspects in the life-cycle of the prion protein.

6 Summary II (German version)

Die transmissiblen spongiformen Enzephalopathien (TSEs) bilden eine Gruppe fataler degenerativer Erkrankungen des zentralen Nervensystems von Mensch und Tier, deren bekannteste Erscheinungsformen die bovine spongiforme Enzephalopathie (BSE) beim Rind, die Traberkrankheit beim Schaf sowie die Creutzfeldt-Jakob-Erkrankung beim Menschen sind. Diese Erkrankungen können als Folge von Mutationen familiär-genetisch bedingt sein, infektiös erworben werden oder ohne erkennbare Ursache (sporadisch) auftreten. Das Auftreten und die Übertragung dieser Erkrankungen sind auf eine posttranslationale Umwandlung des apathogenen zellulären Prion-Proteins (PrP^{c}) in eine infektiöse Isoform (Scrapie-Form, PrP^{Sc}) zurückzuführen, sodass dieses Protein ohne eine damit assoziierte Nukleinsäure als pathogenes Agens (Prion) fungiert. PrP^{c} wird posttranslational glykosyliert und gelangt im Verlauf seiner Maturierung entlang des sekretorischen Transportwegs an die Zelloberfläche, an die es durch einen GPI-Anker verknüpft wird. Die Funktion des Prion-Proteins ist noch unbekannt, obwohl mehrere Untersuchungen eine Bindung von Kupfer an die N-terminal vorliegenden „Octarepeats“ von PrP^{c} feststellen konnten und deshalb dem Prion-Protein eine mit dieser Eigenschaft in Zusammenhang stehende Funktion zugeschrieben wird.

In der vorliegenden Arbeit wurde die physiologische Funktion des N-terminalen Anteils von PrP^{c} im intrazellulären Transport untersucht. Mittels metabolischer Markierung und Oberflächen-Biotinylierung wurde das Verhalten und die Halbwertszeit von PrP-Mutanten, die spezifische Deletionen in der N-terminalen Sequenz aufweisen, mit denen des Wildtyp-Proteins ($wtPrP^{c}$) verglichen. Nach transienter Expression dieser Mutanten in murinen Neuroblastomzellen konnte gezeigt werden, dass die Deletionen weder die biochemischen Eigenschaften noch die Zelloberfächenexpression dieser Proteine beeinflussen, aber dennoch zu einer signifikanten Verlangsamung ihrer Endozytose führen. Die Verlängerung der Internalisierungskinetik erwies sich als abhängig von der Länge der Deletion: die Abspaltung des kompletten N-Terminus erbrachte nahezu eine Inhibierung der Internalisierung des Proteins. Eine Analyse der Degradationskinetik zeigte weiterhin, dass dieser Prozess im gleichen Zusammenhang mit dem N-terminalen Bereich von PrP^{c} steht, da die Halbwertszeit der untersuchten PrP-Mutanten deutlich länger ist als die des Wildtyp-Proteins. Wie durch detaillierte Analyse des sekretorischen Transportweges mittels Immunpräzipitation weiterhin gezeigt werden konnte, erreichen N-terminal verkürzte PrPs die äußere Plasmamembran zu einem späteren Zeitpunkt als das $wtPrP^{c}$. Die Untersuchung der Glykosylierung dieser Proteine mittels Endo-H Verdau ergab, dass die Verzögerungen im Transport zur

Zelloberfläche erst stattfinden, nachdem PrP^c das mid-Golgi Kompartiment erreicht hat. Die Analyse eines chimären PrPs, bestehend aus dem N-Terminus von *Xenopus laevis*, der keine für die Kupferbindung wichtigen Octapeptide enthält, und aus einem N-terminal verkürztem Maus PrP, zeigte, dass sowohl die Endozytose als auch der sekretorische Transportweg dieses Proteins mit dem von murinem $wtPrP^c$ vergleichbar waren. Daraus konnte man schließen, dass der N-Terminus einer phylogenetisch entfernten Spezies den Wildtyp-Phenotyp wiederherstellen kann.

Diese Ergebnisse deuten auf eine wichtige, konservierte Funktion des N-Terminus von PrP^c im gesamten intrazellulären Transport, indem er als Signal für die korrekte Internalisierung und für die Beförderung an die Zelloberfläche dient. Die vorliegenden Daten unterstützen ein Modell, in dem der N-terminale Anteil des Prion-Proteins eine Bindungsstelle für einen transmembranen Rezeptor darstellt, der die Internalisierung bzw. die Eingliederung von PrP^c in die sekretorischen Raft-Kompartimente begünstigt. Es konnte weiterhin erstmals gezeigt werden, dass Kupferbindung an die Octapeptide und intrazellulärer Transport voneinander unabhängige Entitäten im Lebenszyklus des Prion-Proteins darstellen.

7 Reference List

Aguzzi,A., Glatzel,M., Montrasio,F., Prinz,M., Heppner,F.L. (2001). Interventional strategies against prion diseases. Nat.Rev.Neurosci. *2*, 745-749.

Alper,T., Haig,D.A., Clarke,M.C. (1966). The exceptionally small size of the scrapie agent. Biochem.Biophys.Res.Commun. *22*, 278-284.

Anderson,R.M., Donnelly,C.A., Ferguson,N.M., Woolhouse,M.E., Watt,C.J., Udy,H.J., MaWhinney,S., Dunstan,S.P., Southwood,T.R., Wilesmith,J.W., Ryan,J.B., Hoinville,L.J., Hillerton,J.E., Austin,A.R., Wells,G.A. (1996). Transmission dynamics and epidemiology of BSE in British cattle. Nature *382*, 779-788.

Anfinsen,C.B. (1973). Principles that govern the folding of protein chains. Science *181*, 223-230.

Arnold,J.E., Tipler,C., Laszlo,L., Hope,J., Landon,M., Mayer,R.J. (1995). The abnormal isoform of the prion protein accumulates in late-endosome- like organelles in scrapie-infected mouse brain. J.Pathol. *176*, 403-411.

Basler,K., Oesch,B., Scott,M., Westaway,D., Walchli,M., Groth,D.F., McKinley,M.P., Prusiner,S.B., Weissmann,C. (1986). Scrapie and cellular PrP isoforms are encoded by the same chromosomal gene. Cell *46*, 417-428.

Beekes, M. & McBride, P. A. (2000). Early accumulation of pathological PrP in the enteric nervous system and gut-associated lymphoid tissue of hamsters orally infected with scrapie. Neuroscience Letters 278, 181-184.

Bonifacino,J.S., Dell'Angelica,E.C. (1999). Molecular bases for the recognition of tyrosine-based sorting signals. J.Cell Biol. *145*, 923-926.

Borchelt,D.R., Koliatsos,V.E., Guarnieri,M., Pardo,C.A., Sisodia,S.S., Price,D.L. (1994). Rapid anterograde axonal transport of the cellular prion glycoprotein in the peripheral and central nervous systems. J.Biol.Chem. *269*, 14711-14714.

Borchelt,D.R., Scott,M., Taraboulos,A., Stahl,N., Prusiner,S.B. (1990). Scrapie and cellular prion proteins differ in their kinetics of synthesis and topology in cultured cells. J.Cell Biol. *110*, 743-752.

Borchelt,D.R., Taraboulos,A., Prusiner,S.B. (1992). Evidence for synthesis of scrapie prion proteins in the endocytic pathway. J.Biol.Chem. *267*, 16188-16199.

Brown,D.A., Crise,B., Rose,J.K. (1989). Mechanism of membrane anchoring affects polarized expression of two proteins in MDCK cells. Science *245*, 1499-1501.

Brown,D.R., Qin,K., Herms,J.W., Madlung,A., Manson,J., Strome,R., Fraser,P.E., Kruck,T., von Bohlen,A., Schulz-Schaeffer,W., Giese,A., Westaway,D., Kretzschmar,H. (1997a). The cellular prion protein binds copper in vivo. Nature *390*, 684-687.

Brown,D.R., Schmidt,B., Kretzschmar,H.A. (1996). Role of microglia and host prion protein in neurotoxicity of a prion protein fragment. Nature *380*, 345-347.

Brown,D.R., Schmidt,B., Kretzschmar,H.A. (1998). Effects of copper on survival of prion protein knockout neurons and glia. J.Neurochem. *70*, 1686-1693.

Brown,D.R., Schulz-Schaeffer,W.J., Schmidt,B., Kretzschmar,H.A. (1997b). Prion protein-deficient cells show altered response to oxidative stress due to decreased SOD-1 activity. Exp.Neurol. *146*, 104-112.

Brown,D.R., Wong,B.S., Hafiz,F., Clive,C., Haswell,S.J., Jones,I.M. (1999). Normal prion protein has an activity like that of superoxide dismutase. Biochem.J. *344 Pt 1*, 1-5.

Brown, K. L., Stewart, K., Ritchie, D., Mabbott, N. A., Williams, A., Fraser, H., Morrison, W. I. & Bruce, M. E. (1999). Scrapie replication in lymphoid tissues depends on PrP-expressing follicular dendritic cells. Nature Medicine 5, 1308-1312.

Brown,P., Liberski,P.P., Wolff,A., Gajdusek,D.C. (1990). Resistance of scrapie infectivity to steam autoclaving after formaldehyde fixation and limited survival after ashing at 360 degrees C: practical and theoretical implications. J.Infect.Dis. *161*, 467-472.

Bruce,M.E., Chree,A., McConnell,I., Foster,J., Pearson,G., Fraser,H. (1994). Transmission of bovine spongiform encephalopathy and scrapie to mice: strain variation and the species barrier. Philos.Trans.R.Soc.Lond B Biol.Sci. *343*, 405-411.

Bruce, M.E., McConnell, I., Will, R.G. & Ironside, J.W. (2001). Detection of variant Creutzfeldt–Jakob disease (vCJD) infectivity in extraneural tissues. Lancet 358, 208-209

Bruce,M.E., Will,R.G., Ironside,J.W., McConnell,I., Drummond,D., Suttie,A., McCardle,L., Chree,A., Hope,J., Birkett,C., Cousens,S., Fraser,H., Bostock,C.J. (1997). Transmissions to mice indicate that 'new variant' CJD is caused by the BSE agent. Nature *389*, 498-501.

Bueler,H., Aguzzi,A., Sailer,A., Greiner,R.A., Autenried,P., Aguet,M., Weissmann,C. (1993). Mice devoid of PrP are resistant to scrapie. Cell *73*, 1339-1347.

Bueler,H., Fischer,M., Lang,Y., Bluethmann,H., Lipp,H.P., DeArmond,S.J., Prusiner,S.B., Aguet,M., Weissmann,C. (1992). Normal development and behaviour of mice lacking the neuronal cell- surface PrP protein. Nature *356*, 577-582.

Butler,D.A., Scott,M.R., Bockman,J.M., Borchelt,D.R., Taraboulos,A., Hsiao,K.K., Kingsbury,D.T., Prusiner,S.B. (1988). Scrapie-infected murine neuroblastoma cells produce protease-resistant prion proteins. J.Virol. *62*, 1558-1564.

Cardin,A.D., Weintraub,H.J. (1989). Molecular modeling of protein-glycosaminoglycan interactions. Arteriosclerosis *9*, 21-32.

Caughey,B. (1991). In vitro expression and biosynthesis of prion protein. Curr.Top.Microbiol.Immunol. *172*, 93-107.

Caughey,B., Kocisko,D.A., Raymond,G.J., Lansbury,P.T., Jr. (1995). Aggregates of scrapie-associated prion protein induce the cell-free conversion of protease-sensitive prion protein to the protease- resistant state. Chem.Biol. *2*, 807-817.

Caughey,B., Race,R.E., Ernst,D., Buchmeier,M.J., Chesebro,B. (1989). Prion protein biosynthesis in scrapie-infected and uninfected neuroblastoma cells. J.Virol. *63*, 175-181.

Caughey,B., Raymond,G.J. (1991). The scrapie-associated form of PrP is made from a cell surface precursor that is both protease- and phospholipase-sensitive. J.Biol.Chem. *266*, 18217-18223.

Cereghetti,G.M., Schweiger,A., Glockshuber,R., Van Doorslaer,S. (2001). Electron paramagnetic resonance evidence for binding of Cu(2+) to the C- terminal domain of the murine prion protein. Biophys.J. *81*, 516-525.

Chebassier,C., Mouillet-Richard,S., Laplanche,J.L., Kellermann,O., Launay,J.M. (2001). [A signaling function for the prion protein]. Pathol.Biol.(Paris) *49*, 191-193.

Chiesa,R., Drisaldi,B., Quaglio,E., Migheli,A., Piccardo,P., Ghetti,B., Harris,D.A. (2000). Accumulation of protease-resistant prion protein (PrP) and apoptosis of cerebellar granule cells in transgenic mice expressing a PrP insertional mutation. Proc.Natl.Acad.Sci.U.S.A *97*, 5574-5579.

Cohen,F.E., Pan,K.M., Huang,Z., Baldwin,M., Fletterick,R.J., Prusiner,S.B. (1994). Structural clues to prion replication. Science *264*, 530-531.

Colling,S.B., Collinge,J., Jefferys,J.G. (1996). Hippocampal slices from prion protein null mice: disrupted Ca(2+)- activated K+ currents. Neurosci.Lett. *209*, 49-52.

Collinge,J. (1997). Human prion diseases and bovine spongiform encephalopathy (BSE). Hum.Mol.Genet. *6*, 1699-1705.

Collinge,J., Beck,J., Campbell,T., Estibeiro,K., Will,R.G. (1996a). Prion protein gene analysis in new variant cases of Creutzfeldt-Jakob disease. Lancet *348*, 56.

Collinge,J., Brown,J., Hardy,J., Mullan,M., Rossor,M.N., Baker,H., Crow,T.J., Lofthouse,R., Poulter,M., Ridley,R., . (1992). Inherited prion disease with 144 base pair gene insertion. 2. Clinical and pathological features. Brain *115 (Pt 3)*, 687-710.

Collinge,J., Rossor,M. (1996). A new variant of prion disease. Lancet *347*, 916-917.

Collinge,J., Sidle,K.C., Meads,J., Ironside,J., Hill,A.F. (1996b). Molecular analysis of prion strain variation and the aetiology of 'new variant' CJD. Nature *383*, 685-690.

Collinge,J., Whittington,M.A., Sidle,K.C., Smith,C.J., Palmer,M.S., Clarke,A.R., Jefferys,J.G. (1994). Prion protein is necessary for normal synaptic function. Nature *370*, 295-297.

Come,J.H., Fraser,P.E., Lansbury,P.T., Jr. (1993). A kinetic model for amyloid formation in the prion diseases: importance of seeding. Proc.Natl.Acad.Sci.U.S.A *90*, 5959-5963.

Craig,A.M., Banker,G. (1994). Neuronal polarity. Annu.Rev.Neurosci. *17*, 267-310.

Davis,S., Yancopoulos,G.D. (1993). The molecular biology of the CNTF receptor. Curr.Opin.Cell Biol. *5*, 281-285.

DeArmond,S.J., Sanchez,H., Yehiely,F., Qiu,Y., Ninchak-Casey,A., Daggett,V., Camerino,A.P., Cayetano,J., Rogers,M., Groth,D., Torchia,M., Tremblay,P., Scott,M.R.,

Cohen,F.E., Prusiner,S.B. (1997). Selective neuronal targeting in prion disease. Neuron *19*, 1337-1348.

Deddish,P.A., Skidgel,R.A., Kriho,V.B., Li,X.Y., Becker,R.P., Erdos,E.G. (1990). Carboxypeptidase M in Madin-Darby canine kidney cells. Evidence that carboxypeptidase M has a phosphatidylinositol glycan anchor. J.Biol.Chem. *265*, 15083-15089.

Dodelet,V.C., Cashman,N.R. (1998). Prion protein expression in human leukocyte differentiation. Blood *91*, 1556-1561.

Donne,D.G., Viles,J.H., Groth,D., Mehlhorn,I., James,T.L., Cohen,F.E., Prusiner,S.B., Wright,P.E., Dyson,H.J. (1997). Structure of the recombinant full-length hamster prion protein PrP(29-231): the N terminus is highly flexible. Proc.Natl.Acad.Sci.U.S.A *94*, 13452-13457.

Donnelly,C.A., Ferguson,N.M., Ghani,A.C., Anderson,R.M. (2002). Implications of BSE infection screening data for the scale of the British BSE epidemic and current European infection levels. Proc.R.Soc.Lond B Biol.Sci. *269*, 2179-2190.

Eaton,S., Simons,K. (1995). Apical, basal, and lateral cues for epithelial polarization. Cell *82*, 5-8.

Edenhofer,F., Rieger,R., Famulok,M., Wendler,W., Weiss,S., Winnacker,E.L. (1996). Prion protein PrPc interacts with molecular chaperones of the Hsp60 family. J.Virol. *70*, 4724-4728.

Ellgaard,L., Molinari,M., Helenius,A. (1999). Setting the standards: quality control in the secretory pathway. Science *286*, 1882-1888.

Fath,K.R., Burgess,D.R. (1993). Golgi-derived vesicles from developing epithelial cells bind actin filaments and possess myosin-I as a cytoplasmically oriented peripheral membrane protein. J.Cell Biol. *120*, 117-127.

Fiedler,K., Parton,R.G., Kellner,R., Etzold,T., Simons,K. (1994). VIP36, a novel component of glycolipid rafts and exocytic carrier vesicles in epithelial cells. EMBO J. *13*, 1729-1740.

Fischer,M., Rulicke,T., Raeber,A., Sailer,A., Moser,M., Oesch,B., Brandner,S., Aguzzi,A., Weissmann,C. (1996). Prion protein (PrP) with amino-proximal deletions restoring susceptibility of PrP knockout mice to scrapie. EMBO J. *15*, 1255-1264.

Fivaz,M., Vilbois,F., Thurnheer,S., Pasquali,C., Abrami,L., Bickel,P.E., Parton,R.G., van der Goot,F.G. (2002). Differential sorting and fate of endocytosed GPI-anchored proteins. EMBO J. *21*, 3989-4000.

Flechsig,E., Shmerling,D., Hegyi,I., Raeber,A.J., Fischer,M., Cozzio,A., von Mering,C., Aguzzi,A., Weissmann,C. (2000). Prion protein devoid of the octapeptide repeat region restores susceptibility to scrapie in PrP knockout mice. Neuron *27*, 399-408.

Fournier,J.G., Escaig-Haye,F., Billette,d., V, Robain,O. (1995). Ultrastructural localization of cellular prion protein (PrPc) in synaptic boutons of normal hamster hippocampus. C.R.Acad.Sci.III *318*, 339-344.

Gabriel,J.M., Oesch,B., Kretzschmar,H., Scott,M., Prusiner,S.B. (1992). Molecular cloning of a candidate chicken prion protein. Proc.Natl.Acad.Sci.U.S.A *89*, 9097-9101.

Gajdusek,D.C., Gibbs,C.J., Alpers,M. (1966). Experimental transmission of a Kuru-like syndrome to chimpanzees. Nature *209*, 794-796.

Gambetti,P., Parchi,P., Petersen,R.B., Chen,S.G., Lugaresi,E. (1995). Fatal familial insomnia and familial Creutzfeldt-Jakob disease: clinical, pathological and molecular features. Brain Pathol. *5*, 43-51.

Gasset,M., Baldwin,M.A., Fletterick,R.J., Prusiner,S.B. (1993). Perturbation of the secondary structure of the scrapie prion protein under conditions that alter infectivity. Proc.Natl.Acad.Sci.U.S.A *90*, 1-5.

Gauczynski,S, Peyrin J.M., Haik, S., Leucht, C., Hundt, C., Rieger, R., Krasemann, S., Deslys, J.P., Dormont, D., Lasmezas, C.I., Weiss, S. (2001). The 37-kDa/67-kDa laminin receptor acts as the cell-surface receptor for the cellular prion protein. EMBO J 2001 Nov 1;20(21):5863-75

Ghani,A.C., Donnelly,C.A., Ferguson,N.M., Anderson,R.M. (2002). The transmission dynamics of BSE and vCJD. C.R.Acad.Sci.III *325*, 37-47.

Ghetti,B., Piccardo,P., Frangione,B., Bugiani,O., Giaccone,G., Young,K., Prelli,F., Farlow,M.R., Dlouhy,S.R., Tagliavini,F. (1996). Prion protein amyloidosis. Brain Pathol. *6*, 127-145.

Gibbs,C.J., Jr., Gajdusek,D.C., Asher,D.M., Alpers,M.P., Beck,E., Daniel,P.M., Matthews,W.B. (1968). Creutzfeldt-Jakob disease (spongiform encephalopathy): transmission to the chimpanzee. Science *161*, 388-389.

Gilch,S., Winklhofer,K.F., Groschup,M.H., Nunziante,M., Lucassen,R., Spielhaupter,C., Muranyi,W., Riesner,D., Tatzelt,J., Schatzl,H.M. (2001). Intracellular re-routing of prion protein prevents propagation of PrP(Sc) and delays onset of prion disease. EMBO J. *20*, 3957-3966.

Gill,A.C., Ritchie,M.A., Hunt,L.G., Steane,S.E., Davies,K.G., Bocking,S.P., Rhie,A.G., Bennett,A.D., Hope,J. (2000). Post-translational hydroxylation at the N-terminus of the prion protein reveals presence of PPII structure in vivo. EMBO J. *19*, 5324-5331.

Goldfarb,L.G., Petersen,R.B., Tabaton,M., Brown,P., LeBlanc,A.C., Montagna,P., Cortelli,P., Julien,J., Vital,C., Pendelbury,W.W., . (1992). Fatal familial insomnia and familial Creutzfeldt-Jakob disease: disease phenotype determined by a DNA polymorphism. Science *258*, 806-808.

Griffith,J.S. (1967). Self-replication and scrapie. Nature *215*, 1043-1044.

Hao,M., Maxfield,F.R. (2000). Characterization of rapid membrane internalization and recycling. J.Biol.Chem. *275*, 15279-15286.

Haraguchi,T., Fisher,S., Olofsson,S., Endo,T., Groth,D., Tarentino,A., Borchelt,D.R., Teplow,D., Hood,L., Burlingame,A., . (1989). Asparagine-linked glycosylation of the scrapie and cellular prion proteins. Arch.Biochem.Biophys. *274*, 1-13.

Harris,D.A., Falls,D.L., Johnson,F.A., Fischbach,G.D. (1991). A prion-like protein from chicken brain copurifies with an acetylcholine receptor-inducing activity. Proc.Natl.Acad.Sci.U.S.A *88*, 7664-7668.

Harris,D.A., Lele,P., Snider,W.D. (1993). Localization of the mRNA for a chicken prion protein by in situ hybridization. Proc.Natl.Acad.Sci.U.S.A *90*, 4309-4313.

Heppner,F.L., Musahl,C., Arrighi,I., Klein,M.A., Rulicke,T., Oesch,B., Zinkernagel,R.M., Kalinke,U., Aguzzi,A. (2001). Prevention of scrapie pathogenesis by transgenic expression of anti- prion protein antibodies. Science *294*, 178-182.

Herms,J., Tings,T., Gall,S., Madlung,A., Giese,A., Siebert,H., Schurmann,P., Windl,O., Brose,N., Kretzschmar,H. (1999). Evidence of presynaptic location and function of the prion protein. J.Neurosci. *19*, 8866-8875.

Hill,A.F., Butterworth,R.J., Joiner,S., Jackson,G., Rossor,M.N., Thomas,D.J., Frosh,A., Tolley,N., Bell,J.E., Spencer,M., King,A., Al Sarraj,S., Ironside,J.W., Lantos,P.L., Collinge,J. (1999). Investigation of variant Creutzfeldt-Jakob disease and other human prion diseases with tonsil biopsy samples. Lancet *353*, 183-189.

Hill,A.F., Desbruslais,M., Joiner,S., Sidle,K.C., Gowland,I., Collinge,J., Doey,L.J., Lantos,P. (1997). The same prion strain causes vCJD and BSE. Nature *389*, 448-50, 526.

Hilmert,H., Diringer,H. (1984). A rapid and efficient method to enrich SAF-protein from scrapie brains of hamsters. Biosci.Rep. *4*, 165-170.

Hilton, D., Fathers, E., Edwards, P., Ironside, J. & Zajicek, J. (1998). Prion immunoreactivity in appendix before clinical onset of variant Creutzfeldt–Jakob disease. Lancet 352, 703-704

Hooper,N.M., Keen,J.N., Turner,A.J. (1990). Characterization of the glycosyl-phosphatidylinositol-anchored human renal dipeptidase reveals that it is more extensively glycosylated than the pig enzyme. Biochem.J. *265*, 429-433.

Hornemann,S., Korth,C., Oesch,B., Riek,R., Wider,G., Wuthrich,K., Glockshuber,R. (1997). Recombinant full-length murine prion protein, mPrP(23-231): purification and spectroscopic characterization. FEBS Lett. *413*, 277-281.

Hornshaw,M.P., McDermott,J.R., Candy,J.M., Lakey,J.H. (1995). Copper binding to the N-terminal tandem repeat region of mammalian and avian prion protein: structural studies using synthetic peptides. Biochem.Biophys.Res.Commun. *214*, 993-999.

Hosszu,L.L., Baxter,N.J., Jackson,G.S., Power,A., Clarke,A.R., Waltho,J.P., Craven,C.J., Collinge,J. (1999). Structural mobility of the human prion protein probed by backbone hydrogen exchange. Nat.Struct.Biol. *6*, 740-743.

Hsiao,K., Baker,H.F., Crow,T.J., Poulter,M., Owen,F., Terwilliger,J.D., Westaway,D., Ott,J., Prusiner,S.B. (1989). Linkage of a prion protein missense variant to Gerstmann-Straussler syndrome. Nature *338*, 342-345.

Hundt, C., Peyrin, J.M., Haik, S., Gauczynski, S., Leucht, C., Rieger, R., Riley, M.L., Deslys, J.P., Dormont, D., Lasmezas, C.I., Weiss, S. (2001). Identification of interaction domains of the prion protein with its 37-kDa/67-kDa laminin receptor. EMBO J 2001 Nov 1;20(21):5876-86

Hunziker,W., Geuze,H.J. (1996). Intracellular trafficking of lysosomal membrane proteins. Bioessays *18*, 379-389.

Ingram,D.K. (2001). Vaccine development for Alzheimer's disease: a shot of good news. Trends Neurosci. *24*, 305-307.

Jackson,G.S., Murray,I., Hosszu,L.L., Gibbs,N., Waltho,J.P., Clarke,A.R., Collinge,J. (2001). Location and properties of metal-binding sites on the human prion protein. Proc.Natl.Acad.Sci.U.S.A *98*, 8531-8535.

James,T.L., Liu,H., Ulyanov,N.B., Farr-Jones,S., Zhang,H., Donne,D.G., Kaneko,K., Groth,D., Mehlhorn,I., Prusiner,S.B., Cohen,F.E. (1997). Solution structure of a 142-residue recombinant prion protein corresponding to the infectious fragment of the scrapie isoform. Proc.Natl.Acad.Sci.U.S.A *94*, 10086-10091.

Jeffrey,M., Wells,G.A. (1988). Spongiform encephalopathy in a nyala (Tragelaphus angasi). Vet.Pathol. *25*, 398-399.

Kaneko,K., Vey,M., Scott,M., Pilkuhn,S., Cohen,F.E., Prusiner,S.B. (1997a). COOH-terminal sequence of the cellular prion protein directs subcellular trafficking and controls conversion into the scrapie isoform. Proc.Natl.Acad.Sci.U.S.A *94*, 2333-2338.

Kaneko,K., Zulianello,L., Scott,M., Cooper,C.M., Wallace,A.C., James,T.L., Cohen,F.E., Prusiner,S.B. (1997b). Evidence for protein X binding to a discontinuous epitope on the cellular prion protein during scrapie prion propagation. Proc.Natl.Acad.Sci.U.S.A *94*, 10069-10074.

Kirkwood,J.K., Wells,G.A., Wilesmith,J.W., Cunningham,A.A., Jackson,S.I. (1990). Spongiform encephalopathy in an arabian oryx (Oryx leucoryx) and a greater kudu (Tragelaphus strepsiceros). Vet.Rec. *127*, 418-420.

Klein,M.A., Frigg,R., Flechsig,E., Raeber,A.J., Kalinke,U., Bluethmann,H., Bootz,F., Suter,M., Zinkernagel,R.M., Aguzzi,A. (1997). A crucial role for B cells in neuroinvasive scrapie. Nature *390*, 687-690.

Klein,M.A., Kaeser,P.S., Schwarz,P., Weyd,H., Xenarios,I., Zinkernagel,R.M., Carroll,M.C., Verbeek,J.S., Botto,M., Walport,M.J., Molina,H., Kalinke,U., Acha-Orbea,H., Aguzzi,A. (2001). Complement facilitates early prion pathogenesis. Nat.Med. *7*, 488-492.

Kretzschmar,H.A., Prusiner,S.B., Stowring,L.E., DeArmond,S.J. (1986). Scrapie prion proteins are synthesized in neurons. Am.J.Pathol. *122*, 1-5.

Kurschner,C., Morgan,J.I. (1996). Analysis of interaction sites in homo- and heteromeric complexes containing Bcl-2 family members and the cellular prion protein. Brain Res.Mol.Brain Res. *37*, 249-258.

Laemmli,U.K. (1970). Cleavage of structural proteins during the assembly of the head of bacteriophage T4. Nature *227*, 680-685.

Lafont,F., Lecat,S., Verkade,P., Simons,K. (1998). Annexin XIIIb associates with lipid microdomains to function in apical delivery. J.Cell Biol. *142*, 1413-1427.

Lafont,F., Verkade,P., Galli,T., Wimmer,C., Louvard,D., Simons,K. (1999). Raft association of SNAP receptors acting in apical trafficking in Madin-Darby canine kidney cells. Proc.Natl.Acad.Sci.U.S.A *96*, 3734-3738.

Lasmezas,C.I., Deslys,J.P., Demaimay,R., Adjou,K.T., Lamoury,F., Dormont,D., Robain,O., Ironside,J., Hauw,J.J. (1996). BSE transmission to macaques. Nature *381*, 743-744.

Lawson,V.A., Priola,S.A., Wehrly,K., Chesebro,B. (2001). N-terminal truncation of prion protein affects both formation and conformation of abnormal protease resistant prion protein generated in vitro. J.Biol.Chem.

Lecat,S., Verkade,P., Thiele,C., Fiedler,K., Simons,K., Lafont,F. (2000). Different properties of two isoforms of annexin XIII in MDCK cells. J.Cell Sci. *113 (Pt 14)*, 2607-2618.

Lehmann,S., Harris,D.A. (1996). Two mutant prion proteins expressed in cultured cells acquire biochemical properties reminiscent of the scrapie isoform. Proc.Natl.Acad.Sci.U.S.A *93*, 5610-5614.

Lehmann,S., Harris,D.A. (1997). Blockade of glycosylation promotes acquisition of scrapie-like properties by the prion protein in cultured cells. J.Biol.Chem. *272*, 21479-21487.

Lehto,M.T., Sharom,F.J. (1998). Release of the glycosylphosphatidylinositol-anchored enzyme ecto-5'- nucleotidase by phospholipase C: catalytic activation and modulation by the lipid bilayer. Biochem.J. *332 (Pt 1)*, 101-109.

Liemann,S., Glockshuber,R. (1998). Transmissible spongiform encephalopathies. Biochem.Biophys.Res.Commun. *250*, 187-193.

Lisanti,M.P., Caras,I.W., Davitz,M.A., Rodriguez-Boulan,E. (1989). A glycophospholipid membrane anchor acts as an apical targeting signal in polarized epithelial cells. J.Cell Biol. *109*, 2145-2156.

Mabbott,N.A., Bruce,M.E. (2001). The immunobiology of TSE diseases. J.Gen.Virol. *82*, 2307-2318.

Mabbott, N. A., Williams, A., Farquhar, C. F., Pasparakis, M., Kollias, G. & Bruce, M. E. (2000). Tumor necrosis factor-alpha-deficient, but not interleukin-6-deficient, mice resist peripheral infection with scrapie. Journal of Virology 74, 3338-3344.

Madore,N., Smith,K.L., Graham,C.H., Jen,A., Brady,K., Hall,S., Morris,R. (1999). Functionally different GPI proteins are organized in different domains on the neuronal surface. EMBO J. *18*, 6917-6926.

Mallet,W.G., Maxfield,F.R. (1999). Chimeric forms of furin and TGN38 are transported with the plasma membrane in the trans-Golgi network via distinct endosomal pathways. J.Cell Biol. *146*, 345-359.

Marella,M., Lehmann,S., Grassi,J., Chabry,J. (2002). Filipin prevents pathological prion protein accumulation by reducing endocytosis and inducing cellular PrP release. J.Biol.Chem.

Marsh,R.F., Hadlow,W.J. (1992). Transmissible mink encephalopathy. Rev.Sci.Tech. *11*, 539-550.

Matlack,K.E., Mothes,W., Rapoport,T.A. (1998). Protein translocation: tunnel vision. Cell *92*, 381-390.

Matter,K. (2000). Epithelial polarity: sorting out the sorters. Curr.Biol. *10*, R39-R42.

Mayor,S., Sabharanjak,S., Maxfield,F.R. (1998). Cholesterol-dependent retention of GPI-anchored proteins in endosomes. EMBO J. *17*, 4626-4638.

McKnight,S., Tjian,R. (1986). Transcriptional selectivity of viral genes in mammalian cells. Cell *46*, 795-805.

Mellman,I. (1996). Endocytosis and molecular sorting. Annu.Rev.Cell Dev.Biol. *12*, 575-625.

Meyer,R.K., McKinley,M.P., Bowman,K.A., Braunfeld,M.B., Barry,R.A., Prusiner,S.B. (1986). Separation and properties of cellular and scrapie prion proteins. Proc.Natl.Acad.Sci.U.S.A *83*, 2310-2314.

Mizukami,I.F., Faulkner,N.E., Gyetko,M.R., Sitrin,R.G., Todd,R.F., III (1995). Enzyme-linked immunoabsorbent assay detection of a soluble form of urokinase plasminogen activator receptor in vivo. Blood *86* , 203-211.

Mostov,K.E., Verges,M., Altschuler,Y. (2000). Membrane traffic in polarized epithelial cells. Curr.Opin.Cell Biol. *12*, 483-490.

Mukherjee,S., Ghosh,R.N., Maxfield,F.R. (1997). Endocytosis. Physiol Rev. *77*, 759-803.

Muniz,M., Riezman,H. (2000). Intracellular transport of GPI-anchored proteins. EMBO J. *19*, 10-15.

Nichols,B.J., Kenworthy,A.K., Polishchuk,R.S., Lodge,R., Roberts,T.H., Hirschberg,K., Phair,R.D., Lippincott-Schwartz,J. (2001). Rapid cycling of lipid raft markers between the cell surface and Golgi complex. J.Cell Biol. *153*, 529-541.

Nykjaer,A., Petersen,C.M., Moller,B., Jensen,P.H., Moestrup,S.K., Holtet,T.L., Etzerodt,M., Thogersen,H.C., Munch,M., Andreasen,P.A., . (1992). Purified alpha 2-macroglobulin receptor/LDL receptor-related protein binds urokinase.plasminogen activator inhibitor type-1 complex. Evidence that the alpha 2-macroglobulin receptor mediates cellular degradation of urokinase receptor-bound complexes. J.Biol.Chem. *267*, 14543-14546.

Oesch,B., Westaway,D., Walchli,M., McKinley,M.P., Kent,S.B., Aebersold,R., Barry,R.A., Tempst,P., Teplow,D.B., Hood,L.E., . (1985). A cellular gene encodes scrapie PrP 27-30 protein. Cell *40*, 735-746.

Ojakian,G.K., Schwimmer,R. (1988). The polarized distribution of an apical cell surface glycoprotein is maintained by interactions with the cytoskeleton of Madin-Darby canine kidney cells. J.Cell Biol. *107*, 2377-2387.

Owen,F., Poulter,M., Collinge,J., Leach,M., Lofthouse,R., Crow,T.J., Harding,A.E. (1992). A dementing illness associated with a novel insertion in the prion protein gene. Brain Res.Mol.Brain Res. *13*, 155-157.

Owen,F., Poulter,M., Lofthouse,R., Collinge,J., Crow,T.J., Risby,D., Baker,H.F., Ridley,R.M., Hsiao,K., Prusiner,S.B. (1989). Insertion in prion protein gene in familial Creutzfeldt-Jakob disease. Lancet *1*, 51-52.

Owen,F., Poulter,M., Shah,T., Collinge,J., Lofthouse,R., Baker,H., Ridley,R., McVey,J., Crow,T.J. (1990). An in-frame insertion in the prion protein gene in familial Creutzfeldt-Jakob disease. Brain Res.Mol.Brain Res. *7*, 273-276.

Pan,K.M., Baldwin,M., Nguyen,J., Gasset,M., Serban,A., Groth,D., Mehlhorn,I., Huang,Z., Fletterick,R.J., Cohen,F.E., . (1993). Conversion of alpha-helices into beta-sheets features in the formation of the scrapie prion proteins. Proc.Natl.Acad.Sci.U.S.A *90*, 10962-10966.

Pan,K.M., Stahl,N., Prusiner,S.B. (1992). Purification and properties of the cellular prion protein from Syrian hamster brain. Protein Sci. *1*, 1343-1352.

Parchi,P., Castellani,R., Capellari,S., Ghetti,B., Young,K., Chen,S.G., Farlow,M., Dickson,D.W., Sima,A.A., Trojanowski,J.Q., Petersen,R.B., Gambetti,P. (1996). Molecular basis of phenotypic variability in sporadic Creutzfeldt-Jakob disease. Ann.Neurol. *39*, 767-778.

Parchi,P., Petersen,R.B., Chen,S.G., Autilio-Gambetti,L., Capellari,S., Monari,L., Cortelli,P., Montagna,P., Lugaresi,E., Gambetti,P. (1998). Molecular pathology of fatal familial insomnia. Brain Pathol. *8*, 539-548.

Parizek,P., Roeckl,C., Weber,J., Flechsig,E., Aguzzi,A., Raeber,A.J. (2001). Similar turnover and shedding of the cellular prion protein in primary lymphoid and neuronal cells. J.Biol.Chem. *276*, 44627-44632.

Parton,R.G., Joggerst,B., Simons,K. (1994). Regulated internalization of caveolae. J.Cell Biol. *127*, 1199-1215.

Pattison,I.H. (1965). Scrapie in the welsh mountain breed of sheep and its experimental transmission to goats. Vet.Rec. *77*, 1388-1390.

Pauly,P.C., Harris,D.A. (1998). Copper stimulates endocytosis of the prion protein. J.Biol.Chem. *273*, 33107-33110.

Pergami,P., Jaffe,H., Safar,J. (1996). Semipreparative chromatographic method to purify the normal cellular isoform of the prion protein in nondenatured form. Anal.Biochem. *236*, 63-73.

Perini,F., Vidal,R., Ghetti,B., Tagliavini,F., Frangione,B., Prelli,F. (1996). PrP27-30 is a normal soluble prion protein fragment released by human platelets. Biochem.Biophys.Res.Commun. *223*, 572-577.

Prusiner,S.B. (1982). Novel proteinaceous infectious particles cause scrapie. Science *216*, 136-144.

Prusiner,S.B. (1991). Molecular biology of prion diseases. Science *252*, 1515-1522.

Prusiner,S.B. (1998). Prions. Proc.Natl.Acad.Sci.U.S.A *95*, 13363-13383.

Prusiner,S.B., Gajdusek,C., Alpers,M.P. (1982). Kuru with incubation periods exceeding two decades. Ann.Neurol. *12*, 1-9.

Prusiner,S.B., Groth,D., Serban,A., Koehler,R., Foster,D., Torchia,M., Burton,D., Yang,S.L., DeArmond,S.J. (1993). Ablation of the prion protein (PrP) gene in mice prevents scrapie and facilitates production of anti-PrP antibodies. Proc.Natl.Acad.Sci.U.S.A *90*, 10608-10612.

Prusiner,S.B., Groth,D.F., Bolton,D.C., Kent,S.B., Hood,L.E. (1984). Purification and structural studies of a major scrapie prion protein. Cell *38*, 127-134.

Prusiner,S.B., McKinley,M.P., Groth,D.F., Bowman,K.A., Mock,N.I., Cochran,S.P., Masiarz,F.R. (1981). Scrapie agent contains a hydrophobic protein. Proc.Natl.Acad.Sci.U.S.A *78*, 6675-6679.

Prusiner,S.B., Scott,M., Foster,D., Pan,K.M., Groth,D., Mirenda,C., Torchia,M., Yang,S.L., Serban,D., Carlson,G.A., . (1990). Transgenetic studies implicate interactions between homologous PrP isoforms in scrapie prion replication. Cell *63*, 673-686.

Rieger,R., Edenhofer,F., Lasmezas,C.I., Weiss,S. (1997). The human 37-kDa laminin receptor precursor interacts with the prion protein in eukaryotic cells. Nat.Med. *3*, 1383-1388.

Riek,R., Hornemann,S., Wider,G., Billeter,M., Glockshuber,R., Wuthrich,K. (1996). NMR structure of the mouse prion protein domain PrP(121-321). Nature *382*, 180-182.

Riek,R., Hornemann,S., Wider,G., Glockshuber,R., Wuthrich,K. (1997). NMR characterization of the full-length recombinant murine prion protein, mPrP(23-231). FEBS Lett. *413*, 282-288.

Riek,R., Wider,G., Billeter,M., Hornemann,S., Glockshuber,R., Wuthrich,K. (1998). Prion protein NMR structure and familial human spongiform encephalopathies. Proc.Natl.Acad.Sci.U.S.A *95*, 11667-11672.

Robakis,N.K., Devine-Gage,E.A., Jenkins,E.C., Kascsak,R.J., Brown,W.T., Krawczun,M.S., Silverman,W.P. (1986). Localization of a human gene homologous to the PrP gene on the p arm of chromosome 20 and detection of PrP-related antigens in normal human brain. Biochem.Biophys.Res.Commun. *140*, 758-765.

Rodriguez-Boulan,E., Powell,S.K. (1992). Polarity of epithelial and neuronal cells. Annu.Rev.Cell Biol. *8*, 395-427.

Rogers,M., Taraboulos,A., Scott,M., Groth,D., Prusiner,S.B. (1990). Intracellular accumulation of the cellular prion protein after mutagenesis of its Asn-linked glycosylation sites. Glycobiology *1*, 101-109.

Rogers,M., Yehiely,F., Scott,M., Prusiner,S.B. (1993). Conversion of truncated and elongated prion proteins into the scrapie isoform in cultured cells. Proc.Natl.Acad.Sci.U.S.A *90*, 3182-3186.

Saeki,K., Matsumoto,Y., Hirota,Y., Matsumoto,Y., Onodera,T. (1996). Three-exon structure of the gene encoding the rat prion protein and its expression in tissues. Virus Genes *12*, 15-20.

Schatzl,H.M., Da Costa,M., Taylor,L., Cohen,F.E., Prusiner,S.B. (1995). Prion protein gene variation among primates. J.Mol.Biol. *245*, 362-374.

Scheiffele,P., Peranen,J., Simons,K. (1995). N-glycans as apical sorting signals in epithelial cells. Nature *378*, 96-98.

Shyng,S.L., Huber,M.T., Harris,D.A. (1993). A prion protein cycles between the cell surface and an endocytic compartment in cultured neuroblastoma cells. J.Biol.Chem. *268*, 15922-15928.

Shyng,S.L., Lehmann,S., Moulder,K.L., Harris,D.A. (1995a). Sulfated glycans stimulate endocytosis of the cellular isoform of the prion protein, PrPC, in cultured cells. J.Biol.Chem. *270*, 30221-30229.

Shyng,S.L., Moulder,K.L., Lesko,A., Harris,D.A. (1995b). The N-terminal domain of a glycolipid-anchored prion protein is essential for its endocytosis via clathrin-coated pits. J.Biol.Chem. *270*, 14793-14800.

Simons,K., Ikonen,E. (1997). Functional rafts in cell membranes. Nature *387*, 569-572.

Simons,K., van Meer,G. (1988). Lipid sorting in epithelial cells. Biochemistry *27*, 6197-6202.

Skretting,G., Torgersen,M.L., van Deurs,B., Sandvig,K. (1999). Endocytic mechanisms responsible for uptake of GPI-linked diphtheria toxin receptor. J.Cell Sci. *112 (Pt 22)*, 3899-3909.

Smith,T.K., Sharma,D.K., Crossman,A., Dix,A., Brimacombe,J.S., Ferguson,M.A. (1997). Parasite and mammalian GPI biosynthetic pathways can be distinguished using synthetic substrate analogues. EMBO J. *16*, 6667-6675.

Sparkes,R.S., Simon,M., Cohn,V.H., Fournier,R.E., Lem,J., Klisak,I., Heinzmann,C., Blatt,C., Lucero,M., Mohandas,T., . (1986). Assignment of the human and mouse prion protein genes to homologous chromosomes. Proc.Natl.Acad.Sci.U.S.A *83*, 7358-7362.

Spraker,T.R., Miller,M.W., Williams,E.S., Getzy,D.M., Adrian,W.J., Schoonveld,G.G., Spowart,R.A., O'Rourke,K.I., Miller,J.M., Merz,P.A. (1997). Spongiform encephalopathy in free-ranging mule deer (Odocoileus hemionus), white-tailed deer (Odocoileus virginianus) and Rocky Mountain elk (Cervus elaphus nelsoni) in northcentral Colorado. J.Wildl.Dis. *33*, 1-6.

Stahl,N., Baldwin,M.A., Teplow,D.B., Hood,L., Gibson,B.W., Burlingame,A.L., Prusiner,S.B. (1993). Structural studies of the scrapie prion protein using mass spectrometry and amino acid sequencing. Biochemistry *32*, 1991-2002.

Stein,C.A., Khan,T.M., Khaled,Z., Tonkinson,J.L. (1995). Cell surface binding and cellular internalization properties of suramin, a novel antineoplastic agent. Clin.Cancer Res. *1*, 509-517.

Stewart,R.S., Drisaldi,B., Harris,D.A. (2001). A transmembrane form of the prion protein contains an uncleaved signal peptide and is retained in the endoplasmic Reticulum. Mol.Biol.Cell *12*, 881-889.

Strumbo,B., Ronchi,S., Bolis,L.C., Simonic,T. (2001). Molecular cloning of the cDNA coding for Xenopus laevis prion protein. FEBS Lett. *508*, 170-174.

Sumudhu, W., Perera, S., and Hooper, N. M. Ablation of metal ion-induced endocytosis of the prion protein by disease-associated mutation of the octarepeat region. Curr.Biol. 11, No 7, 519-523. 3-4-2001.
Ref Type: Generic

Taraboulos,A., Raeber,A.J., Borchelt,D.R., Serban,D., Prusiner,S.B. (1992). Synthesis and trafficking of prion proteins in cultured cells. Mol.Biol.Cell *3*, 851-863.

Taraboulos,A., Rogers,M., Borchelt,D.R., McKinley,M.P., Scott,M., Serban,D., Prusiner,S.B. (1990a). Acquisition of protease resistance by prion proteins in scrapie- infected cells does not require asparagine-linked glycosylation. Proc.Natl.Acad.Sci.U.S.A *87*, 8262-8266.

Taraboulos,A., Scott,M., Semenov,A., Avrahami,D., Laszlo,L., Prusiner,S.B., Avraham,D. (1995). Cholesterol depletion and modification of COOH-terminal targeting sequence of the prion protein inhibit formation of the scrapie isoform. J.Cell Biol. *129*, 121-132.

Taraboulos,A., Serban,D., Prusiner,S.B. (1990b). Scrapie prion proteins accumulate in the cytoplasm of persistently infected cultured cells. J.Cell Biol. *110*, 2117-2132.

Tarentino,A.L., Plummer,T.H., Jr. (1994). Enzymatic deglycosylation of asparagine-linked glycans: purification, properties, and specificity of oligosaccharide-cleaving enzymes from Flavobacterium meningosepticum. Methods Enzymol. *230*, 44-57.

Telling,G.C., Scott,M., Mastrianni,J., Gabizon,R., Torchia,M., Cohen,F.E., DeArmond,S.J., Prusiner,S.B. (1995). Prion propagation in mice expressing human and chimeric PrP transgenes implicates the interaction of cellular PrP with another protein. Cell *83*, 79-90.

Tobler,I., Gaus,S.E., Deboer,T., Achermann,P., Fischer,M., Rulicke,T., Moser,M., Oesch,B., McBride,P.A., Manson,J.C. (1996). Altered circadian activity rhythms and sleep in mice devoid of prion protein. Nature *380*, 639-642.

Vey,M., Pilkuhn,S., Wille,H., Nixon,R., DeArmond,S.J., Smart,E.J., Anderson,R.G., Taraboulos,A., Prusiner,S.B. (1996). Subcellular colocalization of the cellular and scrapie prion proteins in caveolae-like membranous domains. Proc.Natl.Acad.Sci.U.S.A *93*, 14945-14949.

Viles,J.H., Cohen,F.E., Prusiner,S.B., Goodin,D.B., Wright,P.E., Dyson,H.J. (1999). Copper binding to the prion protein: structural implications of four identical cooperative binding sites. Proc.Natl.Acad.Sci.U.S.A *96*, 2042-2047.

Vorberg,I., Priola,S.A. (2002). Molecular basis of scrapie strain glycoform variation. J.Biol.Chem. *277*, 36775-36781.

Wadsworth,J.D., Hill,A.F., Joiner,S., Jackson,G.S., Clarke,A.R., Collinge,J. (1999). Strain-specific prion-protein conformation determined by metal ions. Nat.Cell Biol. *1*, 55-59.

Walmsley,A.R., Zeng,F., Hooper,N.M. (2001). Membrane topology influences N-glycosylation of the prion protein. EMBO J. *20*, 703-712.

Weissmann,C., Raeber,A.J., Montrasio,F., Hegyi,I., Frigg,R., Klein,M.A., Aguzzi,A. (2001). Prions and the lymphoreticular system. Philos.Trans.R.Soc.Lond B Biol.Sci. *356*, 177-184.

Wells,G.A., Scott,A.C., Johnson,C.T., Gunning,R.F., Hancock,R.D., Jeffrey,M., Dawson,M., Bradley,R. (1987). A novel progressive spongiform encephalopathy in cattle. Vet.Rec. *121*, 419-420.

Westaway,D., Mirenda,C.A., Foster,D., Zebarjadian,Y., Scott,M., Torchia,M., Yang,S.L., Serban,H., DeArmond,S.J., Ebeling,C., . (1991). Paradoxical shortening of scrapie incubation times by expression of prion protein transgenes derived from long incubation period mice. Neuron *7*, 59-68.

Whittal,R.M., Ball,H.L., Cohen,F.E., Burlingame,A.L., Prusiner,S.B., Baldwin,M.A. (2000). Copper binding to octarepeat peptides of the prion protein monitored by mass spectrometry. Protein Sci. *9*, 332-343.

Will,R.G. (1998). New variant Creutzfeldt-Jakob disease. Dev.Biol.Stand. *93*, 79-84.

Will,R.G., Ironside,J.W., Zeidler,M., Cousens,S.N., Estibeiro,K., Alperovitch,A., Poser,S., Pocchiari,M., Hofman,A., Smith,P.G. (1996). A new variant of Creutzfeldt-Jakob disease in the UK. Lancet *347*, 921-925.

Wille,H., Michelitsch,M.D., Guenebaut,V., Supattapone,S., Serban,A., Cohen,F.E., Agard,D.A., Prusiner,S.B. (2002). Structural studies of the scrapie prion protein by electron crystallography. Proc.Natl.Acad.Sci.U.S.A *99*, 3563-3568.

Williamson,R.A., Peretz,D., Smorodinsky,N., Bastidas,R., Serban,H., Mehlhorn,I., DeArmond,S.J., Prusiner,S.B., Burton,D.R. (1996). Circumventing tolerance to generate autologous monoclonal antibodies to the prion protein. Proc.Natl.Acad.Sci.U.S.A *93*, 7279-7282.

Winckler,B., Mellman,I. (1999). Neuronal polarity: controlling the sorting and diffusion of membrane components. Neuron *23*, 637-640.

Windl,O., Dempster,M., Estibeiro,P., Lathe,R. (1995). A candidate marsupial PrP gene reveals two domains conserved in mammalian PrP proteins. Gene *159*, 181-186.

Wopfner,F., Weidenhofer,G., Schneider,R., von Brunn,A., Gilch,S., Schwarz,T.F., Werner,T., Schatzl,H.M. (1999). Analysis of 27 mammalian and 9 avian PrPs reveals high conservation of flexible regions of the prion protein. J.Mol.Biol. *289*, 1163-1178.

Zanusso,G., Petersen,R.B., Jin,T., Jing,Y., Kanoush,R., Ferrari,S., Gambetti,P., Singh,N. (1999). Proteasomal degradation and N-terminal protease resistance of the codon 145 mutant prion protein. J.Biol.Chem. *274*, 23396-23404.

Zeidler,M., Johnstone,E.C., Bamber,R.W., Dickens,C.M., Fisher,C.J., Francis,A.F., Goldbeck,R., Higgo,R., Johnson-Sabine,E.C., Lodge,G.J., McGarry,P., Mitchell,S., Tarlo,L., Turner,M., Ryley,P., Will,R.G. (1997). New variant Creutzfeldt-Jakob disease: psychiatric features. Lancet *350*, 908-910.

Zhao,Y., McCabe,J.B., Vance,J., Berthiaume,L.G. (2000). Palmitoylation of apolipoprotein B is required for proper intracellular sorting and transport of cholesteroyl esters and triglycerides. Mol.Biol.Cell *11*, 721-734.

Zulianello,L., Kaneko,K., Scott,M., Erpel,S., Han,D., Cohen,F.E., Prusiner,S.B. (2000). Dominant-negative inhibition of prion formation diminished by deletion mutagenesis of the prion protein. J.Virol. *74* , 4351-4360.

8 Abbreviations

APS	ammoniumpersulfate
ATCC	American Type Culture Collection
Aa	amino acid
BHK	baby hamster kidney (cells)
Bp	base pairs
BSE	bovine spongiform encephalopathy
CHO	Chinese hamster ovary (cells)
Ci	Curie
CD	circular dichroism
CJD	Creutzfeldt-Jakob disease
CLD	caveolae-like domains
CNS	central nervous system
CWD	chronic wasting disease
Cys	cysteine
DMEM	Dulbecco´s modified Eagle medium
DNA	deoxyribonucleic acid
dNTP	deoxynucleotide
ER	endoplasmic reticulum
ERAD	ER-associated degradation
ERGIC	ER-Golgi intermediate compartment
EDTA	ethylenediaminetetraacetate
Endo-H	Endoglycosidase-H
EtOH	ethanol
FCS	fetal calf serum
FDC	follicular dendritic cells
FFI	fatal familial insomnia
FITC	Fluorescein - Isothyocianate
FSE	feline spongiform encephalopathy
FTIR	Fourier-transform infrared spectroscopy
GPI	glycosyl-phosphatidyl-inositol
GSS	Gerstmann-Sträußler-Scheinker disease
KDa	kilodalton

LR	laminin receptor
LRP	laminin receptor precursor
mAb	monoclonal antibody
MEM	minimal essential medium
Meth	methionine
MetOH	methanol
NMR	nuclear magnetic resonance
OD	optical density
ORF	open reading frame
pAB	ploYclonal antibody
PAGE	polyacrylamide gel electrophoresis
PCR	polymerase chain reaction
PNGase F	N-Glycosidase F
PrP	prion protein
PrP^{c}	cellular non-pathogenic form of the prion protein
PrP^{Sc}	pathogenic form of the prion protein
PK	Proteinase K
REC	recycling endocytic compartment
RT	room temperature
SDS	sodium dodecyl sulfate
SE	sorting endosome
TEMED	N,N,N,N-tetramethylethylendiamin
TGN	trans-Golgi network
TME	transmissible mink encephalopathy
TSE	transmissible spongiform encephalopathy
wt	wild type

9 Publications

Nunziante M., Gilch, S., Schätzl H.M (2003) Essential role of the Prion protein N-Terminus in subcellular trafficking and half-life of cellular Prion protein. The Journal of Biological Chemistry 278, 3726-34

Gilch S., Winklhofer K.F., Groschup M.H., Nunziante M., Lucassen R., Spielhaupter C., Muranyi W., Riesner D., Tatzelt J., Schätzl H.M. (2001) Intracellular re-routing of prion protein prevents propagation of PrP^{Sc} and delays onset of prion disease. The EMBO Journal 20, 3957-66

10 Acknowledgements

I would like to express my gratitude to Prof. Dr. Schätzl for supervising my work, for the provision of all the material, the fruitful discussions and counsel.

I am grateful to Prof. Dr. Conzelmann for being my tutor at the faculty of medicine and to Prof. Dr. Koszinowski for generously allowing my work in his laboratories.

I thank Sabine Gilch and Christian Spielhaupter for their practical assistance, expertise and constructive discussions and for their exceeding patience since day one. I am grateful to the entire Schätzl-Group for the extremely pleasant working atmosphere. Special thanks to Franziska Wopfner for giving of her time and revising this dissertation.

I am also thankful to the colleagues at the Genecentre with whom I have had the pleasure of working. In particular, I appreciate those among them who have became close friends:, Anja Bubeck, Markus Wagner, Madeleine Löfqvist, Carine Menard, Heike Ziegler and Andreas Elsing.

Above all I thank my friends: This work would not have been possible without their continuous support and patience.

11 Curriculum vitae

Name	Maximilian Nunziante
Date of birth	30.09.1969
Place of birth	Catania (Italy)
Nationality	German
Marital status	unmarried
Education	1975-1983 Primary school (Grund- und Mittelschule) Verona (Italy) 1983-1988 Scientific secondary school Galileo Galilei, Verona (Italy)
Secondary school qualification	matriculation standard (allgemeine Hochschulreife)
Higher education	1988-1995 Studies of biological sciences at the University of Padova, (Italy) 1993-1994 Diploma thesis at the institute of histology, Faculty of Medicine, University of Verona (Italy) with Prof. Dr. Armato
PhD studies	November 1998-today Doctoral studies with Prof. Schätzl at the Ludwig-Maximilians-University of Munich, Max-von-Pettenkofer Institute